ASPECTS OF THE STRUCTURE, TECTONIC EVOLUTION AND SEDIMENTATION OF THE TYGERBERG TERRANE, SOUTHWESTERN CAPE PROVINCE.

M.W. VON VEH

1982

A dissertation submitted to the Faculty of Science,
University of Cape Town,
for the degree of Master of Science.

ASPECTS OF THE STRUCTURE, TECTONIC EVOLUTION AND SEDIMENTATION OF THE TYGERBERG TERRANE, SOUTHWESTERN CAPE PROVINCE.

ABSTRACT

A structural, deformational and sedimentalogical analysis of the Sea Point, Signal Hill and Bloubergstrand exposures of the Tygerberg Formation, Malmesbury Group, has been undertaken, through the application of developed geomathematical, digital and graphical computer-based techniques, encompassing the fields of tectonic strain determination, fold shape classification, cross-sectional profile preparation and sedimentary data representation.

Emplacement of the Cape Peninsula granite pluton led to significant tectonic shortening of the sediments, tightening of the pre-existing synclinal fold at Sea Point, and overprinting of the structure by a regional foliation. Strain determinations from deformed metamorphic spotting in the sediments yielded a mean, undirected $\lambda_1 : \lambda_2 : \lambda_3$ value of 1.57:1.24:0.52. This strain increment increases slightly towards the contact and it is proposed that it is non-coaxial to, and late relative to the ca 600Ma orogenic episode. The oblate nature of the strain ellipsoid lends support to the mechanism of radial distension as a means of pluton emplacement.

An insight into the effect of the deformation on the structural configuration of the fold can be gained through a reconstruction of the 'pre-granite emplacement' down-plunge projection. In a reconstructed section, the matching of lithological units along strike was poor.

Through detailed sedimentary logging of both limbs of the fold distinct lithological zones and facies, commonly displaying turbiditic characteristics, were recognised. Significant down-current changes in sedimentary structures, identified from a matching of the zones in the two limbs, are indicative of a small-sized depositional basin. The stratigraphic sequence thickens and coarsens upward and is consequently assigned to the lower and mid fan parts of a prograding submarine fan model.

Mapping of the Bloubergstrand outcrops has led to the recognition of a major NW-striking tectonic discontinuity seperating a N- to NNE-dipping southwestern domain from a NW-striking northeastern domain.

A kinematic interpretation consistent with the geometry of the structural elements found here, is as follows:
An early phase of ductile, right-lateral shearing, in an 040 NE direction, produced mesoscopic drag folding, complex minor folding and extensional features. The effects of the main orogenic episode was to steepen the bedding, modify the minor folds and to overprint a penetrative foliation. Regional relaxation resulted in conjugate, NS-striking, dextral and NNE-striking, sinistral faulting, accompanied by minor kinking, and the development of a poor NNE-striking fracture cleavage. Infilling of tension fissures by sand debris occurred during a subsequent erosional period. Late NW-striking shearing was of a brittle nature.

The volcanic and sedimentary units within the domains are defined and described. A volcanic unit, comprised of interbedded tuffs and porphyritic and brecciated lavas, can be traced along the length of the exposure. The sedimentary facies found here fit with those expected in an upper fan environment.

An earlier orogenic event, pre-dating the deposition of the proximal sediments of the Tygerberg formation and the sediments of parts of the Boland subgroup, and manifested in the complex structural regime of the Swartland terrane, may account for the variation in tectonic style within the Malmesbury Group.

TABLE OF CONTENTS

PART II
THE PRE-CAPE ROCKS AT BLOUBERGSTRAND

1 INTRODUCTION

1-1 GENERAL

The Palaeozoic formations of the Cape Supergroup in the southwestern Cape Province of South Africa rest on a foundation of older formations, which outcrop sporadically within the Cape Fold Belt and on the coastal forelands.

The pre-Cape rocks of the Malmesbury group form a plain on the western foreland. The even surface of this plain is broken by a number of granitic batholiths, as well as by the prominent Table Mountain sandstone outlier of the Cape Peninsula. A thin drift sand veneer covers extensive areas of the plain.

The Malmesbury group rocks, where exposed, display the characteristics of a marine sedimentary assemblage. A wide variety of lithological types are represented; notably schists, shales, greywackes, quartzites, limestones, conglomerates, some extrusive greenstones and minor basic intrusives.

The formations were deformed and metamorphosed to low grades during a late Precambrian orogenic episode, which culminated in the intrusion of the Cape granite suite.

Three major tectonic domains have been recognized in the Malmesbury Group, in which the style and history of deformation appear to differ markedly (Hartnady et al., 1974). Narrow NW-striking belts of shear deformation seperate a central domain (the Swartland Subgroup), from less complexly deformed southwestern and northeastern domains (the Tygerberg Formation and the Boland Subgroup).

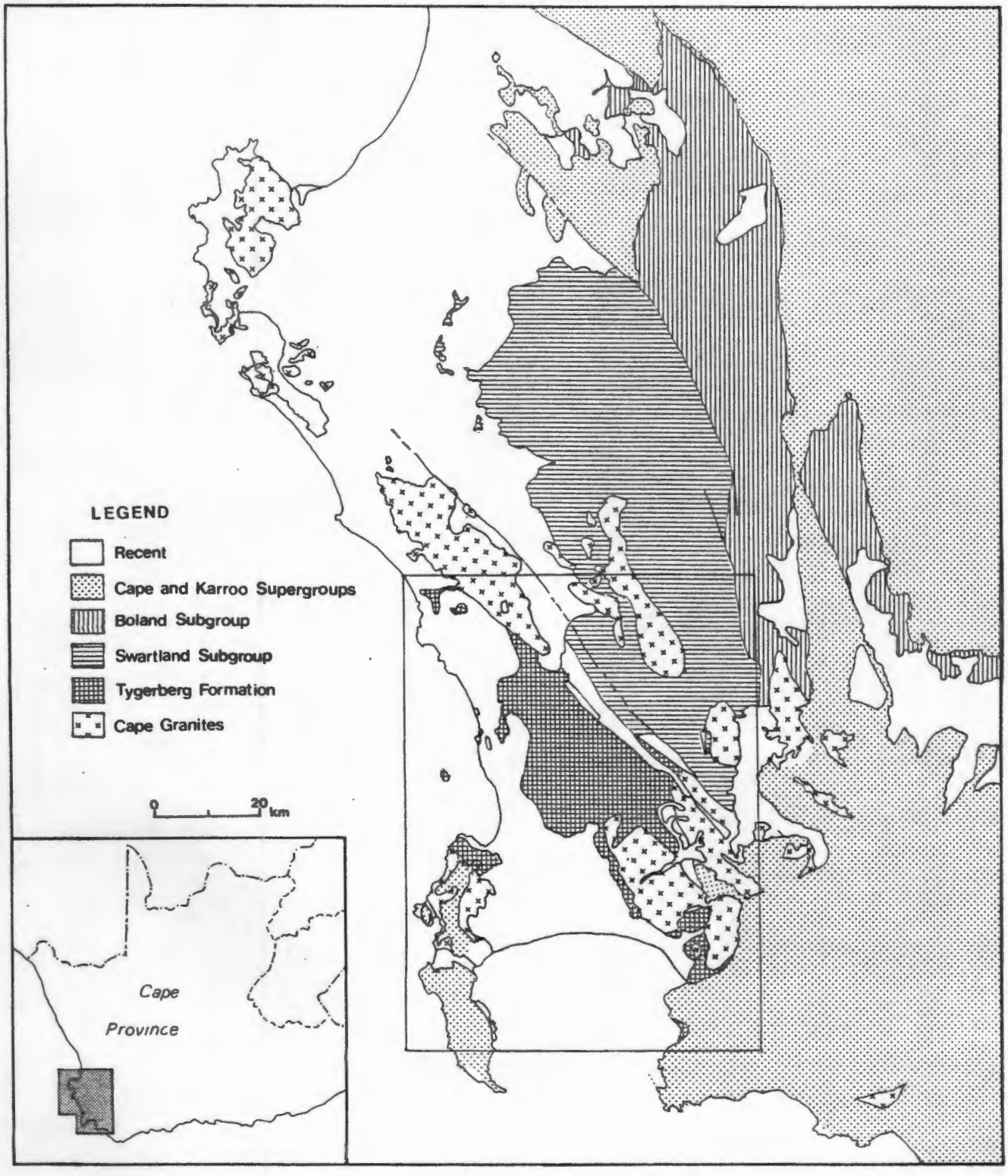

Fig.1.1 Simplified map of the Malmesbury Group. The area covered by Fig 1.1 is shaded in the inset map. The boundaries of Fig 1.2 are indicated on Fig 1.1.

The areas on which this investigation is based are situated in the southwestern Tygerberg 'terrane'*. The Klipheuwel fault zone defines its northeastern boundary (cf. Hartnady et al., 1974).

Reasonable unweathered exposures of this terrane are limited to the Tygerberg hills area, and along the Atlantic coast; at the Cape Town suburb of Sea Point, at the towns of Bloubergstrand and Melkbosstrand, and on Robben Island.

Pelitic and semi-pelitic rocks constitute the principal lithological component. Zones of massively-bedded fine-grained greywackes and sandstones are developed, but limestones, conglomerates and volcanics comprise negligible components.

A moderately-developed axial planar cleavage is commonly developed, but is rarely so intense as to obliterate bedding features.

The large-scale structural pattern appears to be relatively simple, comprising a succession of tight, upright, NW-striking synclines and anticlines.

*Note: Although a lithostratigraphic terminology is currently accepted for the subdivision of the Malmesbury (South African Commission for Stratigraphy (SACS), 1980, p.456), use of the term 'formation' obscures the understanding of the role of structural criteria in the subdivision of the Malmesbury (C.J. Hartnady, pers. comm.).
The term 'terrane', defined as

> "..a fault-bounded entity characterized by a distinctive stratigraphic sequence and/or a structural history differing markedly from those of adjoining neighbours"

(Beck et al., 1980) is therefore informally adopted.

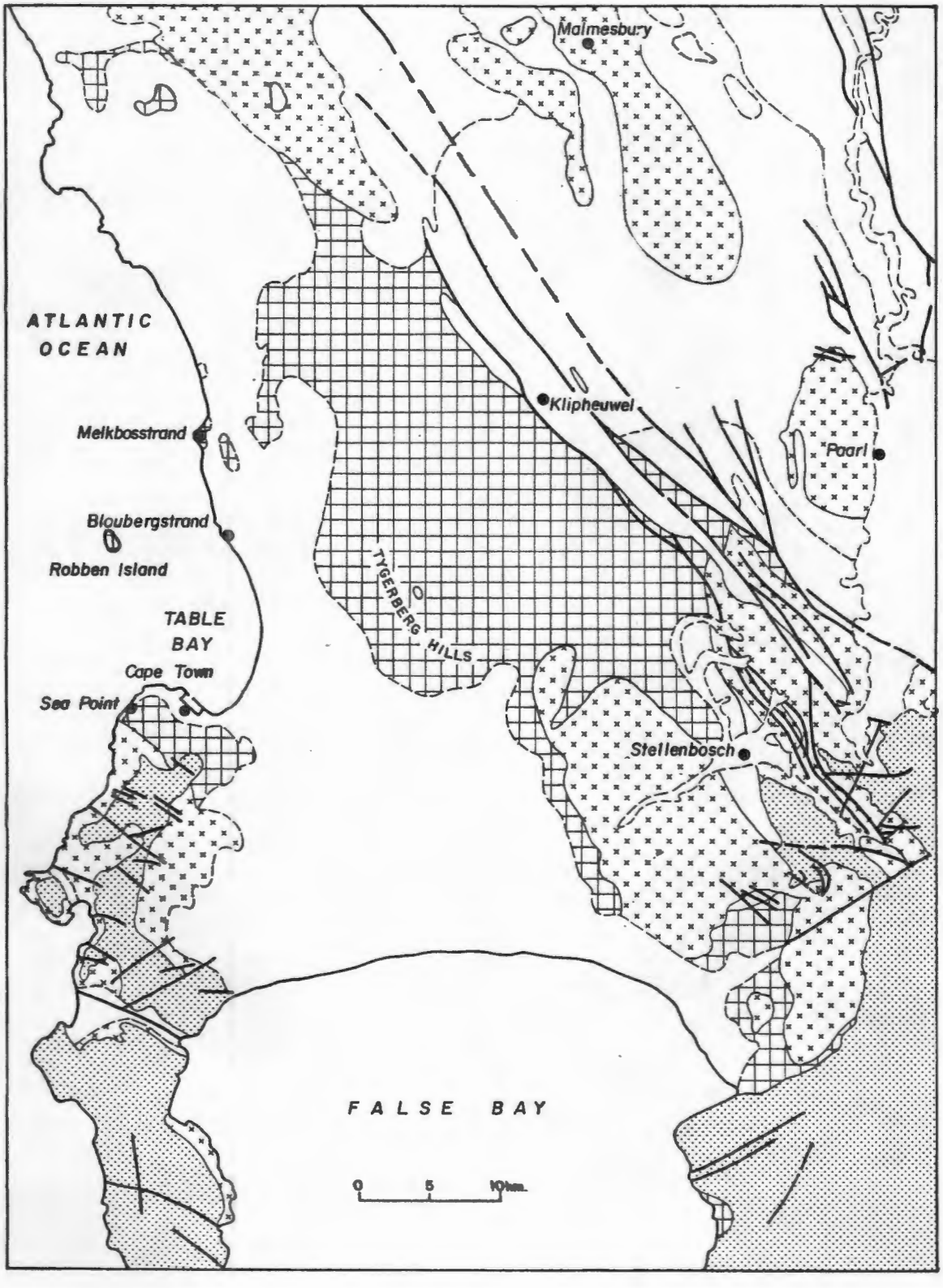

Fig.1.2 Locality map of the Tygerberg terrane.
See Fig.1.1 for legend.

1-2 HISTORICAL REVIEW.

Interest in the Tygerberg terrane appears, in the past, to have been of a somewhat superficial nature, as witnessed by the scarcity of compehensive studies. Concern has focussed largely on its relationship to the adjacent Malmesbury strata and in turn, to the chronological relation of the Malmesbury Group to other Groups (See Hartnady, 1969; SACS, 1980 for reviews).

This lack of attention can be attributed to a number of factors:

a) The general paucity and weathered nature of outcrops;
b) A fairly monotonouos lithology;
c) The lack of known, economically viable, mineral occurences. The rock has been quarried for building material since the seventeenth century. Tin-bearing quartz veins have been worked on a small scale in the Tygerberg Hills;
d) The attraction of unravelling the more complex structural relationships and styles of the adjacent Malmesbury Group formations, as well as of the overlying Cape Fold Belt.

Brief descriptions of the geology of the Tygerberg rocks can be found in most standard textbooks of South African geology (e.g., Rogers & du Toit, 1909; Du Toit, 1954; Haughton, 1969; Truswell, 1977). The area around Cape Town was geologically surveyed by Haughton (1933). Hartnady et al., (1974) proposed that the Tygerberg rocks constitute a tectono-stratigraphically defined domain.

Recently there has been a welcome increase in the number of detailed studies.

These include: a stratigraphical study of the Sea Point exposure (Questiaux, 1978); a metamorphic characterization of this zone (Galloway, 1978); radiometric dating of the Cape Peninsula granite, which gave a concordant U-Pb date of 610±50Ma (Burger & Coertze, 1973), and implies a late Precambrian age for the sediments; an attempted quantification of the deformational effects of this granite emplacement (von Veh, 1980); a detailed structural investigation of the bedrock at, and surrounding the Koeberg nuclear power plant site (see Barker, 1980); and a study of the geology between the Bellville and Agter Paarl areas (de Villiers, 1980).

A major point of current contention concerns the seperation of the Tygerberg terrane from the Swartland Subgroup. De Villiers, in the last-mentioned paper, contests the significance of the northwest striking Klipheuwel fault zone as constituting a major geological boundary (Hartnady et al., 1974), and envisages the Tygerberg rocks to be an integral part of a single, broad anticlinal belt.

Further research into the stratigraphy and structural geometry of the Tygerberg terrane may therefore assist in clarifying its tectonic evolution, relative to that of the adjacent Malmesbury Group rocks.

1-3 PROJECT OBJECTIVES

The underlying objective of this project was to assist in the development and updating of computerised techniques for the quantitative analysis of structural geometry and tectonic strain determination. This opportunity arose through a proposal by the Precambrian Research Unit (PRU) to establish a computer-graphics laboratory to provide the facilities for structural data analysis and modelling. Such tools would provide the stimulus for quantitative digital modelling of deformation kinematics and enable comparison of natural deformation phenomena with experimental models.

The author's tasks were to :

a) refine existing computerised methods of strain determination.
b) implement and adapt acquired computer programmes for drawing cross-sectional profiles.
c) investigate techniques of quantitative fold shape classification.
d) examine ways of graphically displaying stratigraphic columns from field data.

Tasks a) and c) represent a continuation of the writer's earlier work (von Veh, 1980).

Its own intrinsic interest aside, the Tygerberg terrane was treated in this project as it offered suitable examples, close at hand, for the initial testing and application of the above techniques.

The emphasis of the study was placed on the Sea Point and Bloubergstrand stratotypes, since the former contains suitable strain markers as well as 3-dimensional exposure on Signal Hill for drawing cross-sections, and the latter displays abundant minor folding.

With respect to the field work, then, the aims of the project are fairly specific. They are:

a) to investigate the emplacement-related deformation phenomena, encountered in the metasediments, adjacent to the Cape Peninsula pluton.
b) to analyse the sedimentary structures in the Sea Point coastal exposure with the view to obtaining a better insight into the depositional mechanisms and palaeo-environment.
c) to establish a stratigraphic succession at the Bloubergstrand outcrops.
d) to investigate their mesoscopic structural configuration and to attempt a kinematic interpretation of the enigmatic, polyphase folding encountered here.

The above-mentioned areas are, as a result of their separation, treated independently here. Part I is concerned with the pre-Cape rocks in the Northwestern Cape Peninsula. In Part II, the Tygerberg terrane at Bloubergstrand is investigated. The intercorrelation of these outcrops with respect to their tectonic evolution, within the context of a plate tectonic model, is discussed in the conclusions.

The Appendix contains a brief description of the major computer programmes implemented during the course of this work, and a graphic presentation of the sedimentary characteristics of the rocks between Sea Point Pavilion and Three Anchor Bay.

Reference is made throughout the work to applicable computer programmes from which results were obtained, in order to illustrate the nature of their output.

Geological maps of the Sea Point-Mouille Point exposure (Map I) and of the Bloubergstrand outcrops (Map IIA, IIB, IIC) are enclosed.

1-4 ACKNOWLEDGEMENTS

This work was funded by the Precambrian Research Unit.

Sincere thanks and appreciation are extended to Prof. P. Joubert, Director of the Unit, for providing the opportunity to undertake this project; to Dr. C.J. Hartnady, my supervisor, for his guidance and helpful suggestions at all its stages; to Prof. A.R. Duncan, of the Department of Geochemistry, for advice on computer-related matters; to Prof. R. Fisher, of the Department of Land Surveying, for arranging a survey of the Bloubergstrand exposure; to Mrs. R. Kovatz, for kindly drawing maps and diagrams; and to the members of the Precambrian Research Unit, and of the Department of of Geology, for the interest shown in this work.

PART I : THE PRE-CAPE ROCKS OF THE NORTHWESTERN CAPE PENINSULA

2 INTRODUCTION

'The rocks between this plaque and the sea reveal an impressive contact zone of dark slate with pale intrusive granite. This interesting example of contact between a sedimentary and an igneous rock was first recorded by Clarke Abel in 1818. Since its discovery, it has had an inspiring influence on the historical development of geology. Notable among those who have described it is Charles Darwin who visited it in 1836.'

- Inscription of the Historic Monuments Committee on a plaque on the beach front at Saunders Rocks, Sea Point.

2-1 GENERAL

The chief interest of the Tygerberg terrane in the northern Cape Peninsula centres on the contact phenomena displayed by the rocks near and at the junction of the intrusive Cape Peninsula granite pluton. The most classic of the localities at which the contact rocks can be admirably studied is along the foreshore at Sea Point.

The migmatite contact at this locality contains an intimate mixture of granitic lithosomes and hornfelsic palaeosomes having a wavy banded structure.

Descriptions of this zone can be found in Schwarz (1913), Haughton (1933), Scholtz (1946) and Walker & Mathias (1946), amongst others.

A study of the metamorphic effects of the emplacement on the adjacent metasediments was recently undertaken (Galloway, 1978).

In the following chapter, the structural effects of the granite emplacement on them are examined. This is followed, in Chapter 4, by an investigation of the metasediments themselves.

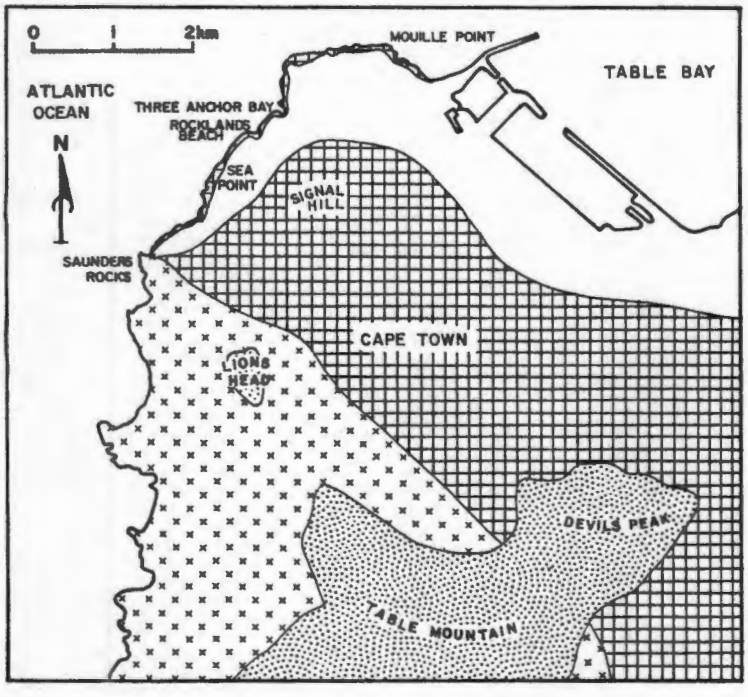

Fig.2.1 Map of the northwestern Cape Peninsula. See Fig.1.1 for legend.

3 TECTONIC ANALYSIS OF THE CAPE PENINSULA PLUTON EMPLACEMENT

3-1 REVIEW OF EMPLACEMENT MECHANISMS

In the last two decades, the study of the tectonics of granite emplacement has flourished due to the development of sophisticated numerical and experimental models and techniques of strain analysis. The general consensus of opinion now is that most granite batholiths are constructed of many separate plutons which were intruded during an extended episodic thermal history.

A popular conception for the emplacement of these plutons is as rising globules of magma or 'diapirs' (Pitcher, 1979). Modelling (cf. Whitehead & Luther, 1975; Ramberg, 1970) has shown that during the initial ascent, the diapir has a bell-shaped form. The base then constricts while the top inflates, the whole taking on a mushroom shape. As the magma rises further, the ductile envelope may close in around the tail of the ascending diapir.

At high levels, as the ductility of the crust decreases and the magma stiffens on cooling, shouldering aside and updoming of the adjacent country rock may occur (Ramsay, 1975; Holder, 1978). This 'piercement' mechanism may culminate in the pluton punching through the crust in the case where there is little overburden to contain its uprise (Pitcher, 1979). Features associated with this forceful mechanism are smoothly concordant contacts, upward drag of the surrounding envelope and radial and concentric fracture patterns in the roof zone.

Alternatively, in some high-level plutons, the magma may remain mobile and the concordant diapirs will then evolve towards angular discordant cauldrons as stoping becomes the dominant means of uprise (Holder, 1978; Pitcher, 1979). Deformational features and thermal recrystallization effects in the country rock will not, in this case, be pronounced.

In the more deep-seated environments, in which the ductility contrast between the pluton and the envelope is small, the piercement mechanism may be modified by the mechanism of radial distension, in which the diapir expands outwards, in pulses, like a balloon, due to the pumping of new magma into its core (Pitcher & Berger, 1972, p.184). In such plutons there is a lack of evidence of upward drag, and strain studies (Ramsay, 1975; Barriere, 1977) identify fabrics of S>L type, in which the strain markers describe pancake ellipsoids involving considerable flattening. This usually results in the production of a schistosity common to the periphery of the pluton and the envelope.

3-2 BACKGROUND AND PRESENT WORK

Recent structural mapping and geochemical analysis on some of the Cape granite batholiths (Schoch et al., 1977), has revealed that they too are comprised of a number of individual plutons, and geochronological studies (Schoch et al., 1975) indicate that their emplacement occurred over an extended period from 630 Ma to about 500 Ma, and was probably of an episodic nature.

Little is known, however, about the tectonics of their emplacement.

Scholtz (1946) considered that they were emplaced along the cores of asymmetrical anticlines in the Malmesbury metasediments during the close of the period in which the latter were deformed.

The question of whether the emplacement was of a forceful diapiric nature, by pushing the country rock aside and upward, or whether the plutons intruded by the 'permissive' mechanisms of stoping and cauldron subsidence, or whether the mechanism of radial distension played a role, has not been satisfactorily resolved.

Read (1951) appears to favour the first mechanism, since, in his view, the Cape granites were emplaced as 'nearly solid masses by softening up the country rocks around them' (op.cit. p.7). Boocock (1956) on the other hand, envisages that 'the granitic material rose along ruptures in the sediments and stoped off large blocks of the country rocks' (op.cit. p.254).

Pitcher and Berger (1972, p.169) have, amongst others, remarked that the mechanism of emplacement of granitic bodies is more often to be determined from the structures of the adjacent country rock than from the granite itself.

Metamorphic and structural studies of the metasediments adjacent to the northern contact of the Cape Peninsula pluton were recently undertaken by Galloway (1978) and Questiaux (1978).

The following contact metamorphic characteristics were recognized: At ~2500 m from the contact, chlorite spots, about 1 mm in diameter, appear, together with a pale biotite. At ~900 m, the incoming of slightly larger cordierite porphyroblasts, and a gradual reddening of the biotite, is accompanied by the disappearance of the chlorite spots. Within 300 m of the contact, the rock becomes completely reconstituted to a K-feldspar-bearing cordierite hornfels.

The metasediments here are folded into a large-scale asymmetrical synclinal fold. Galloway (1978) recognized evidence for a late flattening of the fold adjacent to the granite contact from the ellipsoidal shapes of the metamorphic spots.

Since the Tygerberg formation is generally devoid of structures indicative of a late phase of compression this phenomenon would appear to be emplacement-related.

The aim of this investigation was to provide quantitative data on the deformation recorded by the spots, to thereby investigate its origin and nature, and its effects on the surrounding country rock and to see what information could be gleaned about the mode of granite emplacement.

3-3 METHODS OF STRAIN ANALYSIS EMPLOYED

As far as possible, sampling was undertaken at regular intervals, to examine the regional strain variation. This objective was hampered by inaccessibility, soil cover and lack of porphyroblast development. North-west of Three Anchor Bay no spotting was encountered. Samples clearly displaying the relationship between bedding plane and foliation were preferentially chosen.

The samples were slabbed along orthogonal planes parallel to foliation, lineation and at right angles to both. These directions were assumed to approximate the principal planes of strain.

Due to poor discernibility, small size and wide dispersion of the markers, within samples, numerous methods for estimating their long and short axes were tested. Direct tracings of rock slabs, projected through an Epidioscope, proved to be the most most efficient method, above that of photomicrographs or tracings from slides or thin-sections or rock slabs.

The ratios of the markers' long axes short axes (Rf) and the angular relationships (ϕ_f) of the long axes relative to a coordinate axis system (Fig.3.1) were measured and stored on a computer data file (programme RPHIN), in order to undertake the various computerized methods of strain determination.

$$R_f = \frac{AA'}{BB'}$$

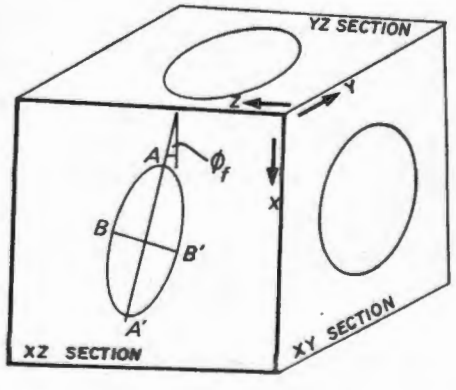

Fig.3.1 Illustration of a rock sample coordinate axis system.

The THETA programme (Peach & Lisle,1979), based on the 'Theta-Curve' method of Lisle (1977), calculates the strain ratio by determining the reciprocal strain ratio needed to produce a statistically random marker orientation (by using the X^2 test).

For the case where the strained markers have non-random fabrics in the unstrained state, the STRANE programme is applicable. This programme also employs the above-mentioned unstraining technique, except that the strain ratio is taken to represent the stage where the orientation of the vector mean of the $\emptyset_f$ values becomes equal to the orientation of the bedding trace for bedding-symmetric unstrained fabrics. For imbricate initial fabrics, the strain ratio is taken to represent the stage where the symmetry of a plot of Rf against $\emptyset_f$ is maximised. Due to recent questioning of the validity of this programme in the literature (de Poar, 1980,1981; Seymour & Boulter, 1979), extensive use was not made thereof.

For combining the measurements of the three orthogonal faces, to yield an average ellipsoid, a method recently developed by Oertel (1978) and Miller and Oertel (1979) (programme STRDET) was employed.

For each orthogonal, but otherwise arbitrarily oriented face, an average ellipse is defined and resultant redundancies in combining the ellipses are reconciled by distributing the error.

If the strain through the sampled volume is inhomogeneous, corrective rotations are applied to the faces (Hildebrandt-Mittlefehldt & Oertel, 1980).

3-4 RESULTS

3-4-1 2-dimensional results

The results from the 'Theta-Curve' method for the XZ section (the face normal to cleavage/parallel to lineation) of samples collected from the Sea Point exposure by the present and by previous workers are plotted in order of increasing distance from the granite contact in Fig.3.2.

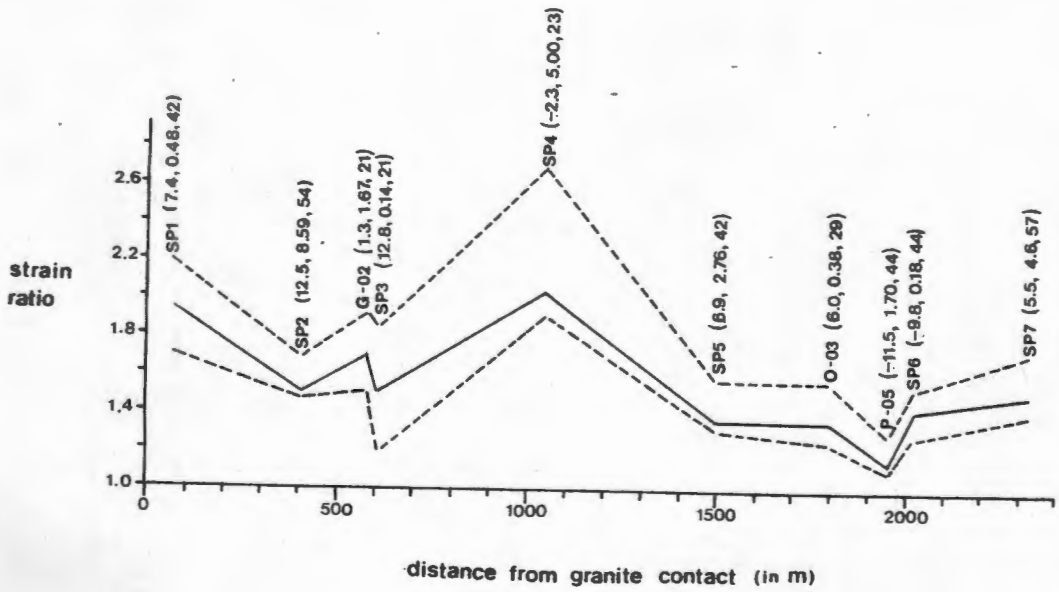

Fig.3.2 Results from the 'Theta-Curve' fitting procedure for XZ sections (THETA programme).
Solid line - Best-fit strain ratio.
Dotted lines - Range of acceptable strain values using a 95% level of confidence (90% for samples SP2 and SP4).
The bracketed values after the sample identification refer to i) vector mean of ϕ_f relative to cleavage trace, ii) the lowest Chi- squared values for 2 degrees of freedom corresponding to the best-fit strain ratio, and iii) the number of samples respectively.

A wide fluctuation of 'best-fitting' strain values, from 1.15 to 2.03 is evident for the XZ sections. A trend of increasing deformation towards the granite contact is however indicated.

3-4-2 3-dimensional results

The results from the STRDET programme for combining measurements of the three faces to yield an average ellipsoid are shown in Figs. 3.3, 3.4 and 3.5.

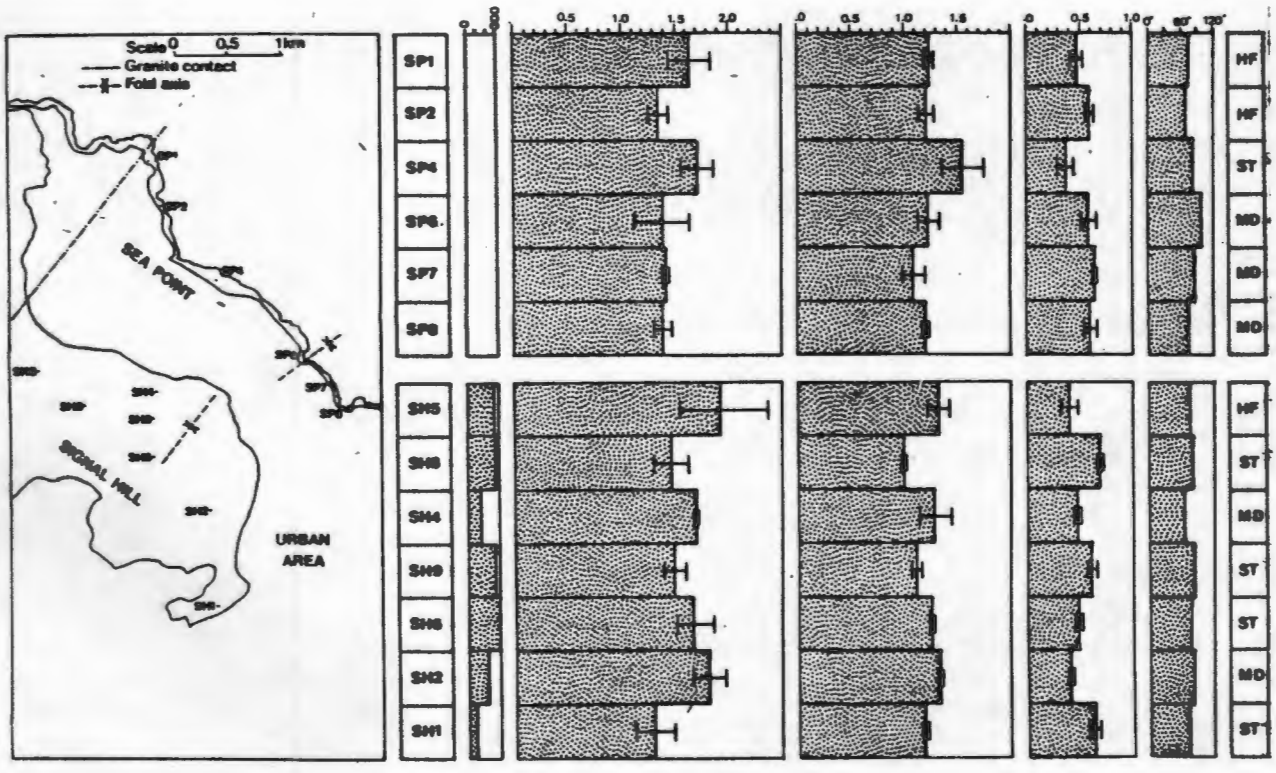

Fig.3.3 Three dimensional finite strain values from the Signal Hill and Sea Point exposures (programme STRDET). The columns below the locality map represent sample identification, station elevation (A.M.S.L), maximum, intermediate and minimum quadratic elongations, principal plane dips and rock type respectively. Principal plane dips are measured relative to a northwesterly strike. The standard errors of the quadratic elongations are bracketed.
Rock types : ST - siltstone, MD - mudstone, HF - hornfels.

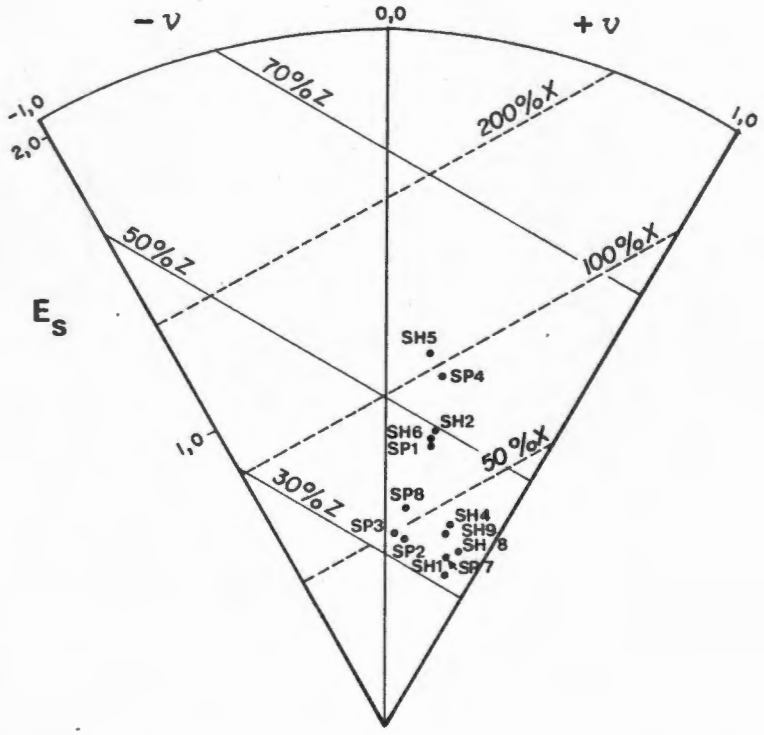

Fig.3.4 Plot of Lode's parameter v and natural logarithmic strain Es.

$$v = \frac{2E2 - (E1 + E3)}{E1 - E3}$$ (Hossack, 1968)

where E1 = ln (1+e1), etc.,
E1 > E2 > E3 and e = $(l - l_o)/l$
where l = length after and l_o = length before strain.

Coward and James (1974) have noted that this parameter provided a range of values (+1 = flattening to -1 = constriction) which are symmetric with respect to the value of plane strain (v = 0).

Natural logarithmic strain or strain magnitude is defined by Nadai (1968) as:

$$Es = 1/\sqrt{3}[(E1-E2)^2 + (E2-E3)^2 + (E3-E1)^2]$$

Parameters are output from programme STRDET.

The deformation is clearly of a flattening type with the strain markers describing oblate ellipsoids (Fig.3.3). As strain magnitudes increase the deformation approaches the plane strain type (Fig.3.4). The trend of increasing strain values towards the contact is also indicated from these figures. This conclusion is supported by the increasing degree of 'drape-around' foliation around spots as the contact is approached (Fig.3.7).

The effect of the elevation on strain variability is uncertain. Although samples SH4 and SH2, at low topographic levels show fairly high strain values, this correlation does not hold for sample SH1 or the Sea point data (Fig.3.3).

Sample position within the fold appears to have a negligible influence, since the strain value of sample SP6, taken from the hinge zone at Rocklands beach, does not differ significantly from that of other samples.

Finding regularities in the data on the basis of criteria other than geographic ones, such as rock types or local stress is equally problematical.

The influence of the rheological properties of the host rock on the strain perturbations is evidenced here by the common presence of tension gashes perpendicular to bedding, in competent horizons. The trend of increasing deformation towards the contact may be partly obscured by the comparatively higher strain values which the incompetent rock samples would record.

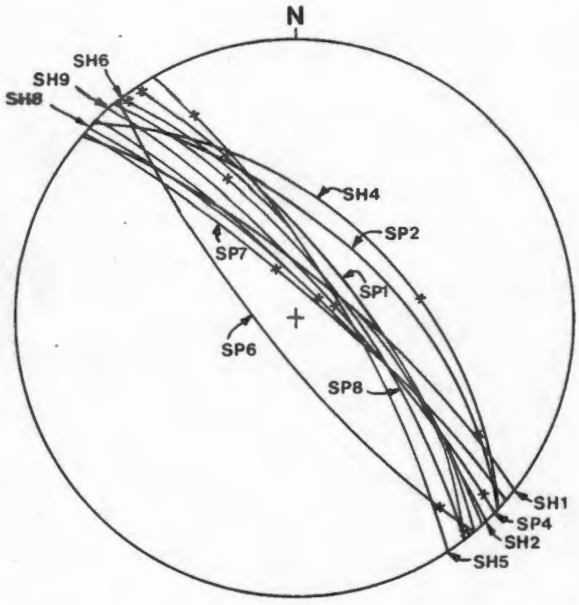

Fig.3.5 Stereogram on which the attitude of the XY plane, as a great circle, and the X - direction, as a cross, have been marked. Output from programme STRDET.

The pitch of the maximum principal axis of the strain ellipsoid (X-axis) in the principal (XY) plane is variable, although frequently sub-horizontal. The XY-plane usually dips in a NE direction, parallel to the dip of the granite contact.

3-4-3 Discussion

Evidence commonly cited that the age of emplacement was late, relative to the ~600 Ma orogenic episode, is the parallel elongation of the Cape granites to the structural trend of the Malmesbury Group, the concordant contacts and the lack of foliation in the intrusive granites (Truswell, 1977). Since prolate prolate ('cigar'-shaped) fabric ellipsoids commonly develop in fold hinges (Ramsay, 1967, p. 220), the oblate ('pancake'-shaped) nature of sample SP6, taken from the hinge zone, supports this conclusion.

The deformation recorded by the markers is then either associated with the waning regional stresses during the close of this episode, or it is the result of the forceful emplacement of the granite pluton.

A positive correlation between the size of the strain markers and the amounts of strain recorded by them, as noted in some samples (von Veh, 1980), would be expected if their deformation was contemporaneous with their growth, and hence, with granite emplacement.

The NE principal plane dip of the strain ellipsoid parallel to the dip of the granite contact suggests that the strain axes associated with the emplacement were non-coaxial to those associated with the main phase of folding.

Further evidence for this suggestion comes from the presence of relict inclusion fabrics in the porphyroblasts, with discontinuous fabric relationships to the matrix (Galloway, 1978).

A possible interpretation for this phenomenon is that during the early stages of emplacement, the porphyroblasts overgrew the pre-existing foliation and as the emplacement progressed, its deformational effects became more prominent, resulting in deformation of the porphyroblasts and draping of the foliation around them.

The existence of a pre-emplacement cleavage is indicated by foliated xenoliths in the migmatitic margin of the granite, as well as by the occasional development of chlorite stringers in siltstone horizons. The stringers generally have a steep southwesterly dip and when this feature is well-developed, differential weathering on exposed bedding planes results in undulations reminiscient of ripple marking.

In both limbs of the fold, as well as in the overturned beds, south of the Sea Point Pavilion, the later foliation, when not constrained to mimic bedding, has a moderate northeasterly vergence. This feature is well displayed in cuttings on the Signal Hill drive.

A late-stage 'overprinting' or 'foliation-rotation' origin for this foliation , as opposed to an axial planar origin, is therefore implied.

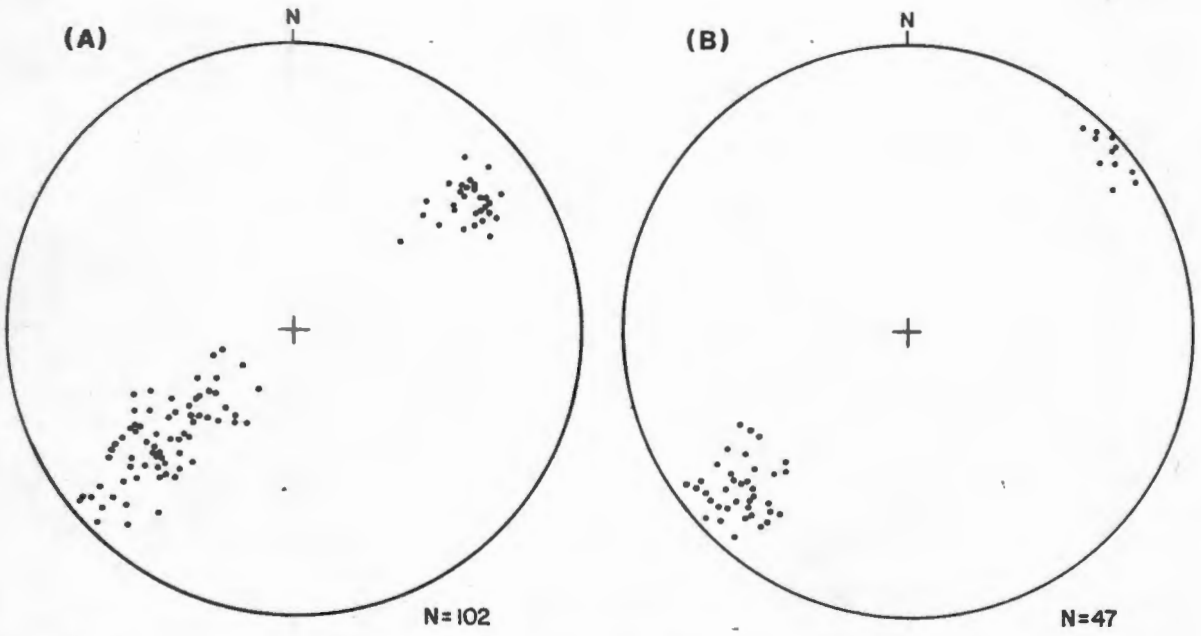

Fig.3.6 Synoptic diagrams of A) poles to bedding and B) poles to foliation, in the Sea Point - Signal Hill area.

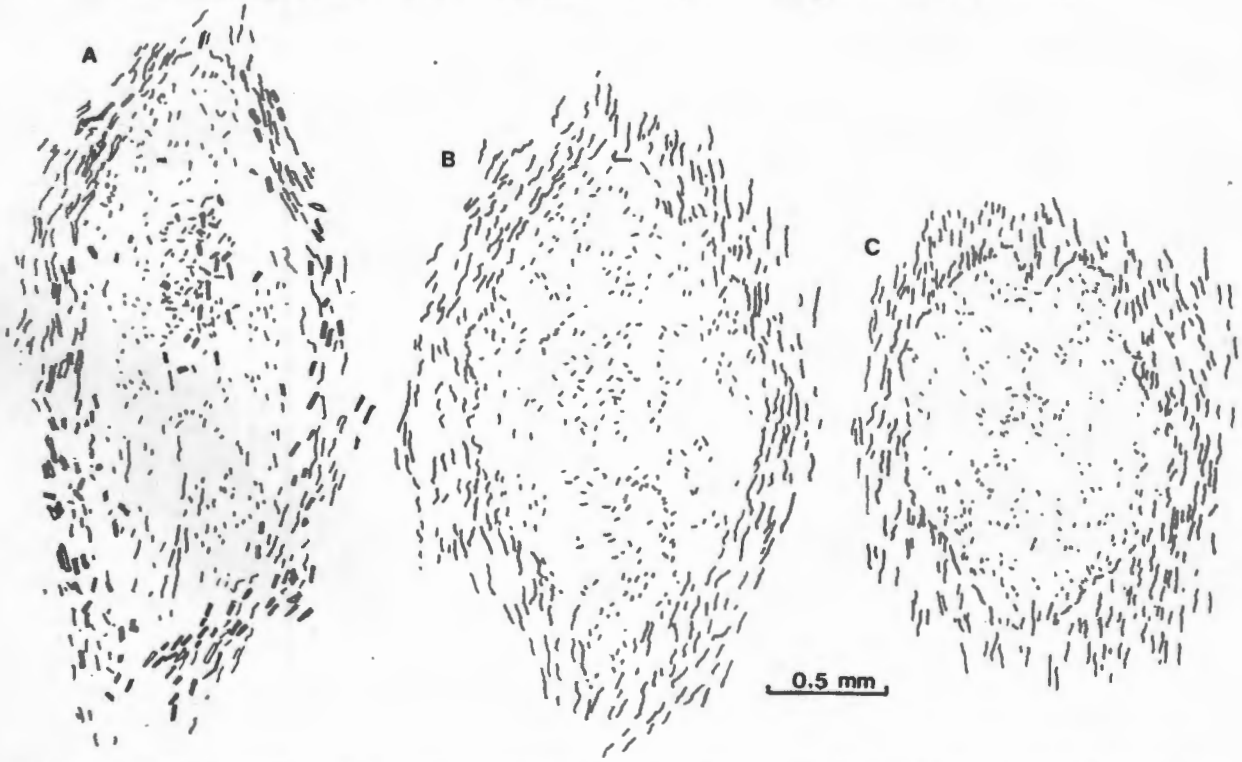

Fig.3.7 Drawings from thin-sections showing the degrees of wrap-around foliation around porphyroblasts. Samples are taken from the Sea Point exposure at approximate distances of 300 m, 900 m and 1500 m from the contact respectively. Note the decrease in the sizes of the porphyroblasts and the randomly oriented inclusion fabrics in the cores.

3-5 ASSESSMENT OF VALIDITY OF RESULTS

A number of assumptions are embodied in the strain analysis technique described above:

a) The particles initially approximated to ellipsoidal shapes.
b) No ductility contrast was present between the particles and the matrix.
c) On the scale of each specimen, the deformation was homogeneous.
d) The initial fabric was random.

No gross divergence from initial ellipsoidal shapes is suspected, since cordierite crystals have orthorhombic to pseudohexagonal forms and chlorite crystals have monoclinic to pseudohexagonal forms.

The assumption, that the markers record the same finite strain as the matrix, is less likely, as the matrix is commonly seen to deflect around the spots (See Fig.3.7). The strain estimates must therefore be regarded as minimum values.

A quantification of this ductility contrast was afforded by the presence of ptygmatically folded pegmatitic veins (Fig.3.8). Although a regional trend of increasing degree of folding of these veins, towards the contact is suggested in the field, the veins at Rocklands beach being virtually planar, a common close association of veins of varying intensities of folding points to a prolonged history of vein formation during deformation.

Strain determination from such markers is accomplished by measuring the arc length/wave length ratios and the orientation of the wavelength lines of two or more veins of differing orientations. A strain estimate can then be made through use of the Mohr construction (see Ramsay, 1967, p.250).

A strain estimate in the vicinity of specimen SP3, yielded an internally consistent strain ratio of 1.95/1, excluding ductile compression, perpendicular to the foliation. SP3 has a strain ratio of 1.52/1. If both strain markers originated from the granite emplacement, a minimum of 30% strain underestimation from the spotting is implied.

Fig.3.8 Ptygmatic quartz veins at a high angle to foliation. Locality : Below Sea Point swimming pool, viewed to the west.

According to Lisle (1977), the goodness of fit of the data to the third and fourth assumptions above, namely for the model of 'homogeneous deformation of random markers' assumption, can be tested for, from the calculated value of Chi-square (X^2) corresponding to the best-fit strain ratio (programme THETA).

Since the X^2 values (5.99 for less than 50 markers and 15.51 for more than 50 markers (Lisle, 1977)), are more than all the X^2 values in this figure, the undeformed orientations of all samples have a 95% statistical chance of coming from a normal (random) distribution. The data therefore compares well with this model of deformation.

Further evidence for this mechanism comes from the close coincidence of the vector mean of ϕ to the cleavage trace (Fig.3.2), symmetric Rf/ϕ diagrams and microscopic shape homogeneity.

3-7 EFFECTS OF EMPLACEMENT

3-7-1 Introduction

A method recently developed by Charlesworth et al (1976), for obtaining computerized cross-sections, was employed to reconstruct the 'pre-emplacement' configuration of the 'Rocklands' synclinal fold, adjacent to the granite contact at Sea Point, and to thereby illustrate the effects of the tectonic strain on it.

3-7-2 Method employed

The cross-sections are constructed by projecting selected points on a folded surface parallel to their fold axis onto the plane of section and by representing the pitch of their trace on the plane of section, by a short line.

A necessary condition for plotting such 'down-plunge' projections is that the structural domain has to be shown to be statistically cylindrical.

The procedure which has to be followed is outlined below:

a) The area is manually divided into subareas within which folding appears to be cylindrical, and the best-fitting fold axis in each subarea is calculated;
b) The cylindricity of the folds in each subarea is statistically tested and the subareas are further subdivided or grouped on the basis of the tests;
c) The boundaries between subareas are located more precisely by calculating the deviations from cylindricity at each outcrop for each subarea;
d) Profiles are prepared for each subarea;
e) A composite plot for the entire area is obtained by rotating the subareas so that their fold axes coincide.

[1] The Null hypothesis of Coplanarity of s-poles is rejected with confidence $1-\alpha$ if $K\lambda_3 > \chi^2_{p-2}(\alpha)$ where $\chi^2_{p-2}(\alpha)$ is the upper 100α percentile point of the χ^2 distribution with p-2 degrees of freedom. K is the concentration parameter measuring roughness and error and is determined by taking repeated measurements of the s-pole at a number of outcrops. λ_3 is the smallest eigenvalue of a matrix T of direction cosines of poles to the folded surface (Watson, 1965).
[2] The Null hypothesis of Coaxiality is rejected with confidence $1-\alpha$ if $(p-4)(\lambda_3 - \lambda_3 a - \lambda_3 b)/2(\lambda_3 a + \lambda_3 b) > F_{2,p-4}(\alpha)$ where λ_3, $\lambda_3 a$ and $\lambda_3 b$ are the smallest eigenvalues of the matrix T for the whole fold and for segments a and b respectively, and where $F_{2,p-4}(\alpha)$ is the upper 100α percentage point of the F distribution with 2 and p-4 degrees of freedom (Charlesworth et al., 1976, eqn. 10).
[3] The Null hypothesis of Equal Scatter is rejected with confidence $1-\alpha$, if $(p_b-2)\lambda_3 a/(p_a-2)\lambda_3 b > F_{p_a-2, p_b-2}(\alpha/2)$, where p_a and p_b are the number of measurements in segments a and b respectively (Charlesworth et al., 1976, eqn. 11).

Statistical tests used for establishing domains of cylindricity.

3-7-3 Application of the method

In order to illustrate the application of this procedure, the method which was followed for the Sea Point - Signal Hill area (Fig.3.9) is detailed below:

Throughout the area, a number of bedding orientation readings were taken at intervals and the Null hypothesis of coplanarity (cylindricity) was tested for (test [1]).

A concentration parameter K value of 103.45 was obtained using 5 bedding orientation measurements from 15 stations (programme MEANS). This fairly high value indicates a low roughness and instrument error.

For 102 s-pole readings, taken over the entire area, a λ_3 value of 1.419 was derived at, using programme CYLTEST.

Since $K\lambda_3 = 146.80$ is more than $\chi^2_{100}(0,05) = 124.34$ (from tables), the Null hypothesis of coplanarity (cylindricity) is rejected.

Since non-cylindricity may be attributed to uncertainty over the value of K, or to large scale roughness features (Charlesworth et al., 1976), clustering of s-poles in segments of a fold, about planes with the same orientation can be tested for (test [2]).

For this test of 'coaxiality' to be valid, the segments must be shown to be cylindrical (using test [1] again, for each segment) and the scatter of measured s-poles in one segment must be the same as in the other (test [3]).

The area was consequently divided into western and eastern subareas, comprising the Sea Point and Signal Hill exposures respectively.

The λ_3 values of T for the two domains were found to be 0.4563 (p=56) and 0.7007 (p=46) respectively.

Since a K value of 108.15 was obtained for the former segment and since $\chi^2_{54}(0.05) = 72.15$ is greater than $K\lambda_3 = 49.35$, the Null hypothesis of coplanarity cannot be rejected for the Sea Point segment.

A K value of 95.24 was obtained for the Signal Hill area, and although the $\chi^2_{44}(0.05) = 60.48$ is less than $K\lambda_3 = 66.73$, the margin of rejection is not considered to be significant due to creep effects and local overturning.

The condition of equal scatter is also met, since the value of the test statistic in [3] is 0.531 is less than $F_{54,44}(0,025) = 1.758$.

Although the conditions for the Null hypothesis of coaxiality are satisfied, this test is rejected since the test statistic in [2] has a value of 11.113 which is more than $F_{2,98}(0,05) = 3.093$.

It is therefore concluded that the segments, but not the whole 'Rocklands' synclinal fold, may be regarded as cylindrical.

The drawing of profiles for the two subareas is therefore justified and a composite profile can then be obtained.

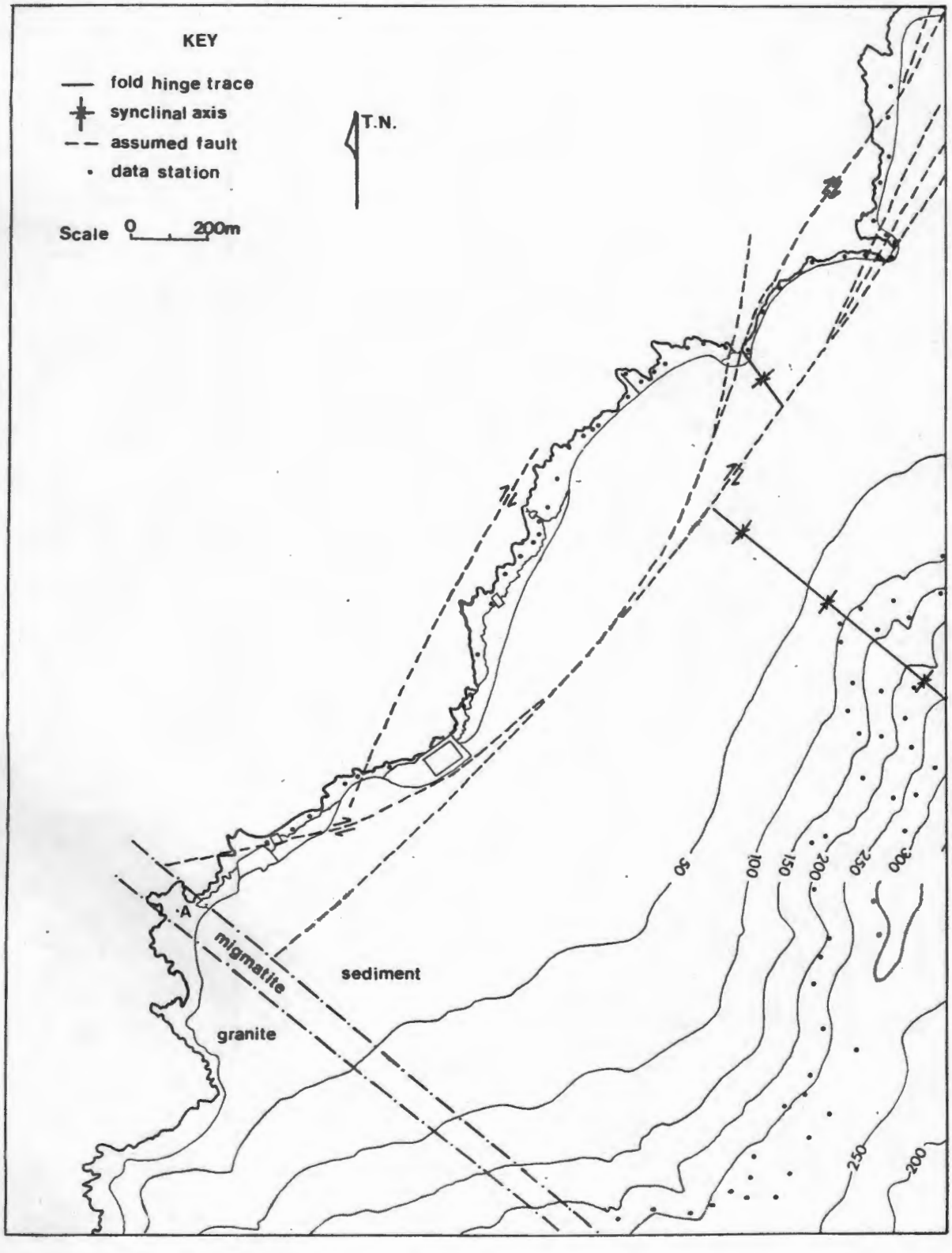

Fig.3.9 Map of the northeastern Cape Peninsula, showing the positions of the fold axis, major faults and the granite contact. The locations of the data stations are represented by dots.

3-7-4 A cross-sectional reconstruction

The drawing of a profile as it looked prior to granite emplacement involved:
a) removing the components of dextral shear in the area (see Fig.3.9);
b) removing the flattening component associated with the emplacement.

Questiaux (1978) noted the dextral displacement and rotation of the axial trace from Signal Hill to Sea Point. Strike slip displacement is in the order of 240 m. A rotation of the fold axis from a trend and plunge of 316°/04° NW for the Signal Hill data to 142°/02° SE for the Sea Point data was determined (programme CYLTEST).

The change in orientation of the fold axis accounts for a 'ductile' shear displacement of 100 m. A further 15 m displacement can be ascribed to the effect of a northeasterly-dipping axial plane (320°/84° NE). The remaining 125 m offset is attributed to 'brittle' shearing between the Sea Point and Signal Hill outcrops.

Evidence for this dextral brittle shear displacement can be seen from the numerous NS - striking, right-lateral faults that are encountered along the coastal exposure (Map I). Dextral faulting is particularly apparent at Three Anchor Bay. Major, silicified breccia zones can be seen at Rocklands Beach and at Green Point.

The parallelism of aplite dykes in the vicinity of the contact, to the fault trend, the lack of displacement of the granite contact between Sea Point and Signal Hill and the silicification of fault breccia suggests a pre- to syn-emplacement age for the faulting.

Figs.3.10 A-E illustrate the nature of the output from the programme SECT5 for drawing cross-sectional profiles.

Figs.3.10 A and B are 'present-day' views of the plane which contains the normal to the fold axis for the Signal Hill and Sea Point subareas respectively. The pitch of the bedding of each data station on these planes is represented by a short line. Prominent clastic unit outcrops are denoted by the letter s.

The profile in the upper part of Fig.3.10 C is the same as in Fig.3.10 A, but in the lower part the Sea Point orientation data have been rotated about a point mid-way between the two areas, so that their fold axis coincides with the Signal Hill fold axis (programme DOMROT). The ductile component of the dextral shear is thereby removed. The effect of this rotation is to change both the position and the orientation of the Sea Point bedding data.

In Fig.3.10 D, the 125 m brittle shear displacement, which is shown in Fig.3.10 C, is also removed. The axial traces of the two subareas are now alligned. The fold asymmetry is clearly apparent. An overall uniformity of limb dip is evident in the more steeply dipping northeastern limb. The southwestern limb displays a greater variability in dip. As the granite contact is approached, the bedding becomes steepened and even overturned.

Removal of the effects of the component of flattening associated with emplacement was undertaken in two stages:

a) removing the effects of rotation of material particles associated with the deformation;
b) restoring the positions of the material points from the deformed to the undeformed state.

The first stage was tackled by manually interpolating the strain values of Fig.3.3 between neighbouring measurements and unstraining the bedding orientation data perpendicular to foliation (programme DEFORM). The axis of greatest elongation was assumed to be the cleavage dip line. An alternative orientation within the principal plane would have a minimal effect on the unstrained bedding attitude due to the uniaxial character of the strain ellipsoid.

For the second stage, the reciprocal mean strain value for the XZ sections for the area was used to map the data points into their initial, undeformed positions. The resultant profile is shown in Fig.3.10 E.

Fig.3.10 E does not represent a reconstruction of the pre-deformational configuration of the domain as such; it merely illustrates the degree of rotation and translation of the bedding data associated with the strain imprint. Reconstituting the profile would require the unstraining of homogeneous subdomains and imparting rigid translations and rotations to the subdomains in a manner that would minimize continuity violation (Cobbold, 1979; Oertel, 1981).

By comparing this profile to Fig.3.10 D, it can be seen that the effect of unstraining the profile is quite pronounced.

The phenomenon of the the overturned bedding South of the Sea Point Pavilion is accentuated, implying the existence of an anticlinal structure here.

The correlation of the major sandstone units between the two areas is poor, although this may in part be due to dip-slip faulting between the two areas.

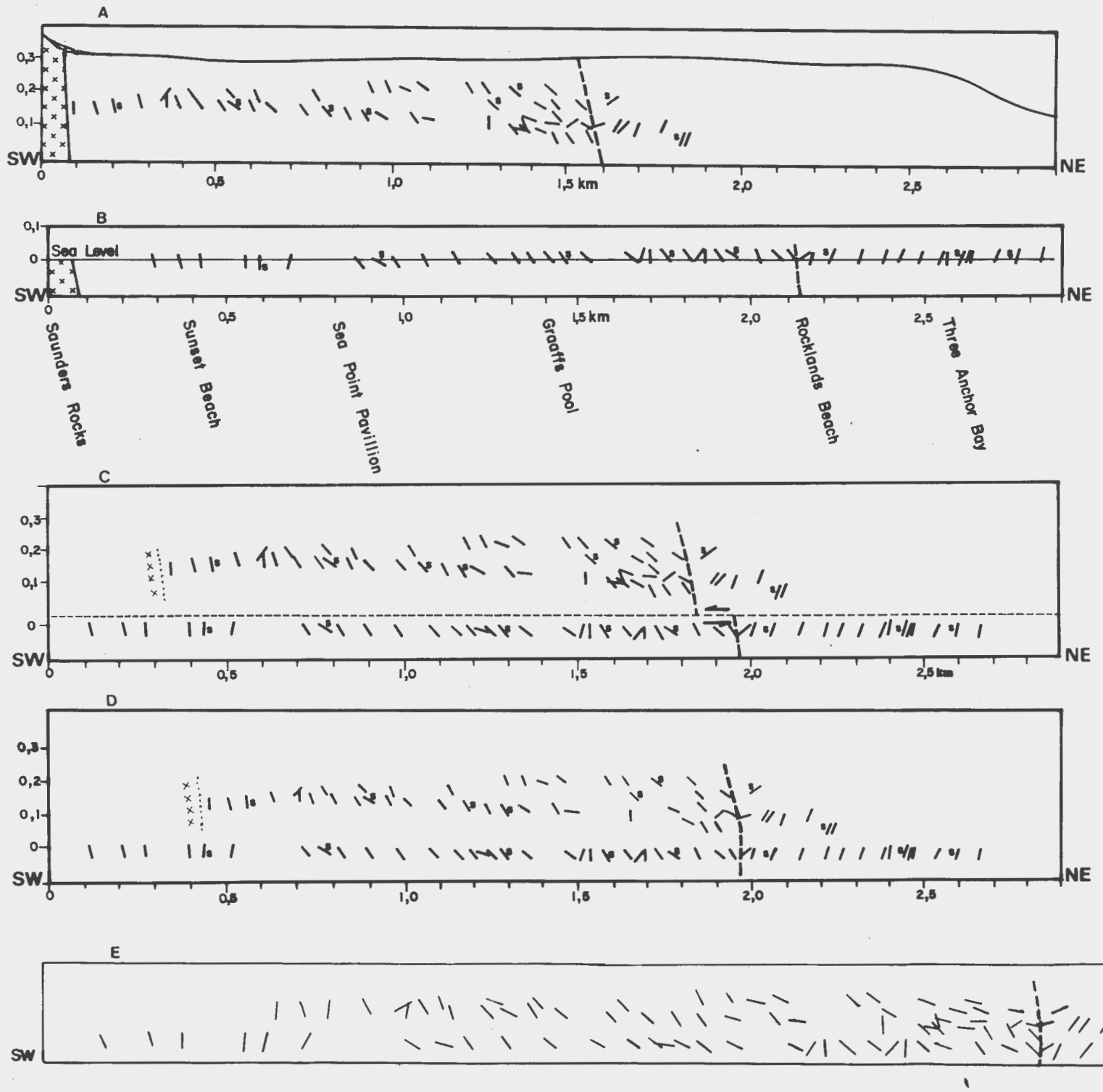

Fig.3.10 Computerised cross-sectional profiles of:
A) the 'present-day' Signal Hill subarea;
B) the 'present-day' Sea Point subarea;
C) the 'pre-ductile shear' configuration of the area (obtained by 'rotating' the data for the Sea Point subarea (in Fig.3.10 B) so that their fold axis coincides with the fold axis for the Signal Hill subarea);
D) the 'pre-ductile and pre-brittle shear' configuration of the area (obtained by removal of the brittle shear displacement in Fig.3.10 C);
E) the 'pre-ductile and pre-brittle shear and pre-flattening' configuration of the area (obtained by removal of the components of flattening from Fig.3.10 D).
The profiles are viewed from the SE towards the NW.
The profile of Signal Hill, the granite contact and the fold axis have been drawn in by hand.

X - axis Distance from beacon at Saunders Rocks (in km.).
Y - axis Elevation above mean sea level (in km.).

3-8 DISCUSSION

The features of the Cape Peninsula pluton and the surrounding rock are such that, on the available evidence, an unequivocal choice between the emplacement mechanisms, as described in the introduction, cannot be made.

The considerable flattening displayed by the strain markers favours the mechanism of radial distension, or 'ballooning' of the pluton.

The forceful or 'piercement' mechanism of emplacement, on the other hand, is favoured by the evidence for steepening and overturning of bedding as the contact is approached, as well as by the faulting in the aureole.

The abundance of inclusions in the granite body, the lack of foliation in its periphery, and its slightly discordant relation to the country rock, could even be used as criteria to support a 'permissive' mechanism of emplacement by stoping.

Since the form of the intrusion is determined by the ductility contrast between the magma and the country rock, and hence by depth in the crust, it may be possible that during the regional deformation, when the ductility contrasts were low, the mechanisms of diapirism and radial distension prevailed, and that during the waning stages, as the ductility contrasts increased, the mechanism of stoping became predominant.

4 AN ANALYSIS OF THE FLYSCH-TYPE SEDIMENTATION IN THE SEA POINT COASTAL EXPOSURE

4-1 INTRODUCTION

4-1-1 Background

Since the milestone paper of Kuenen and Migliorini (1950), which showed that the graded sandstone facies in flysch deposits originated from turbidity currents, the turbidite facies has been intensely studied. As a result, there is extensive general agreement as to the characteristics of a classic turbidite. These are:

a) Erosional markings associated with a sharp base of each sandstone bed.
b) A covering pelitic layer on top of each sandstone.
c) A good bedding regularity.
d) A suite of internal sedimentary structures within each sandstone bed.

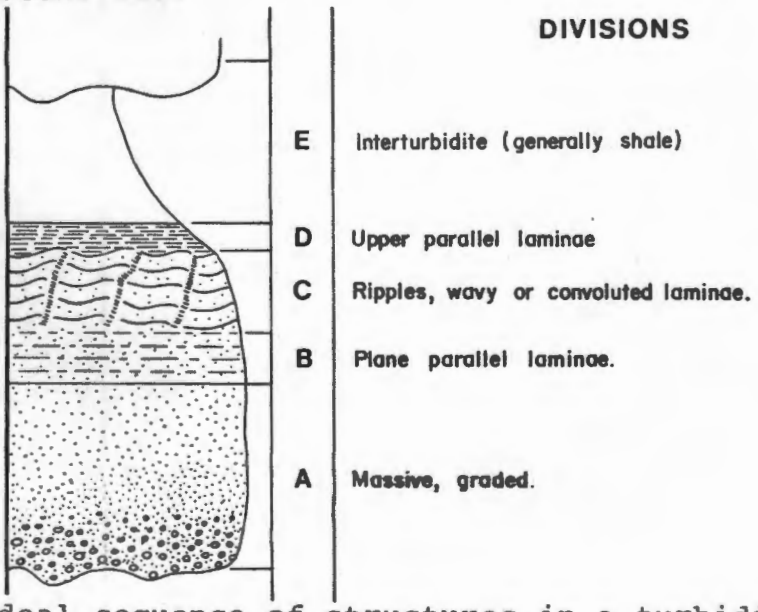

Fig.4.1 Ideal sequence of structures in a turbidite bed. After Bouma (1962).

The recognition that lower or upper intervals of the suite may be missing led to the concept of turbidite 'proximality' (Walker, 1967), whereby bed-thickness and grain-size were assumed to be indicators of relative distance from source. This simple approach was challenged by the development of genetic models of facies associations. It was recognised that thin-bedded facies can be deposited in several depositional environments (Mutti, 1977).

The two depositional models, which evolved from the studies of both ancient and modern deposits, are the lobe-type fan model (Mutti & Ricci-Lucchi, 1972) and the suprafan-type fan model (Normark, 1978; Walker, 1978). These two 'end-member' models reflect different supply-dispersal systems and basin settings. Sand-efficient depositional systems result in unchannelized, low relief sand lobes, whereas inefficient systems build channelized sand bodies, as found in the suprafan of modern fans.

The two models may account for the conflicting evidence concerning the the extent of continuity of individual turbidites. Successful correlations of beds have been documented in the order of 100 kilometers (Hesse, 1974; Hoyt & Fox, 1977), whereas other attempts to correlate turbidites for more than a few kilometers have failed (Enos, 1969; Skipper & Middleton, 1975).

Ancient turbiditic deposits generally display notable thicknesses and a uniformity in stratification (Reineck & Singh, 1973, p.386). Sedimentary structures indicate, however, that the depositional processes were similar to those operating today (Kuenen, 1964). The oldest assemblage of greywackes known, which have been interpreted as turbidites (Kuenen, 1963), is found in the Northern facies tract of the Figtree Group, Swaziland Supergroup. Other examples of southern African, Precambrian deposits of a turbiditic nature are to be found in the eugeosynclinal trough of the Gariep Province (Kroner, 1974), in the Khomas and Kaoko troughs of the Damara Province (Porada & Wittig, 1976; Guj, 1970) and in the pre-Cape rocks of the Kango Group (Le Roux, 1977), the Kaaimans Group (Gresse, 1976) and the Malmesbury Group (Hartnady et al., 1974). All of these examples are found in Pan-African orogenic provinces.

4-1-2 This work

The flysch-type sediments of the Tygerberg terrane at the Sea Point coastal exposure, are of particular interest, since, unlike many of the above-mentioned examples, they are unweathered, well-exposed, and have only been subjected to a low grade of metamorphism and a low intensity of deformation. Due to the folding of the sediments into a large-scale syncline, an almost continuous 4km-long strip is now exposed along the coast.

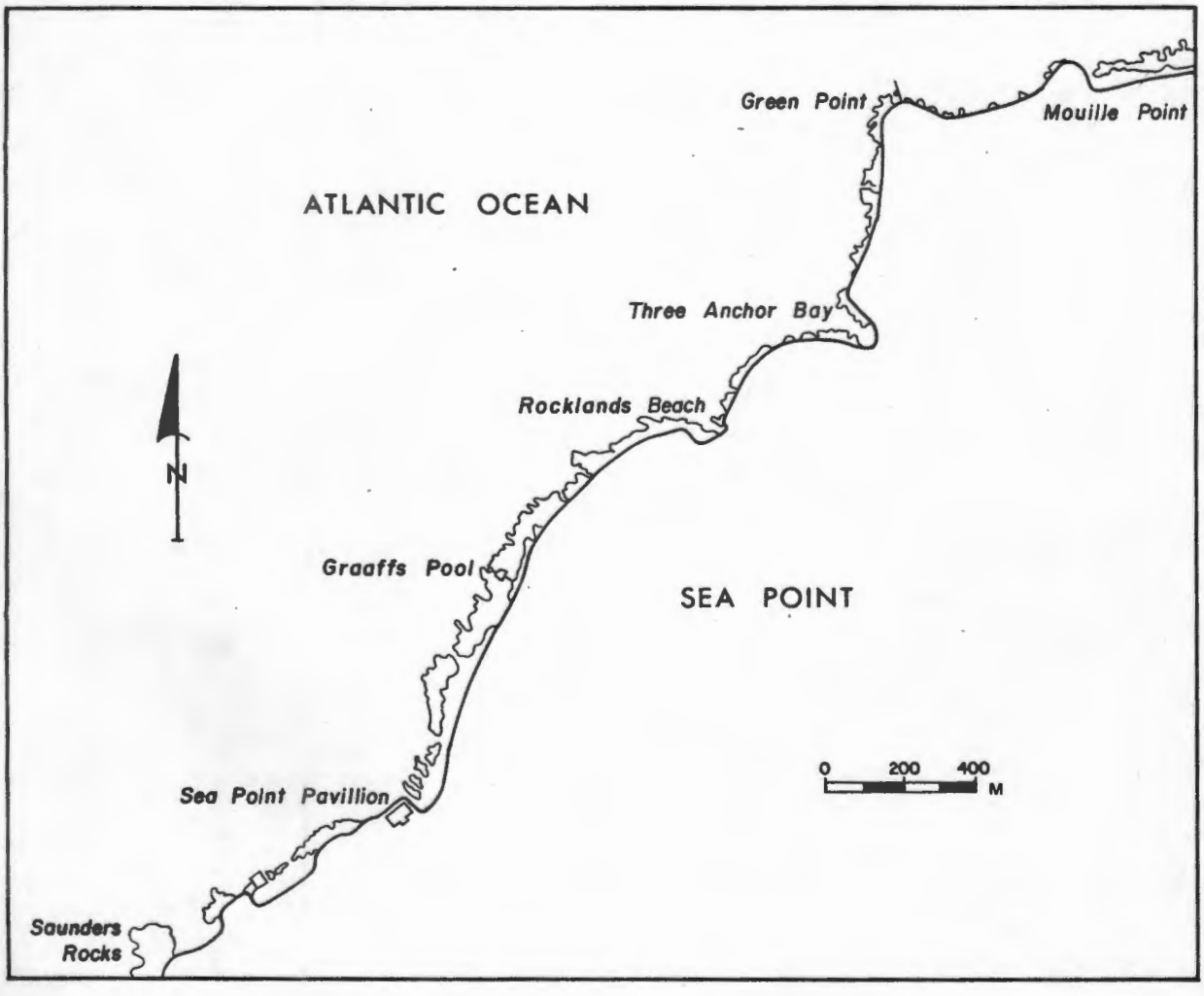

Fig.4.2 The Sea Point exposure of the Tygerberg terrane, Malmesbury Group.

The objective of this study was to obtain a better understanding of their depositional mechanisms and the palaeo-environment.

4-1-3 Methods used

The procedure which was followed was to:

a) Describe the sedimentary structures.
   This was undertaken through a detailed logging of two sections on either side of the fold hinge (from Rocklands beach to Sea Point pavilion, and from Rocklands beach to Three Anchor bay);
b) Identify facies and define their distribution and characteristics;
c) Investigate the extent of lateral continuity of the facies;
d) Relate the facies to their depositional mechanisms and to the palaeo-environment.

Bouma (1962) devised a graphical logging technique for recording 'flysch-type' sequences in detail. Seperate columns in his log are assigned to the rock type, bedding type, bedding plane properties, types of internal sedimentary structures, grain size and carbonate content.

For the purpose of this study it was felt that the scheme was unnecessarily comprehensive and a simplified version was adopted (see introduction to Appendix B). This allowed for rapid computer processing and the legible displaying of the field data.

The data was recorded in the field onto prepared data forms and transferred to data files on computer (programme LOGIN), where it was checked for errors, and corrected for true thicknesses, and graphical stratigraphical logs were then produced (programme LOGPL). These logs are reproduced in Appendix B.

4-2 FACIES ANALYSIS

4-2-1 Facies description

Five distinct facies were differentiated on the basis of the different rock types, bedding thicknesses, internal structures and bedding plane properties.

Their characteristics, facies associations and probable depositional mechanisms are described below in a standardized mode as follows:

1) Lithology	2) Bedding thicknesses
3) Bedding plane characteristics	
4) Internal sedimentary structures	
5) Additional remarks	
6) Facies associations	
7) Hydrodynamic interpretation	

Fig.4.3 Layout for the facies descriptions. Terminology for the thicknesses of beds follows that of Ingram (1954).

FACIES A	
1) Sandstone	2) Thick- to very thick-bedded sandstone Thin mudstone interbeds.
3) Sharp and flat. Sole markings rare.	
4) Massive or diffuse, flat or undulose laminations. Water escape structures rare.	
5) Amalgamation of beds common. Beds generally laterally continuous on outcrop scale.	
6) Facies C rarely facies B or D.	
7) Fluidization, grain flow and high density turbidity flow.	

FACIES B	
1) Sandstone/mudstone.	2) Medium-bedded sandstone beds. Mudstone beds variable.
3) Basal surfaces of sandstones sharp and usually concordant. Upper surfaces are sharp gradational. Trains of symmetrical, transverse ripples common. Lode casts, ball and pillow structures and sole markings rarer.	
4) Sandstone units massive and poorly graded. A poorly developed cross-laminated division may seperate the sand- stone units from the straight- to wavy-laminated overlying mudstones. Corresponds to the A to E divisions of the Bouma sequence (T a-e).	
5) -	
6) Facies C, D and E.	
7) Deposition by turbidity currents in a 'proximal' setting. Some mud settling from suspension.	

FACIES C
1) Greywacke. 2) Thin- to medium-bedded.
3) Sharp and flat. Bedding notably concordant.
4) Characteristic base-missing Bouma sequences, with T b-e or T c-e sequences predominating over T d-e as beds coarsen. The current-ripple laminae of the c-division may be convoluted. The e-division is poorly developed. Grading is poor.
5) Chert layers and thin, ripple-cross laminated sandstones may be intercalated.
6) Facies A and B.
7) Slow vertical accretion from turbidity currents in a 'distal' setting.

FACIES D
1) Mudstone. 2) Thin-bedded or no bedding.
3) Sharp and flat. Small-scale load casts, asymmetrical flame structures, dykes, sills or scours may be present.
4) Massive or laminated. Lamination types range from parallel horizontal to discontinuous wavy to convoluted.
5) In places, very thin, coarse, light-coloured layers may alternate with fine, dark layers.
6) Facies B and E.
7) Continuous or episodic settling of suspension and settling from bottom (contour) currents. Alternating dark and light result from currents with fluctuating velocities.

FACIES E
1) Resedimented mudstone/sandstone : 2) Variable.
3) Sharp or gradational. Slumped sandstone layers may retain their identity and take the form of loops, curves or lenses
4) Layer properties of sandstones may be preserved. Mudstone matrix is commonly featureless, or may display wavy or convoluted laminations.
5) Sandstone dykes may be associated with slumping (zone N18).
6) Facies B and D, rarely C.
7) Slumping and downslope gliding results from an unstable slope or from excessive overload or from liquefaction.

Plate 4.1 Facies A (zone S28).

Plate 4.2 Facies B (zone S20) (30cm. ruler for scale).

Plate 4.3 Facies C (zone S25)

Plate 4.4 Facies D (zone S2)

Plate 4.5 Facies E (zone S11)

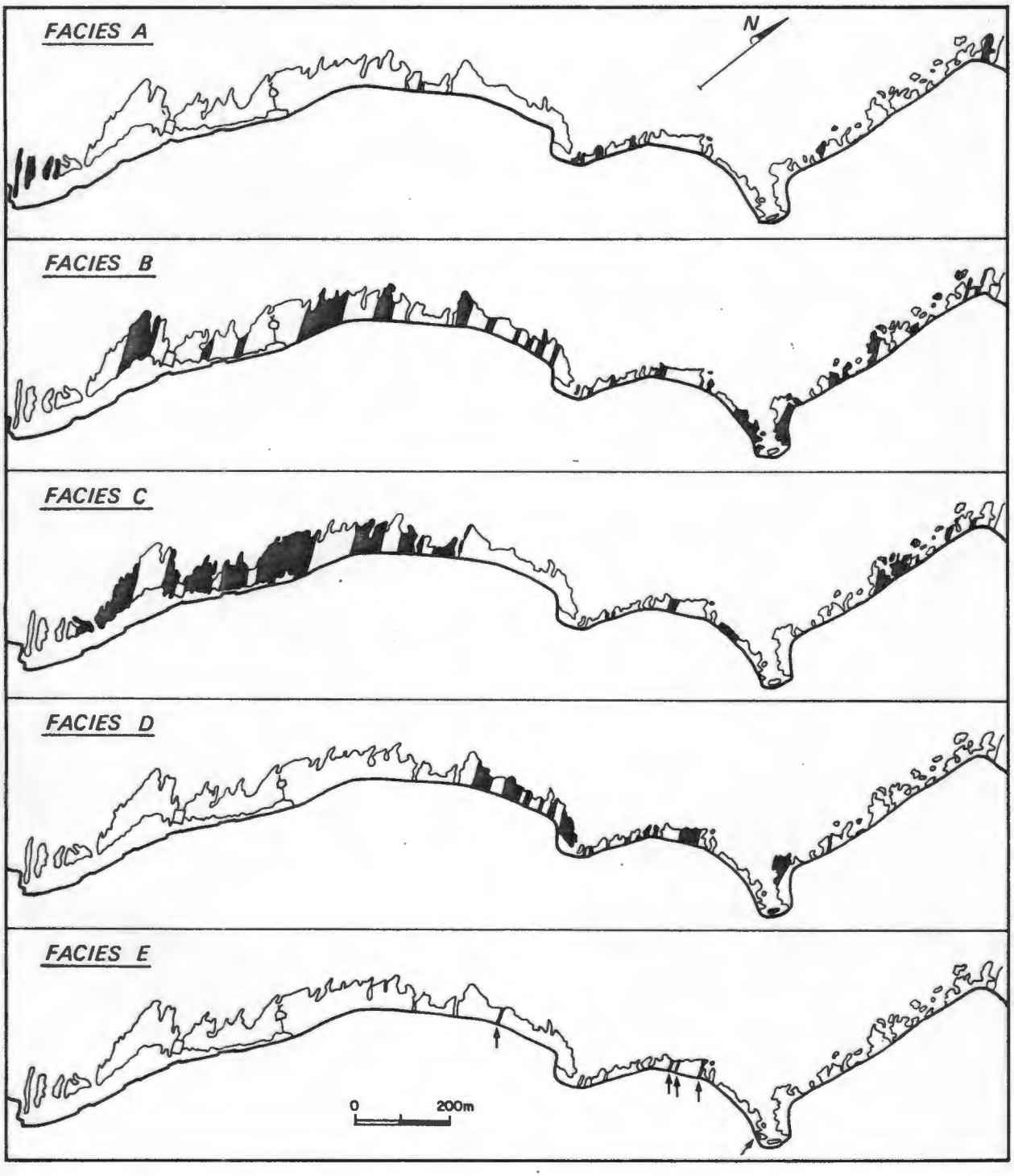

Fig.4.4 Maps of the locations of facies zones (drawn in black) in the Sea Point exposure of the Tygerberg terrane. The facies are defined in the text.

4-2-2 Trends in the vertical sections

The following trends in the vertical sections of both limbs, can be recognised from the sedimentary record:

a) The overall trend is from 'distal' deposition to relatively 'proximal' deposition (Fig.4.5).

b) Facies A zones are, however, more abundant in the lower parts of the sequence, and particularly so beyond the logged sections. (Refer to Map I and first few peaks of Fig.4.5).

c) Facies B zones thin upward, but the sandstone thicknesses within the zones increase upward (Fig.4.6).

d) Facies C zones coarsen upward. In the upper parts of the sequence, beyond Graaff's Pool and Three Anchor Bay, they are superseded by the finer-grained Facies D zones.

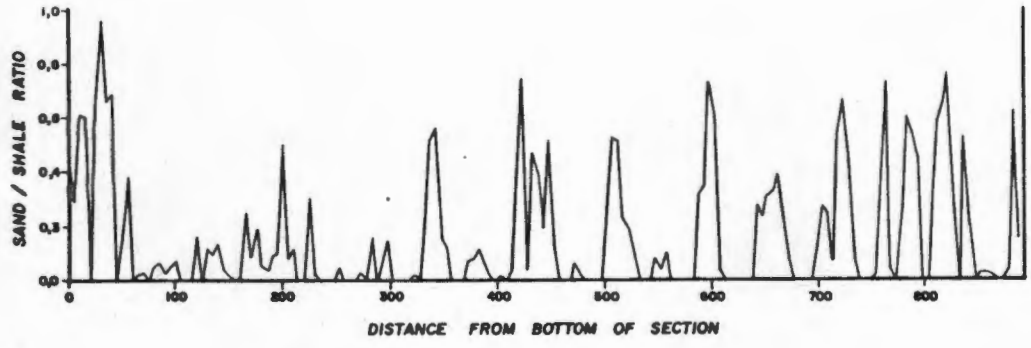

Fig.4.5 Plot of sand/shale ratio against distance from bottom of section for the SW limb. The ratios were calculated for 5 m intervals of the section.

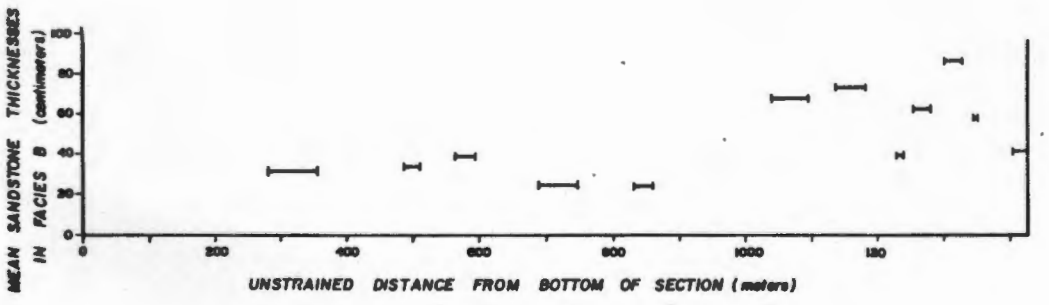

Fig.4.6 Plot of mean sandstone thicknesses against distance from base of section for Facies B in the SW limb. The zone thicknesses are bracketed. All thicknesses have been unstrained to their pre-emplacement values (see Chap.3).

4-2-3 Correlation of sections

Since the mean paleocurrent direction is from a NE direction (Fig.4.7), roughly parallel to the trend of the exposed strip, a good idea of the down-current changes in the sedimentary structures can be gained from a comparison of the sections of the two limbs.

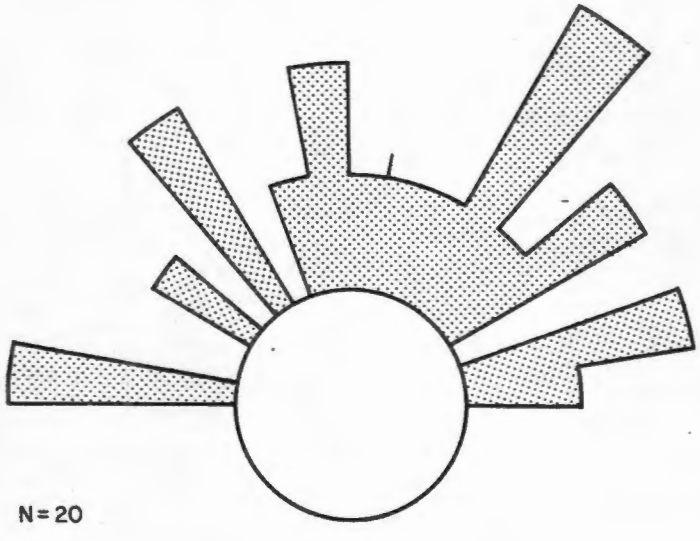

Fig.4.7 Current rose of paleocurrent directionals (cross-lamination dip azimuths).

Matching of the sections was essentially done through a process of extrapolation from the hinge zone. The emphasis was placed on recognizing similar sequences within the sections rather than using thickness or bedding property criteria . These criteria would be affected by the emplacement-related tectonic shortening as well as by the decrease in down-current flow velocities.

The task of correlating sections may be complicated by:

a) Duplication or omission of intervals of the sections due to strike faulting.

A number of strike faults are to be found in this exposure. They take the form of slickensided quartz veins in incompetant horizons. They are probably bedding plane thrusts however, associated with flexural slip folding, and would therefore not result in duplication or suppression of strata;

b) Elimination of parts of the section by erosional channeling.

From the scarcity of unconformities and large scours, it would appear that this process was not generally active. The action of turbidity currents is not believed to be an important means of erosion;

c) Incorporation of extraneous material in one section from a different source.

A unimodal paleocurrent direction would argue against this mechanism. Although a wide fluctuation of paleocurrent directions is indicated (Fig.4.7), the distribution is tentatively regarded as being unimodal;

d) Transposition of layering.

Proof that this process was not operative comes from the abundant younging data (cross-laminations).

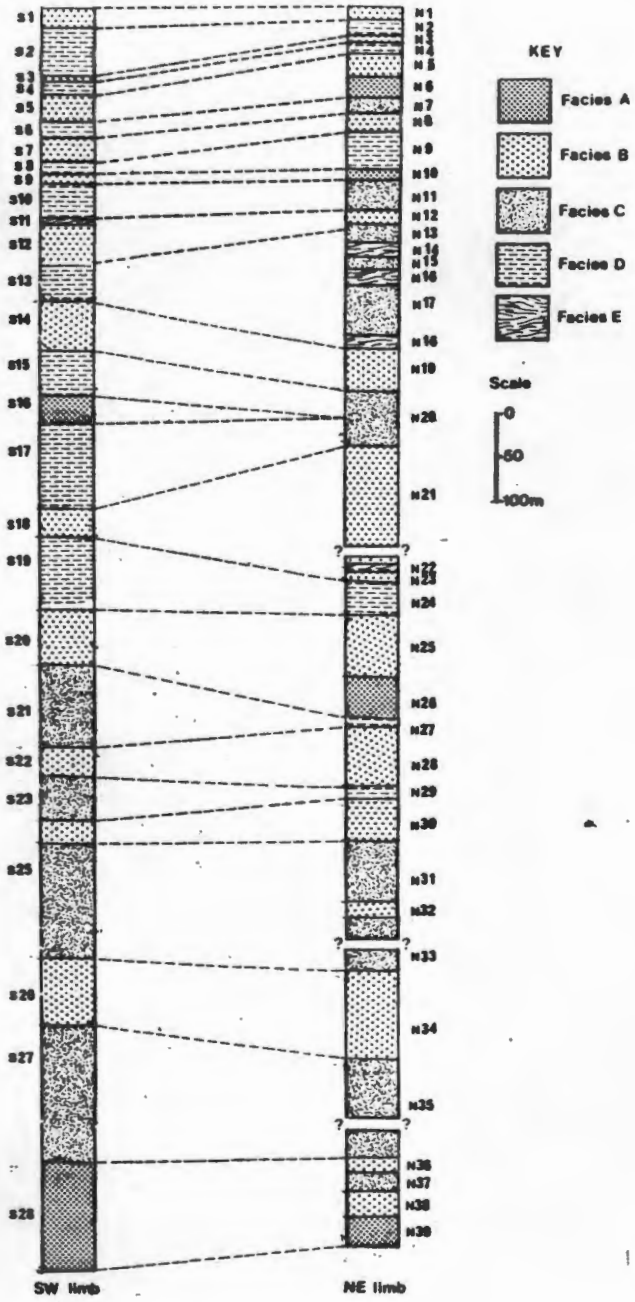

Fig.4.8 Proposed correlation of facies zones in the two limbs of the Rocklands syncline. Limb thicknesses have been corrected for the shortening which accompanied granite emplacement (Chap. 3). Breaks in the sections represent dip faults with unknown displacement.

The matched zones are listed below with comments on the similarities and differences between them. Features which were regarded as fairly reliable indicators for the proposed match are marked with an asterisk (*).

MATCHED ZONES	REMARKS
S1 and N1	S1 thins upward, N1 thickens upward.
S2 and N2	Pronounced down-current increase in zone thickness. Wavy and convoluted laminations not present in N2.
S3 and N3	Sequence is symmetrical and contains three thick sandstone units (*). Erosional features in S3.
S4 and N4	N4 is to a large extent inaccessable.
S5 and N5,N6	Thick sandstone units interbedded with thinner layers. Increase in thickness but decrease in number of these units in S5 due to amalgamation?
S6 and N7	Downcurrent fining. Clastic pulse in middle of zone (*). Layers have sandy bases near bottom of zone.
S7 and N8	Similar layer thickness pattern (Two fining-up sequences?) (*). Down-current layer thinning. Bedding is discontinuous. Two cherts in same stratigraphic positions (*).
S8 and N9	Significant thinning of zone from N9 to S8. Zone coarsens upward.
S9 and N10	Thickening upward sequence (*). Layers thin markedly in S9. Scouring and discontinuous beds in N9.
S10 and N11	Appreciable down-current fining. Upward coarsening in S10.
S11,S12 and N12, top of N13.	Gradual thickening- and coarsening-up, followed by thinning-up sequence (*). The latter sequence is slumped in the southwestern limb.

S13 and bottom of N13 to N18	Dramatic down-current thinning and fining. S13 displays wavy laminations, but no slumping or scouring.
S14 and N19	Thinning-up sequence, with thick sandstone layers in bottom half of zone (*). Sandstone beds are thinner, but thicknesses are more variable in S14.
S15 to S17 and N20	Down-current fining and zone thickening. Marker sandstone beds of S16 are represented by a thin clastic pulse in N20. Occasional thin sandstone beds in S17 and bottom of N20. Chert correlates? Convoluted and ripple-cross laminations more frequent in the NE.
S18 and N21 to N23	General trend of decreasing layer thicknesses. Thicknesses vary laterally near top. In S18, the zone thickness and layer thicknesses have decreased notably, and the rip-up clasts, resedimentation features and sandstone beds with convoluted laminations, of the zones in the NE limb, are absent.
S19 and N24	Down-current coarsening. Silty layers near top of zone.
Upper part of S20 and N25	Slight upward thinning. Layer thicknesses and sandstone percentages decrease from N25 to S20, and the scours, rip-up clasts, load casts and convoluted laminations of N25 are virtually absent in S20.

From this exercise, the following features are evident:

a) The facies zones in the two limbs can be matched, although the match is not always convincing.
b) With increasing distance from the hinge zone, the sedimentary characteristics become more dissimilar.
c) The unit thicknesses, layer thicknesses, sandstone percentages and the sedimentary structures all reflect a marked decrease in the energy of the depositional currents from the NE to the SW.

4-3 PALAEO-ENVIRONMENTAL INTERPRETATION

4-3-1 A synthesis

Hartnady et al. (1974) inferred, from the occurrence of volcanics, that the Tygerberg assemblage had an eugeosynclinal origin analagous to a modern continental rise or even an oceanic trench. A similar setting was envisaged by Tankard et al. (1981) from the evidence for parallel bedding of interbedded turbiditic and hemipelagic deposits.

The development of an amygdaloidal texture in the Bloubergstrand volcanics and the presence of thin limestones in the Tygerberg Hills, do however contradict a deep water depositional origin for these areas (C.J. Hartnady, pers. comm.). This conclusion was also derived at, for the the rocks of the Tygerberg terrane, by Beeson (1976), from the absence of the spilite-keratophyre suite.

There is a similarity between the vertical sequence at Sea Point and the stratigraphic sequence which is expected to develop, at intermediate depths, during active progradation of a submarine fan, from the lower fan to the mid fan region.

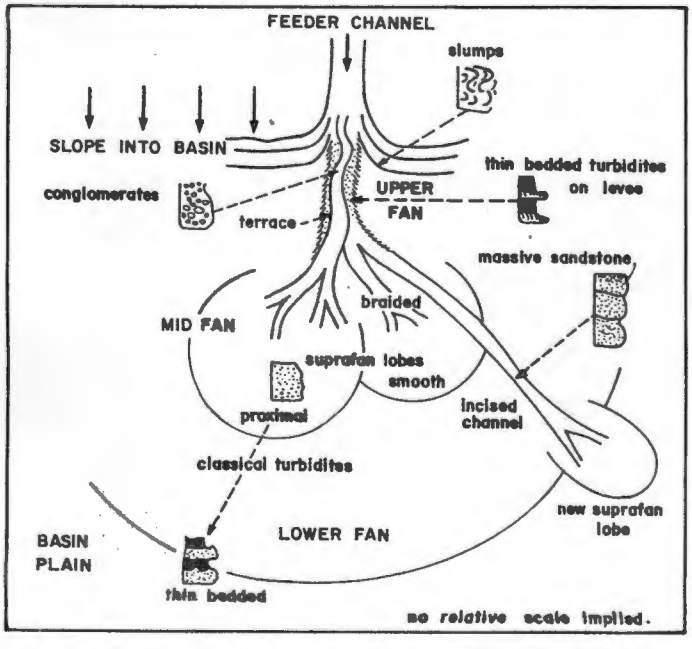

Fig.4.9. Model of submarine-fan deposition, relating facies and depositional environment (after Walker, 1978, p.946).

Walker (1978) predicts that progradation of the lower fan onto the basin plain will result in a sequence of regularly and parallel bedded classic turbidites which become coarser and thicker bedded towards the mid fan (equivalent to Facies C).

The mid fan is built up by lateral switching, coalescing, and supimposition of suprafan lobes (Facies B).

The smooth parts of the lobes gives rise to thickening upward sequences of alternating sandstone/mudstone (zones S7,S9,S12,S16,N8,N10,N23 of Facies B).

Abandoned lobes may receive mudstone veneers (Facies D).

Reestablishment of lobes could lead to superimposed thickening and fining upward sequences (zones S12,S18,S20,N12,N21,N25 of Facies B).

Above the smooth parts, in the suprafan channels, fining-upward sequences develop during channel filling and abandonment (zones S1,S5,S14,N19 of Facies B).

During accelerated progradation, the upper-fan channel cuts downward and outward across the lower fan and a new depositional lobe is constructed on the seaward side of the old fan.

The incised channel deposits consist of massive sandstones (Facies A) with poor lateral continuity.

In summary then, the sediments of the Tygerberg terrane which are exposed at Sea Point are probably turbiditic and hemipelagic deposits which accumulated on a submarine fan of relatively small size, possibly at the foot of the continental slope, but in a tectonically active environment.

PART II : THE PRE-CAPE ROCKS AT BLOUBERGSTRAND

5 INTRODUCTION

5-1 GENERAL

Between the northern Cape Peninsula and the Tygerberg Hills, sporadic exposures of rocks of the Tygerberg terrane are encountered; notably at Robben Island, Bloubergstrand, Blouberg and Melkbosstrand (Fig.5.1). The Bloubergstrand member, situated on the northwestern shore of Table Bay, comprises a 1.5 km belt of unweathered rock.

The lavas and intercalated tuffs which are exposed on either side of Kleinbaai (Fig.5.2) were first described by Haughton (1933). He identified the lava as a trachyte, and the adjacent rocks as 'schists and quartzitic clay-slates'. Subsequent analysis has shown the extrusive to have a more intermediate composition (Hartnady et al., 1974). On geochemical grounds, Hoal (1979) proposed that it originated in an orogenic environment.

Haughton (1933) also noted the common development of shearing phenomena and minor folding. He described the fold axes as dipping in a northerly direction and running approximately NNW, roughly parallel to shear-planes. Unpublished structural studies of an area in the the vicinity of Kreefgat by B.Sc. (Hons.) students of the University of Cape Town, during 1974 and 1975, highlighted the complexity of the folding. They showed that the plunges of the fold axes vary considerably about a NNW plane.

The purpose of this study was firstly to define the distribution of the various rock types in the exposure, and secondly, to analyse and to attempt an interpretation of the kinematics of its structural features.

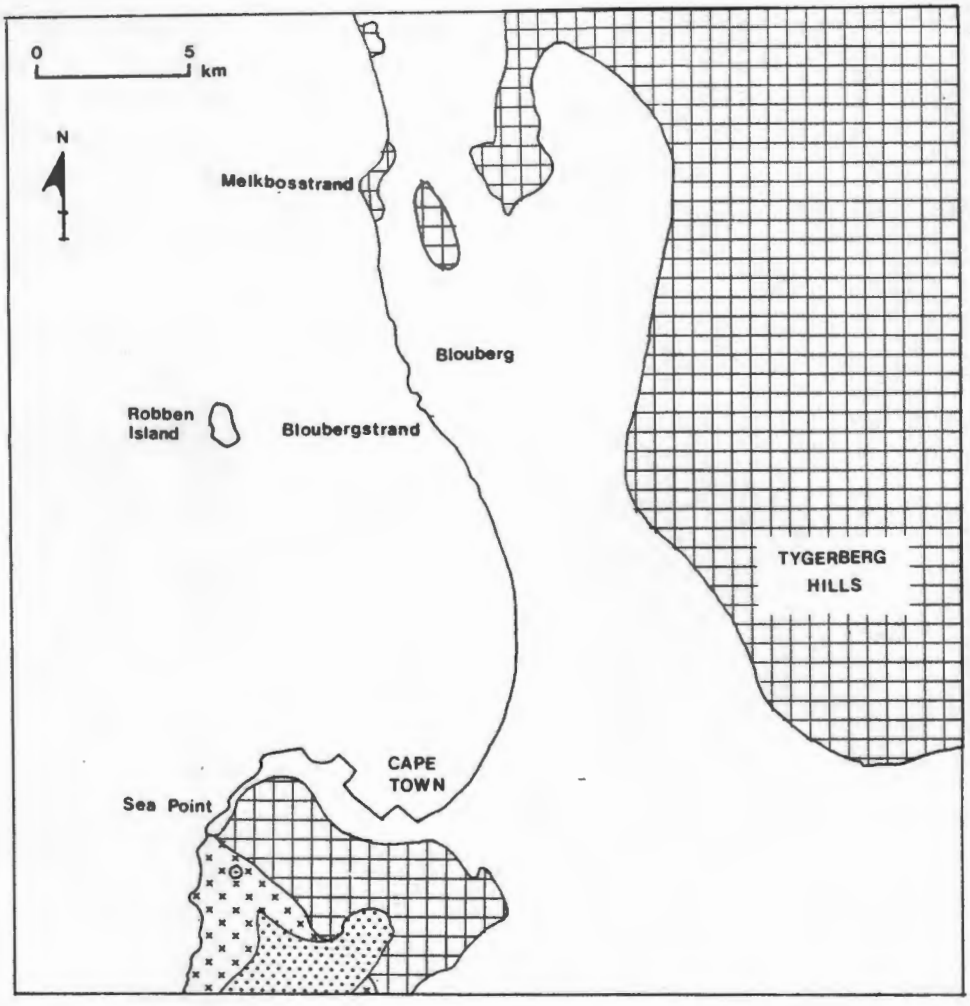

Fig.5.1 Map of the area between the northern Cape Peninsula and the Tygerberg Hills. See Fig.1.1 for legend.

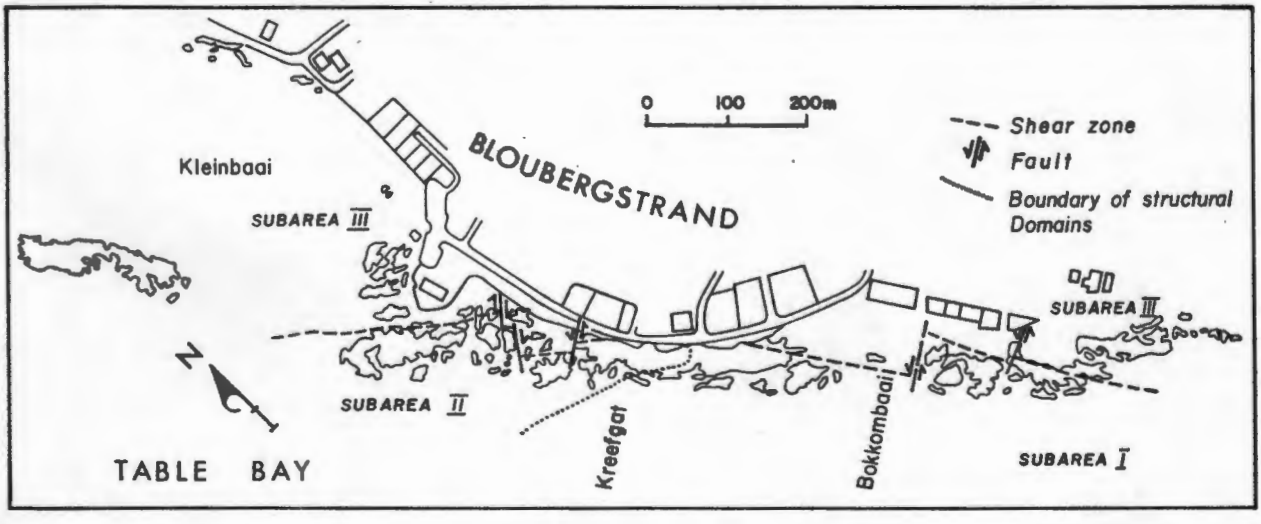

Fig.5.2 Map of the Bloubergstrand outcrops, showing the extent of the shear zone (See text for further explanation).

6 STRATIGRAPHICAL INVESTIGATION

6-1 INTRODUCTORY COMMENTS

The variety of rock types and grain sizes, the relative abundance of younging criteria (cross-bedding) and a fairly simple mesoscopic structure facilitated the establishment of a general stratigraphic succession for the Bloubergstrand outcrops. Due to the localised presence of shearing, transposed folding and complex minor folding, however, the setting up of a detailed succession, particularly with regard to zone thicknesses, would be a difficult task.

A fundamental feature of the stratigraphic succession which is proposed below, is the existence of a major shear zone, separating a northeastern subarea from a structurally unconformable southwestern subarea (Fig.5.2).

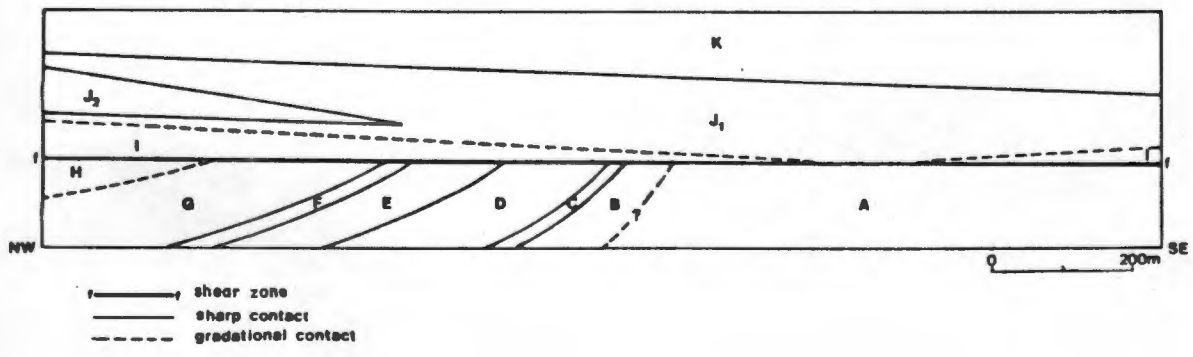

Fig.6.1 Schematic plan view of the Bloubergstrand outcrops showing the relationship of the defined litho-stratigraphic zones to the structural unconformity. Refer to Maps II A-C for a detailed plan view.

6-2 STRATIGRAPHIC SUBDIVISION

6-2-1 Introduction

Descriptions of the salient features of each of the eleven distinct lithostratigraphic zones which have been defined within the two subareas are presented below (Tables 6.1 and 6.2).

The format for the descriptions of the zones is as follows:

: 1) Lithology :
: 2) Bedding thickness :
: 3) Bedding plane characteristics :
: 4) Internal sedimentary structures :
: 5) Colour :
: 6) Comments :

6-2-2 Southwestern subarea

Younging of this subarea is from south to north. The defined zones have been alphabetically named and are described here in their chronostratigraphic order.

Descriptions of lithological zones of the southwestern subarea.

zone A

1) Micaceous and felspathic wacke
2) Very thick
3) Rare, wavy bedding planes defined by thin shale horizons.
4) Massive. At the northernmost extremity of this zone, straight, continuous, alternating dark and light laminae are visible on smoothly weathered surfaces.
5) Pale ochre to aquamarine, weathers to a pale rust colour.
6) Occasional thin reddish-brown sandstone lenses.

zone B

1) Siltstone.
2) Variable, up to 1 m. Thin at base.
3) Sharp and continuous.
4) Massive, or display well-preserved, thin, straight, ripple-cross or convoluted laminations. No conspicuous grading.
5) Variable. Orange, pale brown or blueish-grey.
6) -

zone C

1) Alternating sandstone and mudstone.
2) Medium-bedded, with some very thick (<2 m) sandstone units.
3) Lower bedding planes are sharp and straight for the sandstone beds and gradational for the mudstone beds.
4) Sandstones massive. Diffuse laminations in mudstone layers.
5) Sandstone beds pale ochre. Mudstones green to blue.
6) Rare mudstone fragments (<5 mm) in the sandstone beds.

zone D

1) Mudstone.
2) Medium-bedded (<30 cm).
3) The straight bedding planes are defined by distinct physical breaks.
4) Smoothly weathered surfaces display flat, continuous, thin laminae. A pervasive cleavage obscures layer properties.
5) Blue-grey, weathers to a rust colour.
6) Some light brown sandstone lenses occur near the base.

zone E

1) Alternating siltstone/mudstone.
2) Thin- to medium-bedded.
3) Sharp and straight.
4) Siltstone beds have ripple cross-laminations and are graded. Mudstone beds have straight laminae.
5) Pale brown, pale green, cream.
6) Prominent, discontinuous chert horizons are intercalated and mark both the base and the top of this zone.

zone F

1) Mudstone.
2) Thin.
3) Sharp and straight.
4) Diffuse, thin, straight laminations.
5) Green-blue.
6) Rare thin laminated chert horizons. Penetratively foliated.

zone G
1) Alternating mudstone/siltstone or mudstone/sandstone.
2) Thin- to medium-bedded.
3) Sharp. Bedding often disrupted and attenuated.
4) Sandstones massive. Mudstone straight laminated.
5) Mudstone blue-green. Siltstone green-brown. Sandstone sienna-coloured.
6) -

zone H
1) Arkosic wacke.
2) Very thick.
3) Wavy, discontinuous. Defined by rare thin mudstone partings
4) Massive.
5) Pale ochre, weathers brown.
6) Characteristics similar to zone A.

Table 6.1 Descriptions of lithological zones in the southwestern subarea.

From the above, it can be seen that this subarea is comprised of an assemblage of psammitic and pelitic rocks with a variety of bedding plane and layer properties.

6-2-3 Northeastern subarea

The chronostratigraphic order between this subarea and the southwestern one is unknown. Way-up criteria (cross-bedding) indicates that younging within the subarea is westward from zone I to zone J and eastward from zone K to zone J, implying that zones I and K may be lithological equivalents, with a synclinal hinge passing through zone J.

Descriptions of lithological zones in the northeastern subarea.

zone I

1) Alternating siltstone/mudstone.
2) Thin-bedded in the south. Thin- to medium-bedded in the north.
3) Basal surfaces of siltstone beds sharp and concordant.
4) Ripple cross-laminated siltstone grading into straight laminated mudstone. A straight laminated mudstone is found at Bokkombaai.
5) Siltstone green-brown. Mudstone blue-green.
6) Contact with zone J is gradational in grain-size and colour. In the north, the zone is similar to zone G, although bedding has a greater lateral persistence.

zone J

1) Tuff in the south (J1 in Fig.3.2), interbedded with andesitic lava in the north (J2).
2) - 4) A penetrative schistosity has obliterated bedding structures.
5) Red, weathers pale green.
6) Angular, amygdaloidal and vesicular blocks of lava, tuffaceous agglomerates and andesitic lavas are interbedded in J2:

zone K
1) Mudstone.
2) In the north, bedding is inconspicuous in the lower part of the zone and thin-bedded in the upper part. In the south, it is medium-bedded.
3) Sharp. Straight or wavy.
4) Generally indistinct. Upward coarsening of the zone is evidenced by beds displaying proximal turbiditic characteristics at the southernmost outcrop, by massive or ripple cross-laminated sandstone lenses further north, and by thin interbedded siltstones at Kleinbaai.
5) Bright olive-green or mauve, in the south. Further north, a pale pinkish brown colour, that weathers to a pale olive green colour.
6) -

Table 6.2 Descriptions of lithological zones in the northeastern subarea.

Owing to limited exposure in this subarea, its stratigraphic subdivision may well be oversimplified. The defined zones need not be laterally continuous. For example, the nature of the sediments grouped under zone K varies widely.

6-3 PALAEO-ENVIRONMENTAL INTERPRETATION

6-3-1 Discussion

The sediments of the Bloubergstrand exposure contrast with those at Sea Point in the following respects:

a) The presence of interbedded volcanics;
b) A significant increase in thickness and degree of immaturity of the massive argillaceous sandstone horizons (zones A and H);
c) A decrease in layer thickness and coarseness of the alternating sandstone/mudstone zones;
d) A greater abundance of pelites.

Whereas the rocks at Sea Point were assigned to the lower fan and mid fan parts of a prograding submarine fan, the Bloubergstrand rocks, located in an up-current direction, resemble deposits of the upper fan environment (See Fig.4.9).

Zones A and H are interpreted as channel fill deposits. The absence of conglomerates can be attributed to the lack of coarse clasts in the source area. The 'distal' alternating siltstone/mudstone and mudstone zones may represent the levee or back-levee environments of the upper fan. In the proximity of the Bloubergstrand outcrops, at Robben Island, slumping of layering, in the form of 'loops and curves some tens of metres across' (de Villiers, 1980, p.67), has occurred. This phenomenon is to be expected in an upper fan environment because of the steeper gradients. The extensively developed quartzites of the Tygerberg Hills could represent the feeder channel deposits in the upper reaches of the upper fan.

The indication therefore is that the sediments of the Tygerberg terrane were derived from a proximally located hinterland, presumably from the region where the Swartland Subgroup is today exposed.

7 STRUCTURAL ANALYSIS

7-1 FABRIC ANALYSIS

7-1-1 Introduction

As noted in the introduction to PART II, the Bloubergstrand outcrops are marked by the presence of shearing phenomena. The shears are persistent features, which can be traced along almost the entire length of the exposure. They vary from diffuse zones of attenuation and boudinage, to discrete zones of mylonitisation Although they are frequently offset by late faulting and may be imperceptible in the foliated pelites, due to their rough parallelism with the schistosity, it appears that they constitute segments of a single, continuous shear zone, which curves from an azimuth of ~130° in the vicinity of Kreefgat to ~150° in the south (Fig.5.2,Map IIA-C). A sinistral fault, passing through Bokkombaai, would however need to be invoked.

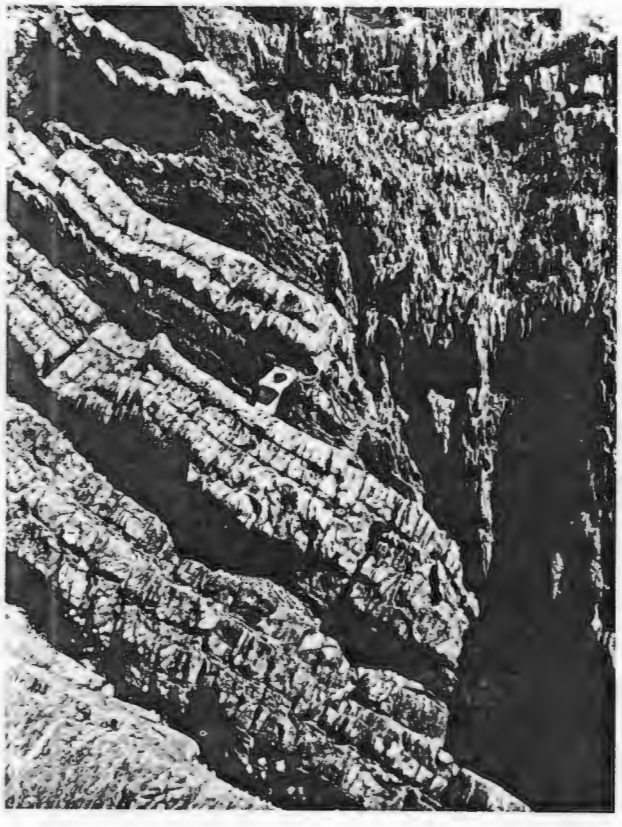

Plate 7.1 Bedding in zone C truncated by the shear zone. View is to the NW.

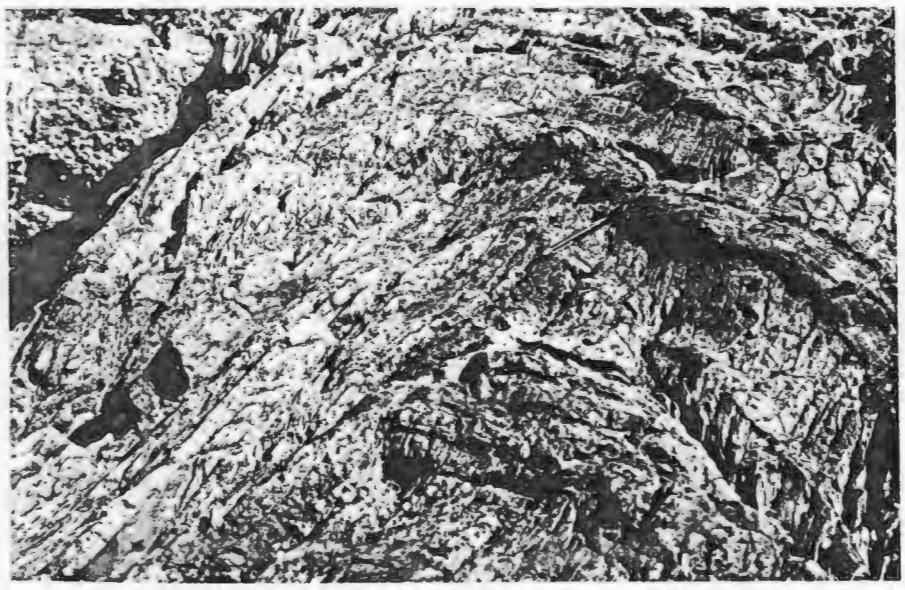

Plate 7.2 Drag folding of layering near the base of zone D. The shear zone is in the top left-hand corner. View is to the SE.

7-1-2 Structural subdivision

Three structural subareas have been distinguished on the basis of, inter alia, location with respect to the shear zone, bedding attitudes, and the presence or absence of minor folding (see Fig.5.2):

Description of the structural subareas.

	Subarea I	Subarea II	Subarea III
Location	SW of shear zone in the south. (zones A-D)	SW of shear zone in the north. (zones E-H)	NE of shear zone. (zones I-K)
Identifying characteristics.	W to NWW strike of the steeply dipping bedding. Minor folds rare. Shears are discrete zones of mylonitization.	NWW strike of bedding. Complex minor folding. Shears are diffuse zones of attenuation and boudinaging.	NW strike of bedding. Minor folds absent. Shears are generally absent.
Mean bedding pole	282°/83° N	302°/89° NE	139°/89° SW
Bedding relations	Although bedding relations inconpicuous in zones A and D, a progressive NE swing of bedding to the south is evident. (Fig.6.1).	Bedding pole distribution is scattered due to minor folding.	Strike corresponds to the regional trend.

Mean pole to foliation:	332°/87° NE	320°/86° NE	329°/90°
Foliation type.	Penetrative sub-vertical slaty cleavage that overprints structures. In competent zones (zone A), a NNW-striking fracture cleavage predominates.	A slaty cleavage overprints the incompetent layers of minor folds. It may however mimic them as competent layers are approached. In competent layers a poor fracture cleavage is normal to bedding.	Slaty cleavage type, with a predictable orientation.

Table 7.1 Description of the structural subareas.

A tectonic database system, PRUDE, developed by C.J. Hartnady for the management of tectonic orientation and location data, was used to statistically process the structural data and to plot the stereographic projections.

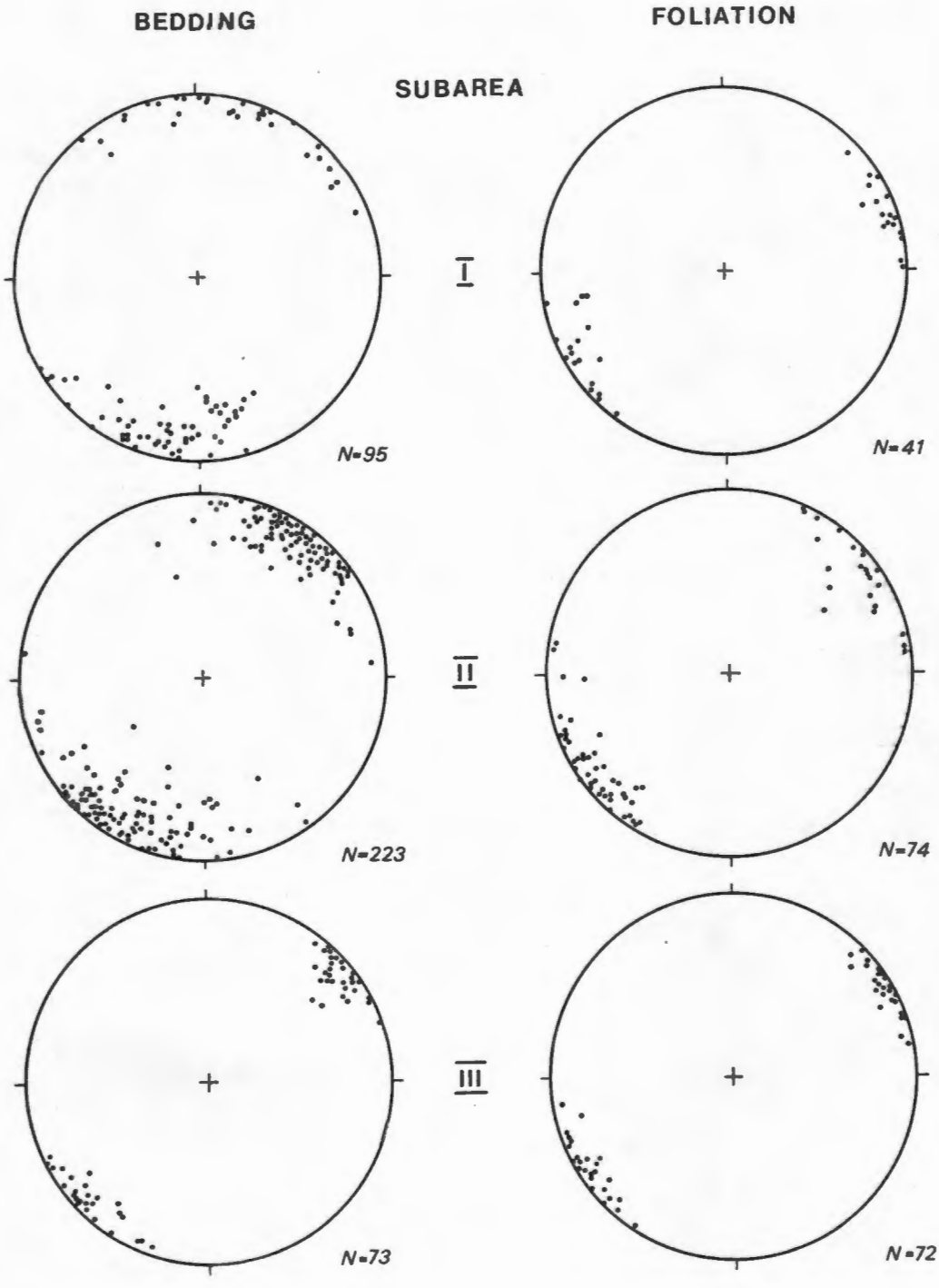

Fig.7.1 Lower hemisphere equal area stereographic plots of structural data for subareas I-III.

7-2 QUANTITATIVE FOLD SHAPE STUDY

7-2-1 Description of the folding

A study of the minor folds in Subarea II was undertaken, through the use of a number of field photographs of fold profiles. The wavelengths of these folds vary considerably, from tens of centimetres for thin beds, to a few metres for thick beds. They also show a considerable variation in symmetry, with long to short limb ratios of up to 3/1, and with both 'S' and 'Z' senses of symmetry being represented.

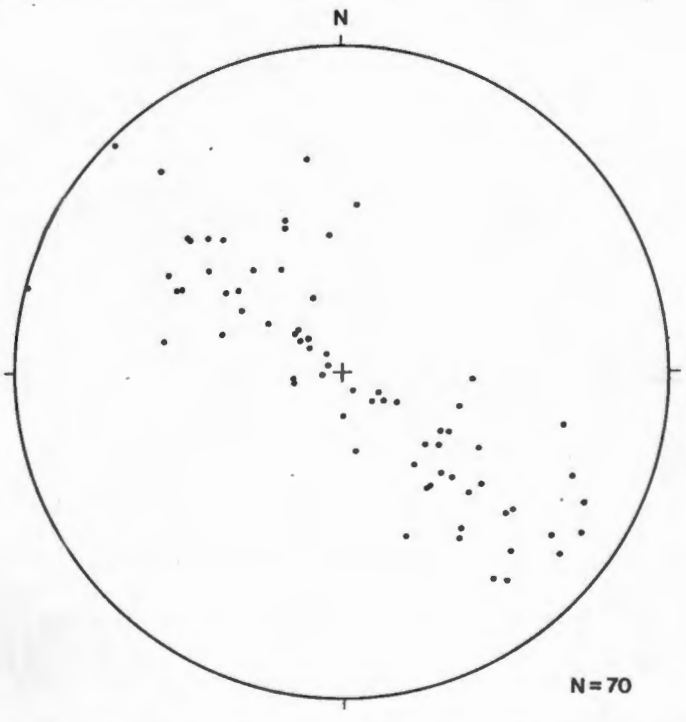

Fig.7.2 Lower hemisphere equal area stereographic plot of minor fold axes (pole to best-fit plane 042°/01° SW).

The fold axes define a diffuse girdle about a great circle. No systematic variation in the spatial distribution of the axial orientations could be discerned. Axial traces cannot be followed for any considerable distance and are often curvilinear. Plunges may vary considerably along trace and the folds may even be doubly-plunging.

To illustrate the diversity of fold style, the morphological characteristics of a number of structures are illustrated and briefly described below:

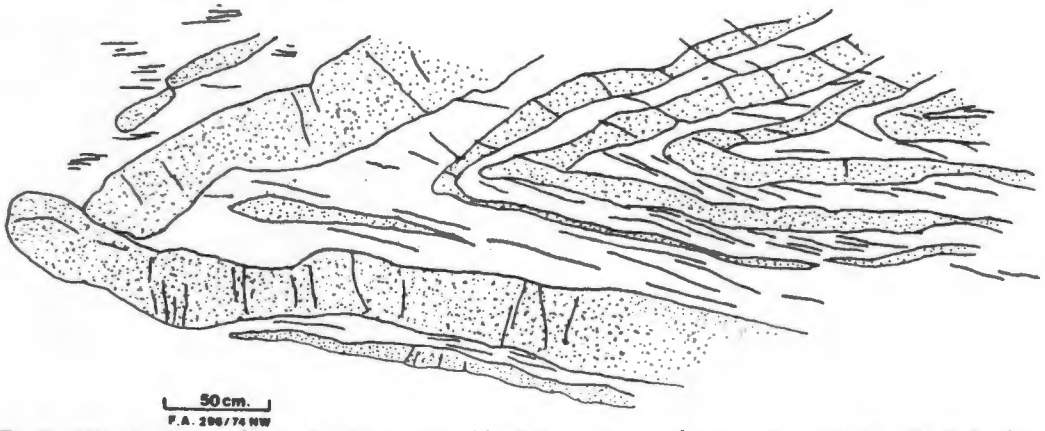

Fig.7.3 Sketch of a large upright plunging chevron fold in alternating siltstone/mudstone (zone E). Siltstone beds are stippled.

The limb length incompatibility of the anomalously thick layer is accomodated by a limb thrust. The thin layers display pinching. Flow of incompetent material into hinge zones has occurred. A slaty cleavage parallels bedding and transects fold cores in the one limb, and becomes a refracting fracture cleavage cutting the layers at a high angle in the other limb.

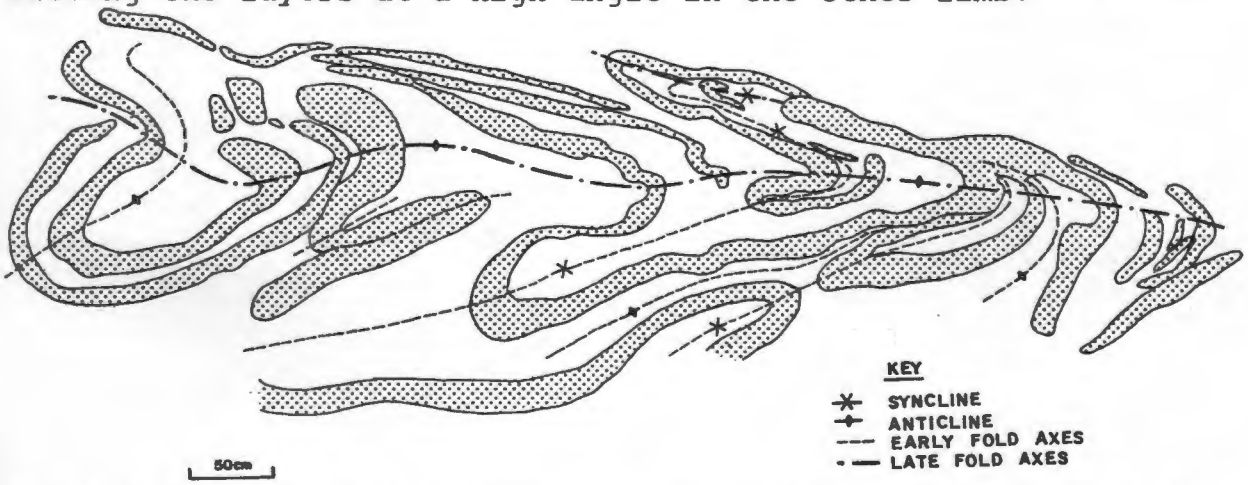

Fig.7.4 An example of overprinting of early, tight folds by a later fold generation in alternating siltstone/mudstone layers (zone E). The early folds are non-periodic, asymmetrical, plunging inclined folds. The later, close folds have vertical axial planes and horizontal fold axes, striking 132° SE. View is to the SE.

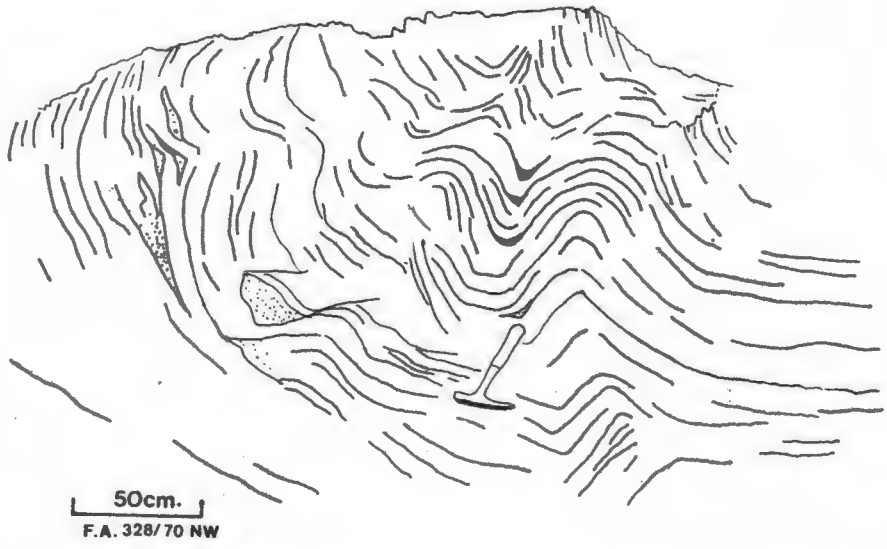

Fig.7.5 Sketch of an open synform in a porphyritic andesite (zone J). View is to the NW.

Discrete fractures define the boundaries of the thin homogeneous layers. The layers are progressively deformed as the core is approached. Incipient kinking gives way initially to parallel folds. Dilation spaces then develop in the hinge zones, the style of folding becomes cuspate (tight antiforms and open synforms), and finally the antiforms are faulted out.

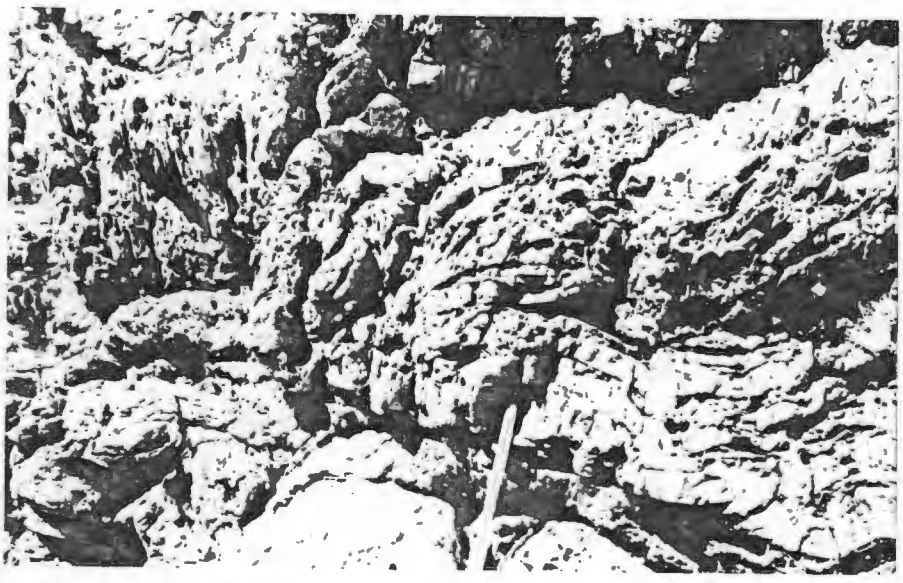

Plate 7.3 A recumbent fold in zone E. View is to the N.

Plate 7.4 Asymmetrical fold adjacent to a discrete shear in zone B. View is to the W.

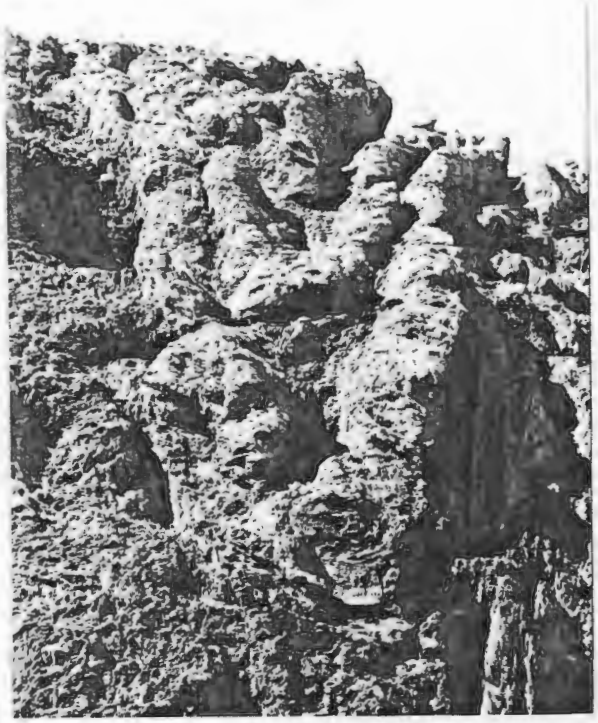

Plate 7.5 Close fold bounded by shear joints in zone E. View is to the SSE.

Plate 7.6 Asymmetrical fold in zone E. View is to the NW.

Plate 7.7 Chevron folding of thin competent layers in zone E.

7-2-2 Fold layer geometry

In order to analyse the relationships of the bounding surfaces of the folds, the quantitative fold classification method of Ramsay (1967, p.359-372) was adopted.

Method used

A computer programme (programme FOLDS) was written for rapidly obtaining dip isogons and evaluating the thickness parameters of folded layers from field photographs.

The method entails a smoothing of the surfaces by a least-squares routine; locating points of equal slope to find the dip isogons; ascertaining their lengths and the angles between the isogons and normals to tangents of the folded surface (ϕ); and using these two parameters to determine orthogonal thicknesses (t_α) and thicknesses parallel to the hinge (T_α) (see Fig.7.6 for explanation). Plots are produced to show the variations of $t'_\alpha = t_\alpha/t_o$ or $T'_\alpha = T_\alpha/t_o$, where t_o is the thickness at the hinge.

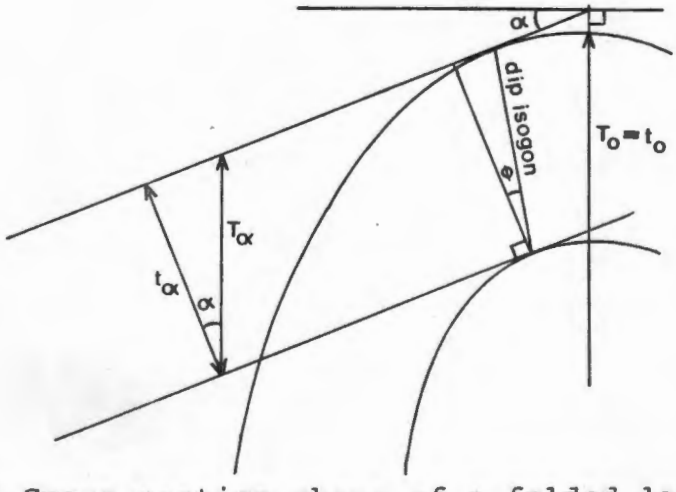

Fig.7.6 Cross-section shape of a folded layer showing fold thickness parameter definitions.

Results

In Fig.7.7 A-C, the variations in t_α with α are graphically expressed for competent, incompetent and relatively homogeneous beds respectively. Although the last-mentioned group may exhibit graded bedding, the distinction between competent and incompetent layering is poor.

The competent beds show marked variations of thickness in the hinge zone; from subclass 1B parallel folds, to subclass 1A folds, with strongly convergent dip isogons. In the limbs, the structures are modified to take up the geometrical forms of folds with weakly convergent isogons (subclass 1C).

The incompetent layers show, without exception, a marked thickening in the hinge zone and may therefore be classified as Class 3 folds (divergent isogons).

The layers of little competence contrast accord closely with the subclass 1C fold model, without hinge zone modifications.

Internal deformation of competent buckled layers in well-stratified rocks is commonly accomodated by flexural slip and gives rise to subclass 1B parallel folds (Ramsay, 1967). Superimposing a homogeneous strain leads to flattening of the parallel shape, and modification of the fold to a subclass 1C model.

The subclass 1A modification in the hinges of the competent structures can be attributed either to hinge collapse, that adjusts the fold geometry to hinge dilation; or to bulbous structures that develop due to limb length incompatibility, if an anomalously thick layer is present, intercalated in a regular sequence (Ramsay, 1974).

If competent layers are close to each other, a superimposed homogeneous strain will lead to squeezing of the incompetent surrounding material into the hinge zone region, producing Class 3 folds.

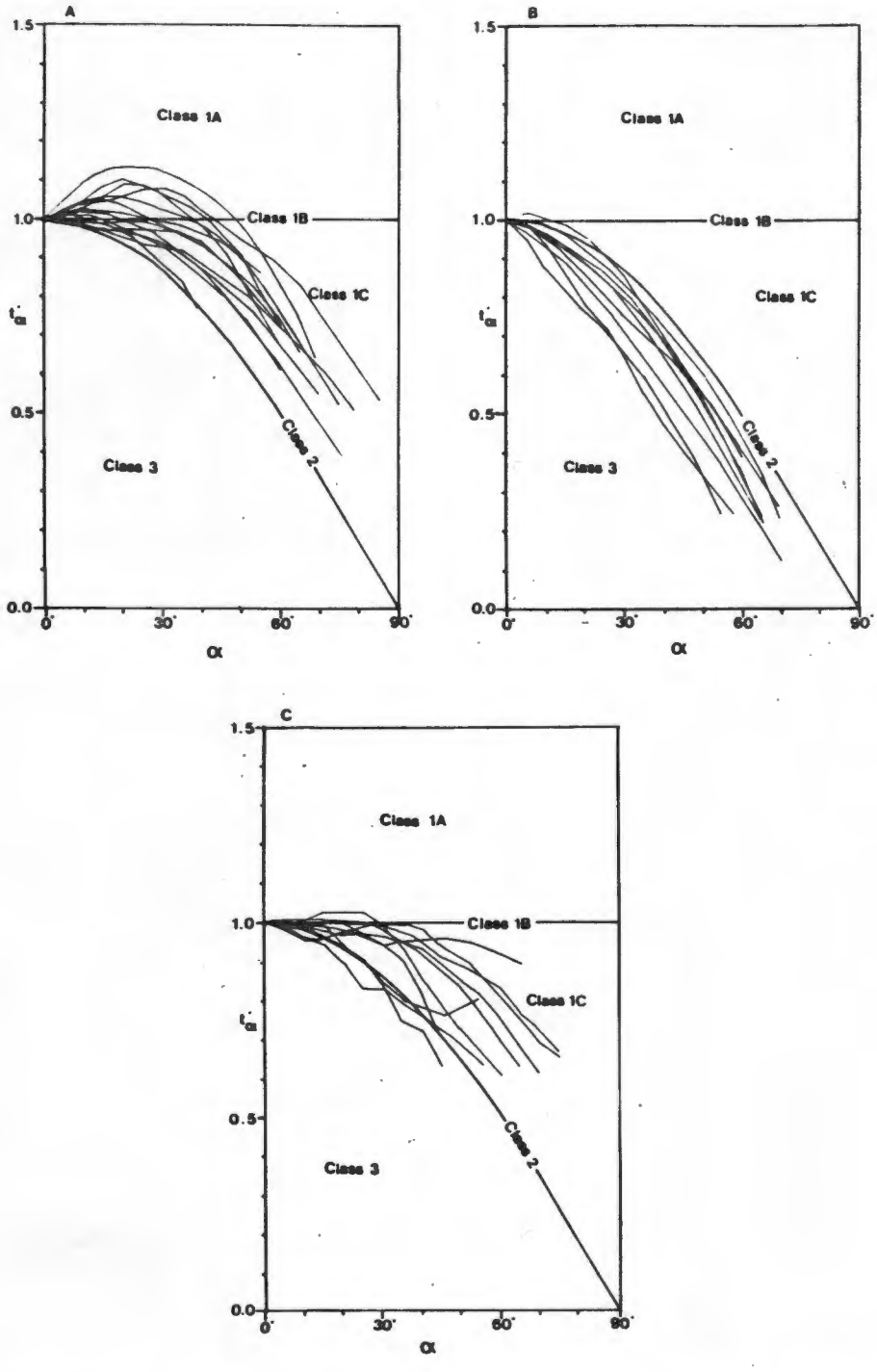

Fig.7.7 Orthogonal thickness variations with dip, for folds at the Bloubergstrand exposure. The fundamental fold classes are shown. Isogon measurements are at 5° intervals. A - Competent layers. B - Incompetent layers. C - Layers of little competence contrast.

7-2-3 Fold surface geometry

Methods used

In order to describe the shape of single folded surfaces, the technique of harmonic analysis of 'quarter-wavelength' units, as described in Hudleston (1973), was adopted. The first two odd coefficients of the Fourier sine series are sensitive parameters of fold shape.

To this end, a computer programme (programme SHAPE) was drawn up. Points on the fold surface, between hinge and inflection points are digitised at small intervals. The programme then evaluates the first two odd coefficients, b_1 and b_3, according to simplified expressions derived by Stabler (1968). A plot is produced for classifying the fold surface, according to the categories of 'shape' and 'amplitude', as defined by Hudleston (1973).

The size of the first coefficient b_1, is related to the fold amplitude/ wavelength ratio, or fold tightness. The ratio of the third coefficient b_3 to the first, b_1, is sensitive to changes in fold shape (Hudleston, 1973).

Results

Frequency histograms of the size of b_1 for the competent siltstone beds, with thicknesses of less than 10 cm, between 10 and 20 cm and greater than 20 cm, appear in Fig.7.8 A,B and C respectively.

Examination of the synthesised data reveals that the distributions are asymmetrical and that the mean size of b_1 decreases significantly as bedding thickness increases.

The folds less than 10 cm thick, plot in the proximity of Hudleston's 'amplitude' category 3 and are therefore close folds. The folds with thicknesses between 10 and 20 cm have a more variable tightness but fall, to a large extent, between 'amplitude' categories 2 and 3, and are therefore open to close folds. Folds greater than 20 cm thick, all plot between categories 1 to 3 and can be termed as gentle to open folds.

These results are in agreement with a prediction of Sherwin and Chapple (1968), that fold amplification is proportional to wavelength/thickness ratios.

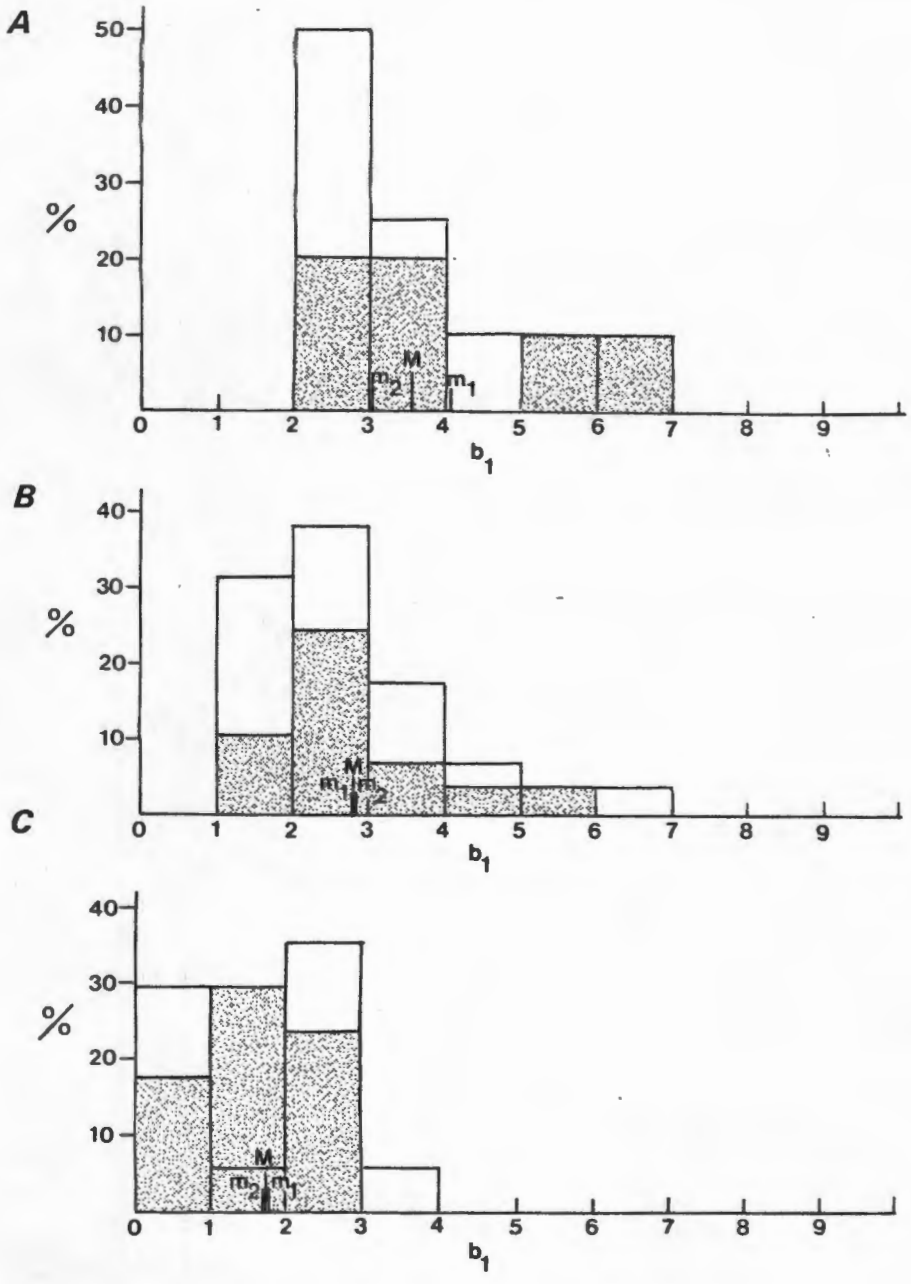

Fig.7.8 Frequency histograms of the value of b_1. The shaded section is for inner arcs of folds, the unshaded section is for outer arcs. m_1 is the mean for inner arcs and m_2 is the mean for outer arcs. M is the total mean. A - 12 folds (6 inner arcs, 6 outer arcs) with layer thicknesses less than 10 cm. B - 29 folds (14 inner arcs, 15 outer arcs) with thicknesses between 10 and 20 cm. C - 17 folds (8 inner arcs, 9 outer arcs) with thicknesses greater than 20 cm.

Seperate histograms of the ratio b_3/b_1 for the three groups, as defined above are drawn in Fig.7.9 A-C.

It is apparent that their distributions are roughly symmetrical about their means.

The thin beds generally plot between Hudleston's 'shape' categories E and F (chevron folds), whereas the thicker beds plot between categories C and F (semi-ellipses to chevron folds).

The mean b_3/b_1 values for inner arcs of competent beds are consistently lower than those of outer arcs, implying that their their hinges are sharper. This result accords with the above observation that the hinges of competent beds are of subclass 1B or 1A, and of class 3 for incompetent beds.

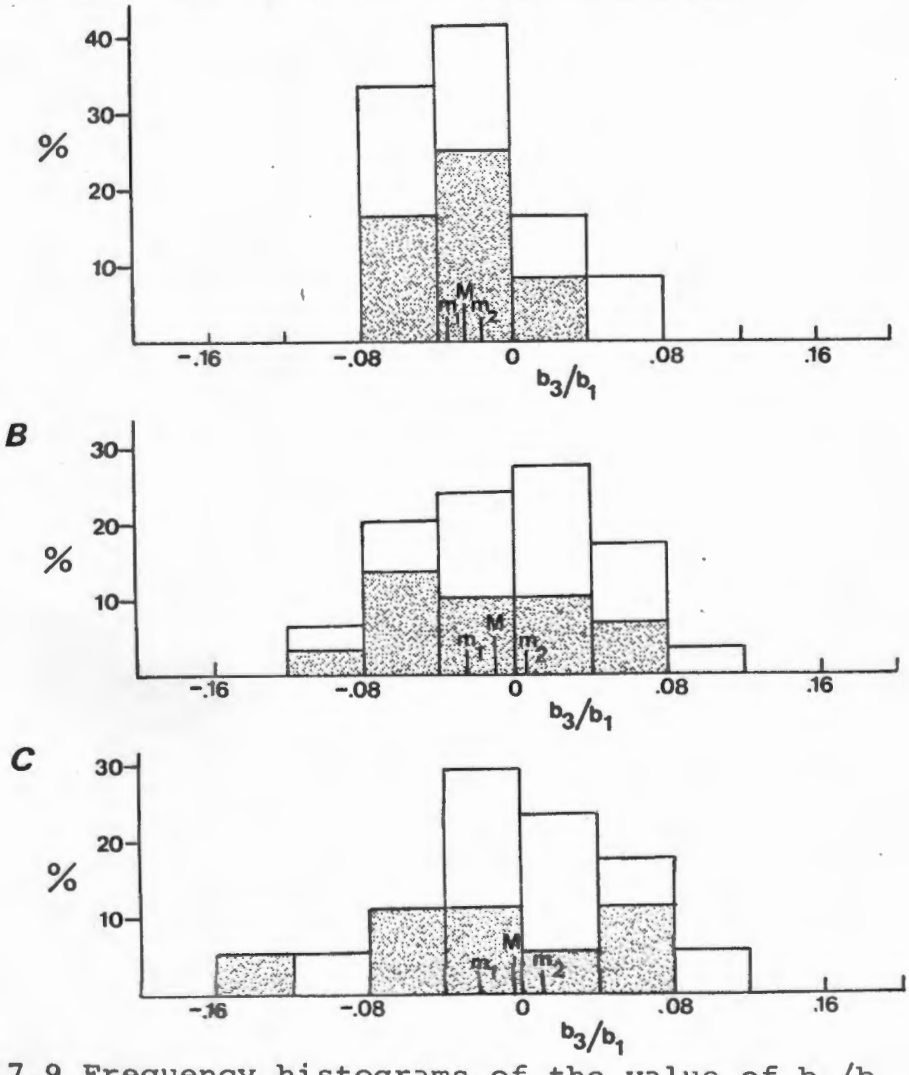

Fig.7.9 Frequency histograms of the value of b_3/b_1. See Fig.7.8 for further description.

7-3 FAULTS AND JOINTS

A variety of planar discontinuities, which are not confined to any particular subarea, occur at Bloubergstrand.

7-3-1 Faults

Brecciation and fault drag is associated with a number of major strike-slip faults. The faults have displacements in the order of metres. A conjugate fault pattern, comprised of dextral faults with a trend of ~030° NNW and sinistral faults trending ~070° NWW can be discerned from Map II.

7-3-2 Shear joints

The anastomosing network of bifurcating and rejoining sub-vertical fractures are a striking feature of the exposure.

An investigation of their orientations reveals that all directions are present, but that a distinct maximum is found between 140° and 150° and is accompanied by submaxima between 100° - 110° and 40° - 50° (See Fig.7.10). The lineaments about 145° are relatively longer than those of other directions.

The amount and sense of offset of the joints is largely unpredictable, although sinistral displacements appear to predominate. Prominent marker beds may terminate abruptly against the joints, with no counterpart being found across them.

The joint planes are sites of preferential pressure solution activity, frequently exhibiting quartz and calcite filling and deflection of the adjacent foliation towards parallelism with them.

7-3-3 Extension joints

In the isotropic rocks, straight a-c joints, with a NEE-SWW strike, roughly perpendicular to fold axes and foliation, are common. A subhorizontal joint set is invariably associated with quartz veining.

In some of the extension joints, as well as in tension gashes, in zone A, a blue-green mudstone filling is present, which may have been deposited during a late erosional period.

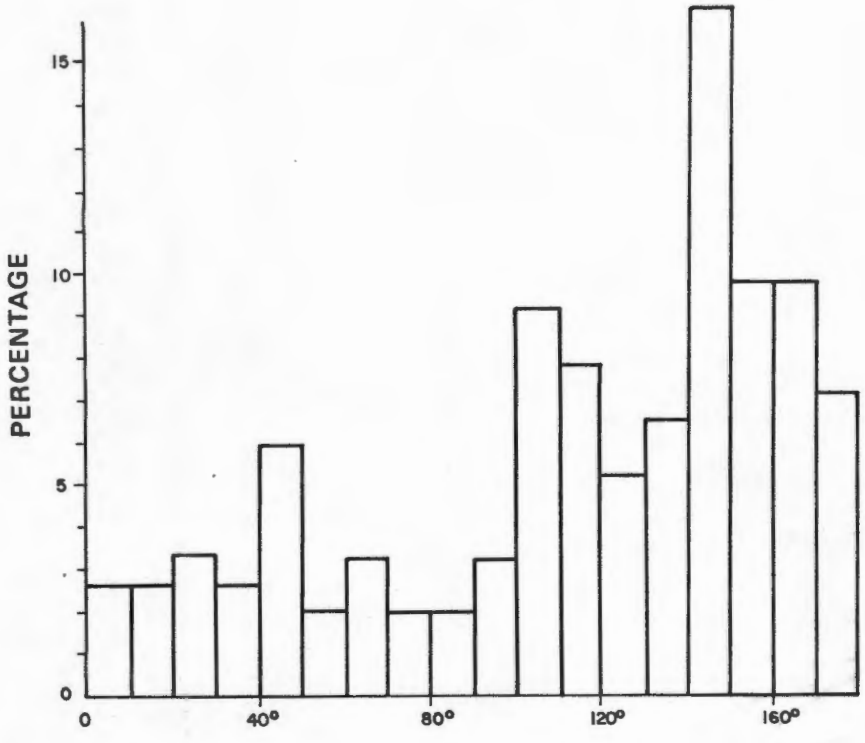

Fig.7.10 Histogram of frequency per azimuth (in %) of shear joints, longer than 10m, taken from Map II A-C. Frequency: n = 155.

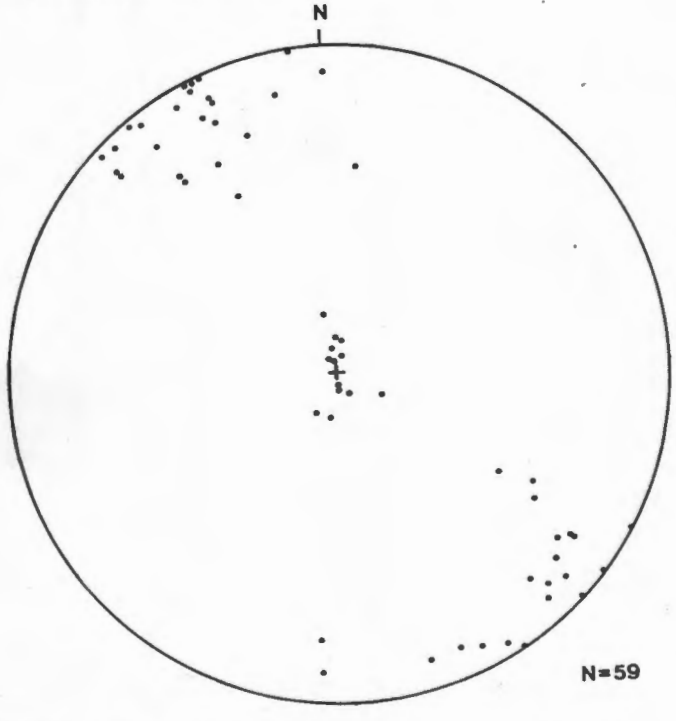

Fig.7.11 Lower hemisphere equal area stereographic plot of poles to extension joint planes.

7-4 KINEMATIC INTERPRETATION.

7-4-1 Early ductile simple shear event

The salient features of the minor folds described above, that are compatible with their initiation under a dominant simple shear regime are the following:

a) Their localised occurrence, both on an outcrop and a regional scale;
b) Their intimate association with shear zones;
c) Their asymmetry, non-cylindricity and non-periodicity;
d) The great circle distribution of the fold axes. During progressive simple shear deformation, fold axes rotate towards the prevailing maximum principal axis of the strain ellipsoid (Grocott & Watterson, 1980).

The gross difference in the strike of the layering on opposing sides of the shear zone is considered to be a consequence of large-scale drag folding.

The progressive north-eastward rotation in the strike of bedding to the south is somewhat enigmatic. An interpretation may be sought in:

a) A model of synsedimentary shearing;
b) Scissor-faulting with progressively increasing throw of the southwestern block, to the south; or
c) Further, obliquely oriented shearing immediately offshore.

7-4-2 Pure shear event

The following criteria form the basis for ascribing the structures related to the ~600 Ma orogenic episode to a later niche in the time scale than those related to the early ductile shearing event:

a) The extensive overprinting of fold structures by the regional foliation;
b) Similarity in orientation of superimposed folds to the regional (145°) trend (eg., Fig.7.4);
c) The ubiquitous evidence of a superimposed homogeneous strain component (Class 1b modified by Class 1c folds and hinge zone modifications). Parallel folds modified by a later heterogeneous shear parallel to the axial surface would have resulted in Class 1c modified by Class 1a folds (Ramsay, 1967, p.409).

The conjugate strike-slip faulting, the incipient NNW-striking fracture cleavage in competent zones and the relatively rare kink-bands and tension gashes could all be attributed to the tectonic relaxation which followed this event.

7-4-3 Late brittle simple shear

The pattern of the network of shear joints which cross-cuts the exposure bears a resemblance to that observed experimentally in a left-lateral wrench fault system, by Wilcox et al. (1973).

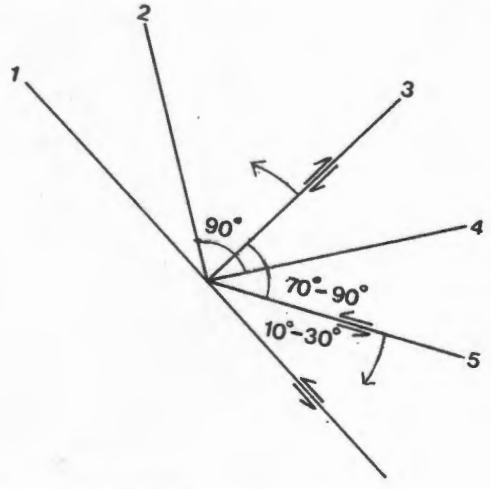

1) main wrench
2) minimum compression; en echelon folds
3) antithetic fault
4) maximum compression, normal faults
5) synthetic fault

Fig.7.12 The expected 'primary tectonic elements' for a left-lateral wrench fault system, based on the main wrench striking 145°.

Master joints at 145° and pinnate fractures at 45° and 110° are to be expected (Fig.7.10).

The fold axes orientations, however, are incompatible with this scheme, as is the sense of curvature of layering immediately north of Bokkombaai.

It is therefore proposed that early shearing was largely of a ductile, possibly dextral nature, and preceded the ~600 Ma orogenic event, whereas the later shearing which postdated this event, was of a brittle, mainly sinistral type. The latter period of rotational strain may have been extensive. Seismic activity is still being recorded in the region (Fernandez and Guzman, 1979).

The depressed elevation of the Cape Flats region compared to that of the flanking Cape Peninsula, Bottelaryberg and Drakenstein ranges, has been attributed to erosion along major NW - trending zones of structural weakness (Theron, 1974). Although the evidence for such zones is hidden by the extensive recent sand cover, the shearing phenomenon at Bloubergstrand does lend support for their existence.

7-5 CONCLUDING REMARK

It should be borne in mind that the above structural and kinematic interpretations may well be somewhat idealized. The intention of the study, however, was to provide a framework for further research into the undoubtedly complex deformational history of this exposure.

8 CONCLUSION

8-1 TECTONIC EVOLUTION OF THE TYGERBERG TERRANE

8-1-1 Parameters for a model

The following observations are of fundamental importance to the formulation of an integrated model of the tectonic evolution of the Tygerberg terrane:

a) The Malmesbury Group appears to have formed adjacent to a continental margin (Kalahari Province) to the northeast;
b) Two major pre-Cape fault zones divide the Malmesbury Group into three domains, with differing tectonic characteristics. Polyphase deformation in the central domain contrasts with simple folds of a single generation in the southwestern domain and in parts of the northeastern domain;
c) The sediments of the Tygerberg terrane appear to have been derived from a proximally located source (Chap. 6);
d) The Cape granites in places intrude and in other places are in tectonic contact with the Malmesbury Group. Although a 'post-Malmesbury' age for the Cape granites has been repeatedly demonstrated from intrusive contacts such as the one at Sea Point, Hartnady (1969, p. 60) cites evidence such as peripheral deformation of granites and a lack of contact thermal metamorphism to support a 'pre-Malmesbury' age for some granitic rocks in the Boland.

In the last decade, an overwhelming amount of evidence has demonstrated the association of compressive and magmatic mobile belts with zones of crustal subduction at continental margins. By analogy, it seems possible that subduction was occurring beneath the western margin of the Kalahari Province during the late-Precambrian deformation of the Malmesbury formations.

A recent approach towards the understanding of the tectonics of the subduction model has been to recognize the existence of two basically different models of subduction (Uyeda, 1982; Dewey, 1982): One in which the subducting plate and the upper landward plate are closely coupled causing a compressional stress regime in the arc and back arc regions (Chilean-type); the other in which they are virtually decoupled causing a tensional stress regime and extensional spreading in the back arc region (Mariana-type). The mode of subduction may be controlled by the motion of the upper plate relative to the subducting slab; or the different modes may represent different stages of an evolutionary process: subduction starts in the former mode and evolves towards the latter mode as the angle of thrusting increases with increasing age and weight of the subducting slab.

The subduction model which is outlined below and schematically illustrated in Fig.8.1 utilizes this two basic modes to account for the above features. Terminology follows that of Dickinson and Seely (1979) and Dewey (1982).

8-1-2 The model

early depositional phase

A compressional (Chilean-type) arc-trench system was generated by plate consumption adjacent to the continental margin. The arc- and back-arc derived sediments of the Swartland Subgroup in the central domain were deposited in the fore-arc region.

It has been estimated that the maximum age for the deposition of the Malmesbury Group lies within the range of late ages for the '1000 million year event' in southern Namaqualand and from granitic samples cored beneath the Karroo in the western Cape Province i.e. from 830-980 Ma (Hartnady et al., 1974).

early compressive phase

Continued underthrusting by the oceanic plate led to complex Cordilleran- type deformation and emplacement of the older, 'basement' granites.

late depositional phase

The mode of subduction evolved to the Mariana-type, resulting in the formation of an outward-migrating extensional arc.

The turbiditic and hemipelagic sediments of the Tygerberg terrane in the southwestern domain accumulated as submarine fans in the newly-formed fore-arc basin, whereas the sediments of the Boland subgroup in the northeastern domain were deposited in the foundering back-arc region.

A minimum age for this phase may be the Rb-Sr isochron of 595±45 Ma determined by Allsop and Kolbe (1965) from pelites of the Tygerberg terrane. They concluded that it represented the date of 'isotopic homogenization' by diagenesis or metamorphism of the rocks and that the deposition cannot have greatly exceeded this age.

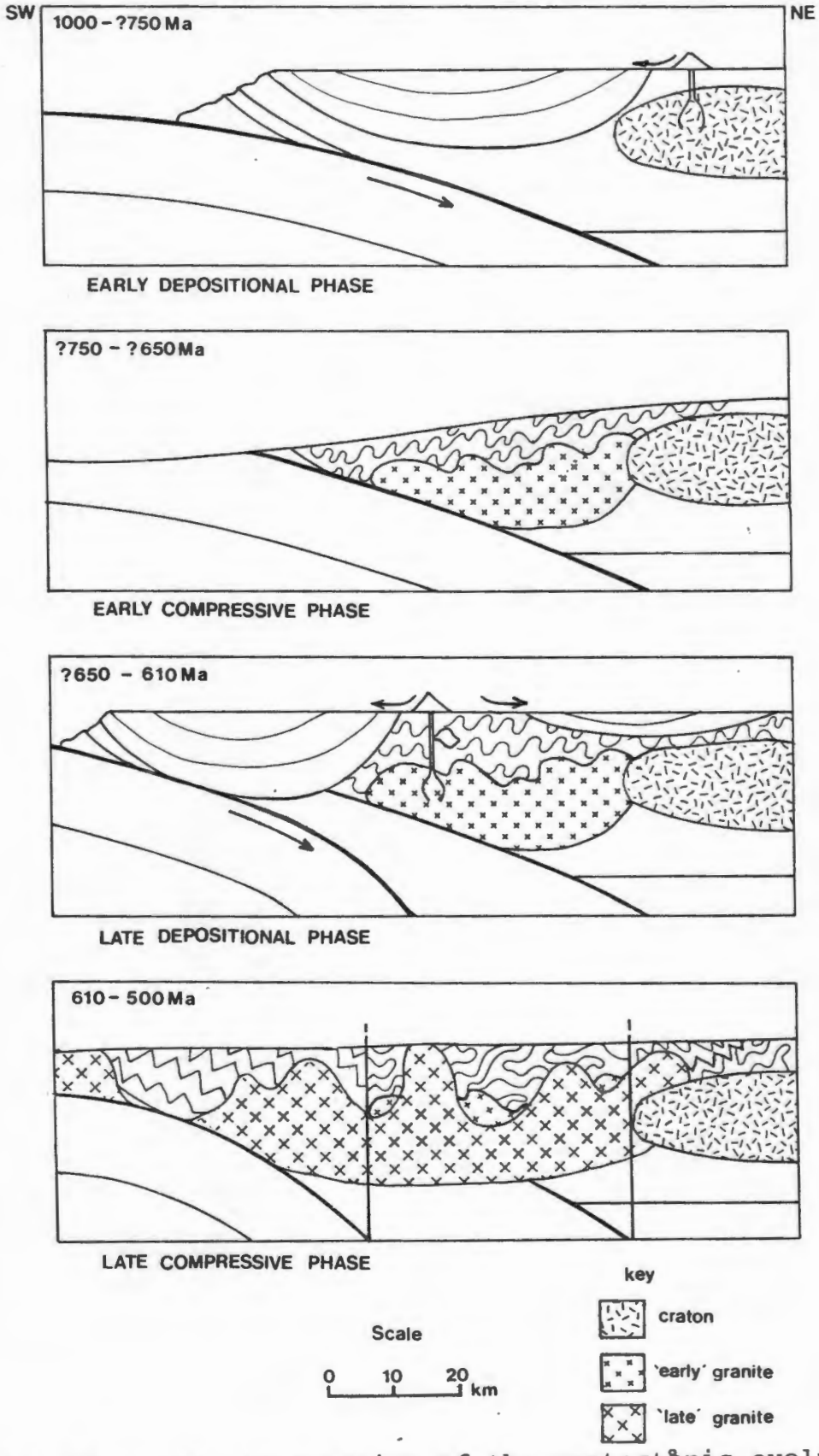

Fig.8.1 Schematic illustration of the geotectonic evolution of the Malmesbury Group.

late compressive phase

Continued subduction or collision with an exotic terrane resulted in cessation of deposition, deformation of all the previously formed sediment and the production of wide spread plutonism (the 'intrusive' granite batholiths). The granites were emplaced as small diapic plutons which deformed the adjacent country rock.

On the available isotopic evidence Hartnady et al., (1974) considered this orogenic episode to have spanned the time from 500 Ma to about 610 Ma.

8-1-3 Conclusion: a cautionary note

Although a model of this kind may provide some solutions, many problems remain:
No direct evidence of a subduction zone such as ophiolites, tectonic melanges, or blue shist have been found in the Malmesbury Group; Some areas of complex deformation are to be found in the northeastern domain (Hartnady, 1969); The sense of symmetry of the late crenulation cleavage fabric in the Porseleinberg formation of the Swartland subgroup is incompatible with a NE-dipping subduction zone.

Perhaps the tectonic evolution of the Malmesbury Group will become clearer when the relative importance of the collision/ accretion process in the formation of orogenic belts and even the role of rigid plate interactions during the Precambrian Era are more fully understood.

9 REFERENCES CITED

ALLSOPP, H.L. and KOLBE, P., 1965 - Isotopic age determinations on the Cape granite and intruded Malmesbury sediments, Cape Peninsula, South Africa: Geochem. Cosmochim. Acta., 29, 1115-1130.

BARKER, O.B., 1980 - Palaeo-proof from the piddock. Nuclear Active, 22, 2-8.

BARRIERE, M., 1977 - Deformation associated with the Ploumanac'h intrusive complex, Brittany. J. geol. Soc. London, 134, 311-324.

BECK, M., COX, A. and JONES, D.L., 1980 - Penrose conference report - Mesozoic and Cenozoic microplate tectonics of western North America. Geology, 8, 454-456.

BEESON, R., 1975 - Petrography of sediments of the Malmesbury Group in the Philadelphia area, Cape Province. Ann. Geol. Surv., 11, 129-134.

BOOCOCK, C., 1956 - The structural features and inclusions of the Cape Peninsula granite. Trans. R. Soc. S.Afr., 33, 243-277.

BOUMA, A.H., 1962 - Sedimentology of some flysch deposits. Elsevier, 168 pp.

BURGER, A.J. and COERTZE, F.J., 1973 - Radiometric age measurements on rocks from southern Africa to the end of 1971. Geol. Surv. S. Afr., 58.

CHARLESWORTH, H.A.K., LANGENBERG, C.W. and RAMSDEN, J., 1976 - Determining axes, axial planes and sections of macroscopic folds using computer-based methods. Can. J. Earth. Sci., 13, 54-65.

COBBOLD, P.R., 1979 - Removal of finite deformation using strain trajectories. J. Struct. Geol., 1, 67-72.

COWARD, M.P. and JAMES, P.R., 1974 - The deformation patterns of two Archaean greenstone belts in Rhodesia and Botswana. Precamb. Res., 1, 235-258.

DE POAR, D.G., 1980 - Some limitations of the Rf/ϕ technique of strain analysis. Tectonophysics, 64, T29-T31.

----------, 1981 - Some limitations of the Rf/ϕ technique of strain analysis - A reply. Tectonophysics, 81, 158.

DE VILLIERS, J.E., 1980 - The geology of the country between Bellville and Agter Paarl. Trans. geol. Soc. S. Afr., 83, 63-67.

DEWEY, J.F., 1982 - Episodicity, sequence, and style at convergent plate boundaries. Geol. Assoc. Canada, Spec. Paper 20, 552-573.

DICKINSON, W.R. and SEELY, D.R., 1979 - Structure and stratigraphy of forearc regions. Bull. Am. Ass. Petrol. Geol., 63, 2-31.

DU TOIT, A.L., 1954 - The geology of South Africa. 3rd Ed. Oliver and Boyd. 611 pp.

DUNNET, D. and SIDDANS, A.W.B., 1971 - Nonrandom sedimentary fabrics and their modification by strain. Tectonophysics, 12, 307-325.

ENOS, P., 1969 - Anatomy of a flysch. J. sedim. Petrol., 39, 680-723.

FERNANDEZ, L.M. and GUZMAN, J.A., 1979 - Seismic history of Southern Africa. Seismol. Ser. geol. Surv. S. Afr, 9, 20 pp.

GALLOWAY, S., 1978 - A metamorphic, structural and mineralogical consideration of the Tygerberg formation. Unpubl. B.Sc. Hons. Thesis, Dept. of Geology, Univ. Cape Town, 35 pp.

GENDZWILL, D.J. and STAUFFER, M.R., 1981 - Analysis of triaxial ellipsoids: Their shapes, plane sections, and plane projections. Math. Geol., 13, 2, 135-150.

GROCOTT, J. and WATTERSON, J., 1980 - Strain profile of a boundary within a large ductile shear zone. J. Struct. Geol., 2, 111-118.

GRAY, N.H., GEISER, P.A. and GEISER, J.R., 1980 - On the least squares fit of small and great circles to spherically projected orientation data. Jour. Math. Geol., 12, 173-184.

GRESSE, P.G., 1976 - The structure and metamorphism of the pre-Cape rocks in the coastal strip, south of George. Unpubl. M.Sc. thesis, Univ. Stellenbosch.

GUJ, P., 1970 - The Damara Mobile Belt in the southwestern Kaokoveld, southwest Africa. Bull. Precambr. Res. Unit, Univ. Cape Town, 8, pp.

HARTNADY, C.J., 1969 - Structural analysis of some pre-Cape formations in the Western Province. Bull. Precambr. Res. Unit, Univ. Cape Town, 6, 69 pp.

----------, NEWTON, A.R. and THERON, J.N., 1974 - Stratigraphy and structure of the Malmesbury Group in the southwestern Cape. Bull. Precambr. Res. Unit, Univ. Cape Town, 15, 193-213.

HAUGHTON, S.H., 1933 - The geology of Cape Town and ajoining country. Expl. of sheet 247. Geol. Surv. S. Afr.

----------, 1969 - Geological history of Southern Africa. Oliver and Boyd, 535 pp.

HESSE, R., 1974 - Long-distance continuity of turbidites: possible evidence for an Early Cretaceous trench-abyssal plain in the East Alps. Bull. geol. Soc. Am., 85, 859-870.

HILDEBRAND - MITTLEFEHLDT, N. and OERTEL, G., 1980 - Strain determination from the measurement of pebble shapes: the special case of a bent foliation. Tectonophysics, 67, T1-T7.

HOAL, B.G., 1979 - The tectonic significance of pre-Cape calc-alkaline rocks in the southwestern Cape Province, with special reference to the Brewelskloof area (Abstract). In: Geol. Soc. S. Afr., GEOKONGRES, 79, Part I, 462 pp.

HOLDER, M.T., 1978 - Granite emplacement models (Abstract). In: UPTON, B.G.J., Emplacement and crystallisation of minor intrusives. Geol. Soc. London, 135, 459.

HOSSACK, J.R., 1968 - Pebble deformation and thrusting in the Bygdin area (Southern Norway). Tectonophysics, 5, 315-339.

HOYT, W.H. and FOX, P.J., 1977 - Long-distance turbidite correlations in Horseshoe Abyssal Plain. Bull. Am. Ass. Petrol. Geol., 61, 797.

HUDLESTON, P.J., 1973 - Fold morphology and some geometrical implications of theories of fold development. Tectonophysics, 16, 1-46.

INGRAM, R.L., 1954 - Terminology for the thickness of stratification and parting units in sedimentary rocks. Geol. Soc. Am. Bull, 65, 937-938.

KRONER, A., 1974 - The Gariep Group, Part I: Late Precambrian formations in the western Richtersveld, northern Cape Province. Bull. Precambr. Res. Unit, Univ. Cape Town, 13, 115 pp.

KUENEN, Ph.H. and MIGLIORINI, C.I., 1950 - Turbidity currents as a cause of graded bedding. Jour. Geol., 58, 91-127.

----------, 1963 - Turbidites in South Africa. Trans. geol. Soc. S. Afr., 66, 19-24.

----------, 1964 - Deep-sea sands and ancient turbidites. In: BOUMA, A.H., (Ed.), Turbidites, Elsevier, 264 pp.

LE ROUX, J.P., 1977 - The stratigraphy, sedimentology and structure of the Cango Group, North of Outshoorn. Unpubl. M.Sc. thesis, Univ. Stellenbosch.

LISLE, R.J., 1977 - Estimation of the tectonic strain ratio from the mean shape of deformed elliptical markers. Geol. Mijnbouw, 56, 140-144.

MILLER, D.M. and OERTEL, G., 1979 - Strain determination from the measurement of pebble shapes: a modification. Tectonophysics, 55, T11-T13.

MUTTI, E., 1977 - Distinctive thin-bedded turbidite facies and related depositional environments in the Eocene Hecho Group (South-central Pyrenees, Spain). Sedimentology, 24, 107-131.

---------, and RICCI LUCCHI, F., 1972 - Le torbiditi dell' Apennino settentrionale: introduzione all'analisi di facies. Mem. Soc. Geol. Ital., 11, 161-199.

NADAI, A., 1968 - Theory of Flow and Fracture of Solids. Eng. Soc. Monogr., McGraw Hill, New York, N.Y., 705 pp.

NORMARK, W.R., 1978 - Fan valleys, channels and depositional lobes on modern submarine fans: Characters for recognition of sandy turbidite environments. Bull. Am. Ass. Petrol. Geol., 62, 912-931.

OERTEL, G., 1978 - Strain determination from the measurement of shapes. Tectonophysics, 50, T1-T7.

OERTEL, G., 1981 - Strain estimation from scattered observations in an inhomogeneously deformed domain of rocks. Tectonophysics, 77, 133-150.

PEACH, C.J. and LISLE, R.J., 1979 - A Fortran IV programme for the analysis of tectonic strain using deformed elliptical markers. Comp. and Geosc., 5, 325-334.

PITCHER, W.S., 1979 - The nature, ascent and emplacement of granitic magmas. J. geol. Soc. London, 136, 627-662.

----------, and BERGER, A.R., 1972 - The Geology of Donegal: A study of Granite Emplacement and Unroofing. Wiley Intersci., N.Y., 434 pp.

PORADA, H. and WITTIG, R., 1976 - Das Chausib-Turbidit becken am Sudrand des Damara-Orogens, Sudwest-Afrika. Geol. Rundsch. 65, 1002-1019.

QUESTIAUX, J.M., 1978 - Aspects of the stratigraphy, structure and sedimentology of the Tygerberg formation, in the northwestern Cape Peninsula. Unpubl. B.Sc. Hons. Thesis, Dept. of Geology, Univ. Cape Town, 47 pp.

RAMBERG, H., 1970 - Model studies in relation to intrusion of plutonic bodies. In: NEWALL, G. and RAST, N. (eds.). Mechanism of igneous intrusion. Spec. Iss. Geol. J., 2, 261-286.

RAMSAY, J.G., 1967 - Folding and fracturing of rocks. Mc-Graw Hill, 568 pp.

----------, 1974 - Development of chevron folds. Bull. geol. Soc. Am., 85, 1741-1754.

----------, 1975 - The structure in the Chindamora Batholith (Abstract). Annu. Rep. res. Inst. Afr. Geol. Leeds, 19, 81.

READ, H.H., 1951 - Metamorphism and granitisation: Alex L. du Toit Mem. Lect. No. 2. Trans. geol. Soc. S. Afr., 54 (annex.), 27 pp.

REINECK, H.E. and SINGH, I.B., 1975 - Depositional sedimentary environments. Springer Verlag, 439 pp.

ROGERS, A.W. and DU TOIT, A.L., 1909 - An introduction to the geology of the Cape Colony. Longmans, Green and Co., 491 pp.

SCHOCH, A.E., LEYGONIE, F.E. and BURGER, A.J., 1975 - U-Pb ages for Cape granites from the Saldanha batholith: A preliminary report. Trans. geol. Soc. S. Afr., 7, 97-100.

----------, LETERRIER, J. and DE LA ROCHE, H., 1977 - Major element geochemical trends in the Cape Granites. Trans. geol. Soc. S. Afr., 80, 197-209.

SCHOLTZ, D.L., 1946 - On the younger Pre-Cambrian plutons of the Cape Province. Proc. geol. Soc. S. Afr., 49, 35-82.

SCHWARZ, E.H., 1913 - The Sea Point granite-slate contact. Trans. geol. Soc. S. Afr., 16, 33-38.

SEYMOUR, D.B. and BOULTER, C.A., 1979 - Tests of computerized strain analysis methods by the analysis of simulated deformation of natural unstrained sedimentary fabrics. Tectonophysics, 58, 221-235.

SHERWIN, J.A. and CHAPPLE, W.M., 1968 - Wavelengths of single layer folds: Comparison between theory and observation. Am. J. Sci., 266, 199-213.

SKIPPER, K. and MIDDLETON, G.V., 1975 - The sedimentary structures and depositional mechanisms of certain Ordovician turbidites, Cloridorme Formation, Gaspe Peninsula, Quebec. Can. J. Earth Sci., 12, 1934-1952.

SOUTH AFRICAN COMMITTEE FOR STRATIGRAPHY (SACS), 1980 - Stratigraphy of South Africa, Part I (Comp. L. E. Kent). Lithostratigraphy of the Republic of South Africa, etc. Handb. Geol. Surv. S. Afr., 8.

STABLER, C.L., 1968 - Simplified Fourier analysis of fold shapes. Tectonophysics, 6, 343-350.

STUMP, E., 1976 - On the late Precambrian - early Proterozoic metavolcanic and metasedimentary rocks of the Queen Maud mountains, Antartica, and a comparison with rocks of similar age for Southern Africa. Inst. of Polar Studies, Ohio State Univ., 62, 1-212.

TANKARD, A.J., ERIKSSON, K.A., HOBDAY, D.K., HUNTER, D.R., MINTER, W.E.L., 1981 - Crustal evolution of Southern Africa. Springer-Verlag. 480 pp.

THERON, J.N., 1974 - Die seismiese geskiedenis van die Suid-westelike Kaapprovinsie. In: Seismol. Ser. geol. Surv. S. Afr., 4, 48 pp.

TRUSWELL, J.F., 1977 - The geological evolution of South Africa. Rustica Press. 218 pp.

UYEDA, S., 1982 - Subduction zones: An introduction to comparative subductology. Tectonophysics, 81, 133-159.

VON VEH, M., 1980 - Development of systems for digitizer and computer in the study of structural fabrics, and their application to selected samples from the Malmesbury Group. Unpubl. B.Sc. Hons. Thesis, Univ. Cape Town, 37 pp.

WALKER, F. and MATHIAS, M., 1946 - The petrology of two granite-slate contacts at Cape Town, South Africa. Quart. J. geol. Soc. London, 52, 499-521.

WALKER, R.G., 1967 - Turbidite sedimentary structures and their relationship to proximal and distal depositional environments. J. sedim. Petrol., 37, 25-43.

WALKER, R.G., 1978 - Deep-water sandstone facies and ancient submarine fans: Models for exploration for stratigraphic traps. Bull. Am. Ass. Petrol. Geol. 62, 932-966.

WATSON, G.S., 1965 - Equatorial distributions on a sphere. Biometrika, 52, 193-203.

WHITEHEAD, A. and LUTHER, D.S., 1975 - Dynamics of laboratory diapir and plume models. J. geophys. Res., 80, 705-717.

WILCOX, R.E., HARDING, T.P. and SEELY, D.R., 1973 - Basic wrench tectonics. Bull. Am. Ass. Petrol. Geol., 57, 74-96.

APPENDIX A

PROGRAMME DESCRIPTIONS

A brief description of each of the major computer programmes, implemented during the course of this study is given below. Source and executable versions of these programmes are located on the University of Cape Town Univac 1100 mainframe or Dept. of Geochemistry HP1000 microcomputer. The appropriate references are given in brackets.

Structural analysis

MEANS - Computes a mean orientation, Fisher's K concentration parameter and a pooled estimate of K from stations where multiple readings of structural orientation are available (Charlesworth et al., 1976).

CYLTEST - Calculates the best-fit fold axis and the sum of squared errors, for cylindrical folds. A map is produced showing the magnitude of the deviation from cylindricity at each station (Charlesworth et al., 1976).

DOMROT - Rotates the orientations and space coordinates of surfaces in a domain, about a given point, so that its fold axis becomes parallel to that of an adjacent domain. This enables a composite section, with a constant direction of projection, across an area consisting of several cylindrical domains, to be constructed (Charlesworth et al., 1976).

SECT5 - Computes and plots cross sections of fold data (Charlesworth et al., 1976).

LSQFIT - Calculates the angular radius and direction cosines of the centre of the small circle, best fitting a given set of poles. Following the method of Gray et al. (1980), convergence to a best fit centre was not obtained and the programme requires further testing.

SHAPE - Calculates the first three harmonic coefficients of the Fourier Sine series, resulting from the analysis of a 'quarter-wavelength' unit, according to simplified expressions derived by Stabler (1968). The programme requires as input the digitized coordinates of points, at small intervals, between the hinge and inflection points. A plot of the third coefficient against the first is produced.

FOLDS - determines the parameters required for fold classification, based on the changes and rates of change of inclination of the two bounding surfaces of a fold profile (Ramsay, 1967). The two fold surfaces between the hinges and and inflection points are digitised at small intervals. The following parameters are determined for each point of intersection of a dip isogon with the fold surface :

i. Orthogonal thickness / thickness at the hinge.
ii. Thickness parallel to the axial surface / thickness at the hinge.
iii. Angle between the normal to the tangent to the fold surface and the dip isogon (Hudleston, 1973).

A plot of the first or second parameter against value of the dip isogon is produced.

Strain analysis

FOLDS - Features are incorporated in the above programme for assessing the amount of superimposed compressive strain in flattened parallel folds. Its value is empirically determined from the slope of the best-fit straight line of t'_α against $\cos^2\alpha$ (cf. Hudleston, 1973, p.38). The standard error provides a measure of the goodness of fit of the data to a model of homogeneous flattening of Class 1b parallel folds. Curves, representing the family of folds with various values of λ_2/λ_1 , the superimposed strain, can be plotted on the t'_α/α or T'_α/α plots for obtaining a visual estimate.

RPHIN - A programme for digitizing the estimated long and short axes of elliptical particles relative to a coordinate system. Axial ratios, long axes orientations, axes lengths and ellipse centroid positions are stored on disk file or magnetic tape. An option is incorporated for plotting an Rf/Phi scatter diagram.

THETA - Calculates the vector mean of Φ_F values, the median Φ_F direction, the strain ratio and range of acceptable strain values. χ^2 /strain ratio, Rf/Φ and Ri/Θ graphs are plotted (Peach & Lisle, 1979).

STRANE - Determines the strain ratio, original ratios and orientations of elliptical particles with a primary planar or semi-planar fabric (Dunnet & Siddans, 1971).

STRDET - Derives the strain ellipsoid from the ellipse measurements from three orthogonal sections. A second-rank tensor, associated errors, principal values and errors, principal axes direction angle matrix and errors, Lode's parameter and strain intensity are calculated. Histograms of tensor components relative to specimen coordinates are plotted (Oertel, 1978; Miller & Oertel, 1979). Corrections are undertaken if the orientation of the foliation plane is non-homogeneous (Hildebrand-Mittlefehldt & Oertel, 1980).

INVEL - Determines the strain ellipsoid for the case where the three plane sections are non-parallel (Gendzwill & Stauffer, 1981).

DEFORM - Calculates the change in orientation of a line or plane when subjected to a finite strain.

Sedimentary analysis

LOGIN - An interactive programme for inputting data from measured stratigraphic sections to a disk file in a coded format.

LOGPR - produces a symbolic bedding thickness log on a line printer from data entered via programme LOGIN.

LOGPL - plots a graphic log of a stratigraphic section on the HP7245 plotter/printer from data entered via programme LOGIN.

APPENDIX B

SEDIMENTOLOGICAL GRAPHS

Description of graphic logs

A brief description of the various columns and symbols in the sedimentological graphs follows:

Column 1 : Zone identification. This column is used to indicate the proposed zonal subdivision, based on rock type, bedding thicknesses and bedding properties.

Column 2 : Thickness of column in meters. Scale is 1:500.

Column 3 : Logarithmic layer thickness. Due to the small scale of the graphic log, this column was included to improve the representation of thickness variability. A rock unit was regarded as constituting a layer if it was bounded by a discrete change in lithology, or a sharp physical break, or both, and excludes laminations.

Column 4 : Rock type. Names are based on lithological grounds.


Sandstone.


Argillaceous sandstone.


Thin alternating siltstone/mudstone.


Greywacke.


Mudstone.

The different gradations of sharpness of the bedding planes are -

——— Sharp.

—··— Transition gradual, but rapid.

····· Transition gradual and slow.

A distinction is made between a flat and an irregular contact.

——— Flat contact.

 Irregular contact.

Column 6 : Bedding plane properties.

 Load casts.

 Ripple marks.

— Tool marks.

 Erosional surface.

Column 7 : Layer properties. This column has been subdivided into nine subcolumns, one for each property. The occurrence of every structure is designated in its subcolumn by a vertical block giving the interval over which it occurs.

 Massive.

 Graded.

 Straight laminations.

 Wavy laminations.

 Ripple-cross laminations.

 Slump structures.

 Scour structure.

 Convoluted laminations.

The last, blank subcolumn is intended for any additional layer properties and was, in this case, used to indicate the presence of intraclasts.

Column 8 : Remarks. Any comments regarding locality or sedimentalogical or structural features.

Graphic log of the SW limb, Rocklands Syncline.

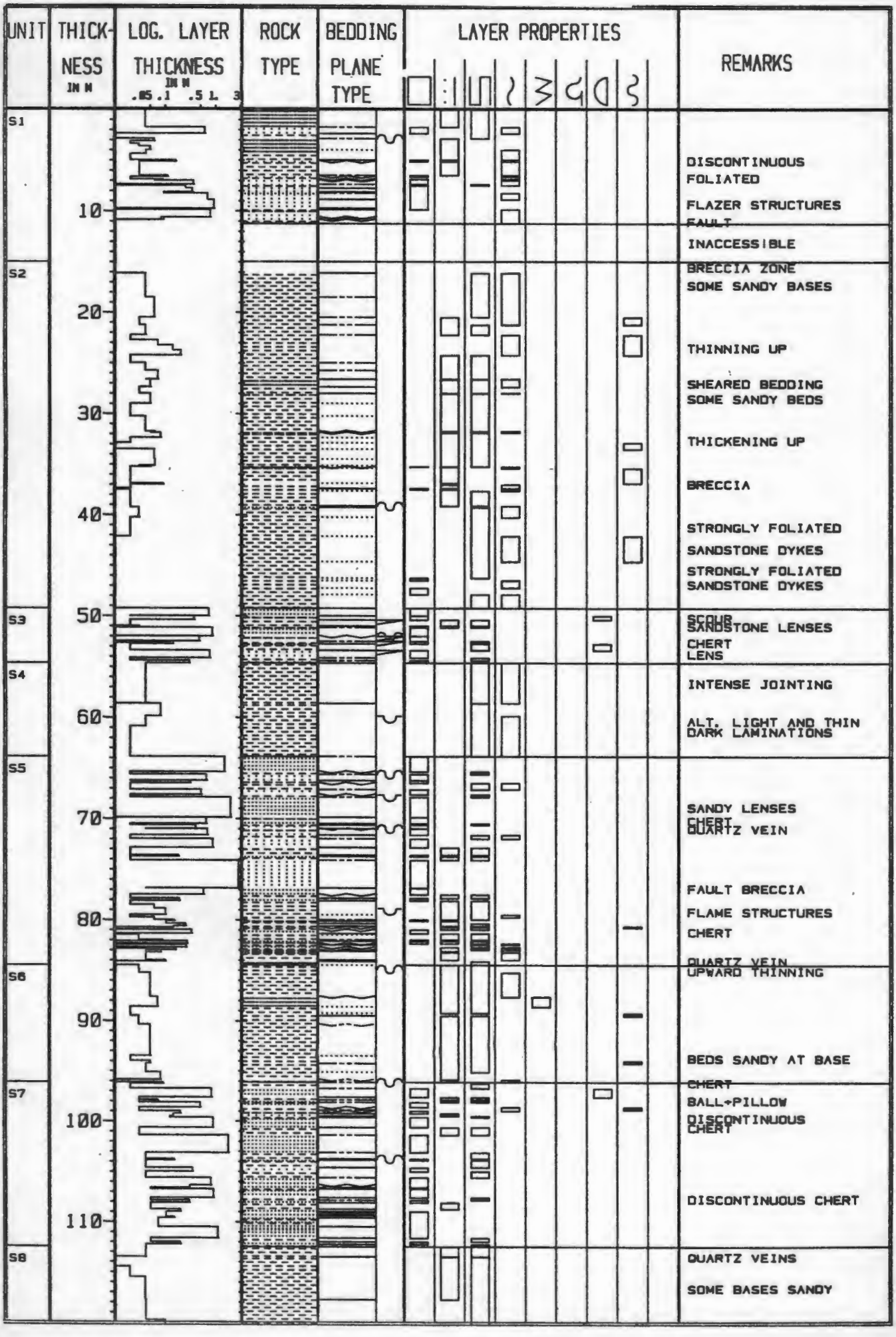

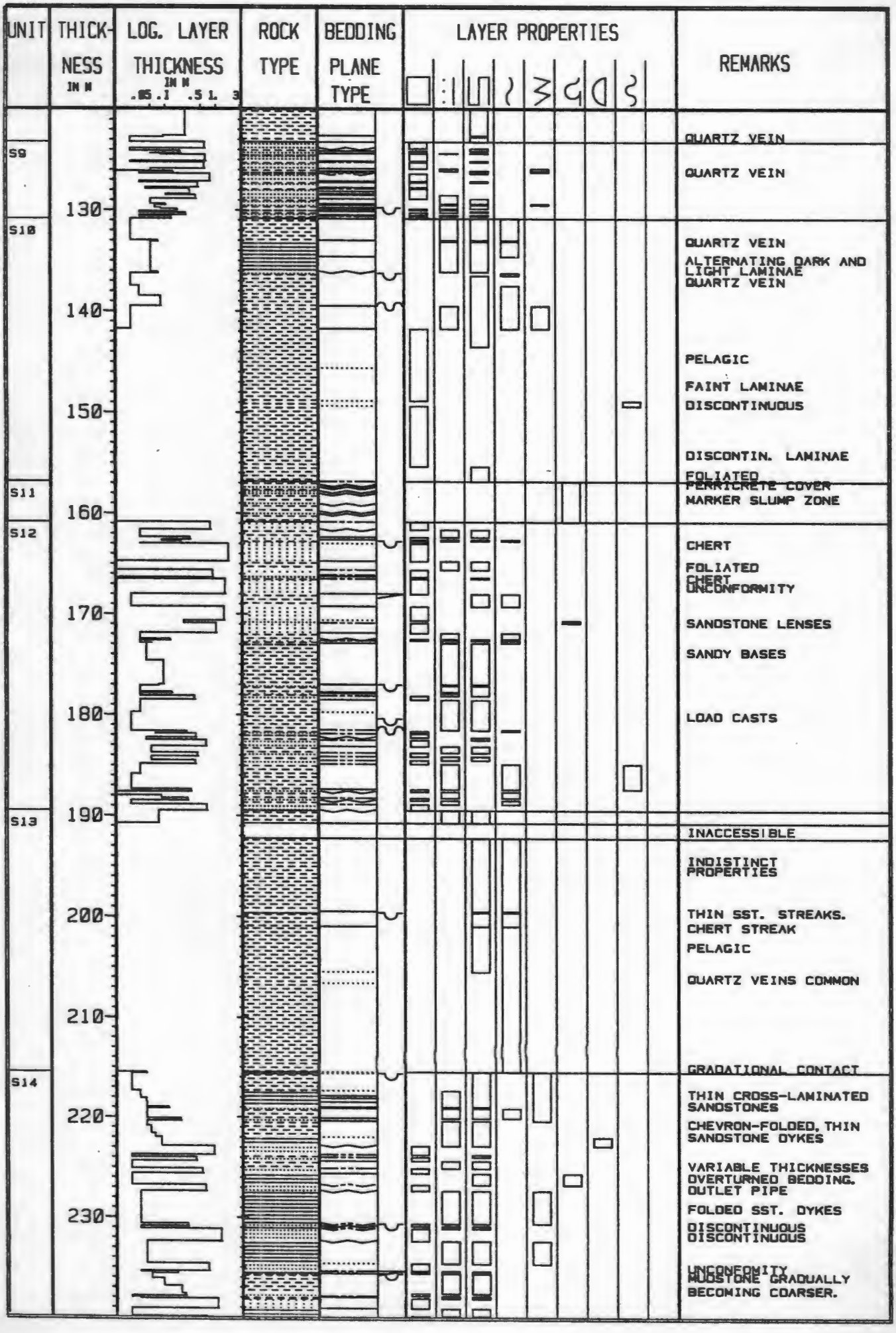
UNIT
THICK-NESS IN M
LOG. LAYER THICKNESS IN M .05 .1 .5 1. 3
ROCK TYPE
BEDDING PLANE TYPE
LAYER PROPERTIES
REMARKS
S9
S10
S11
S12
S13
S14
130
140
150
160
170
180
190
200
210
220
230
QUARTZ VEIN
QUARTZ VEIN
QUARTZ VEIN
ALTERNATING DARK AND LIGHT LAMINAE
QUARTZ VEIN
PELAGIC
FAINT LAMINAE
DISCONTINUOUS
DISCONTIN. LAMINAE
FOLIATED
FERRICRETE COVER
MARKER SLUMP ZONE
CHERT
FOLIATED CHERT
UNCONFORMITY
SANDSTONE LENSES
SANDY BASES
LOAD CASTS
INACCESSIBLE
INDISTINCT PROPERTIES
THIN SST. STREAKS.
CHERT STREAK
PELAGIC
QUARTZ VEINS COMMON
GRADATIONAL CONTACT
THIN CROSS-LAMINATED SANDSTONES
CHEVRON-FOLDED, THIN SANDSTONE DYKES
VARIABLE THICKNESSES
OVERTURNED BEDDING.
OUTLET PIPE
FOLDED SST. DYKES
DISCONTINUOUS
DISCONTINUOUS
UNCONFORMITY
MUDSTONE GRADUALLY BECOMING COARSER.

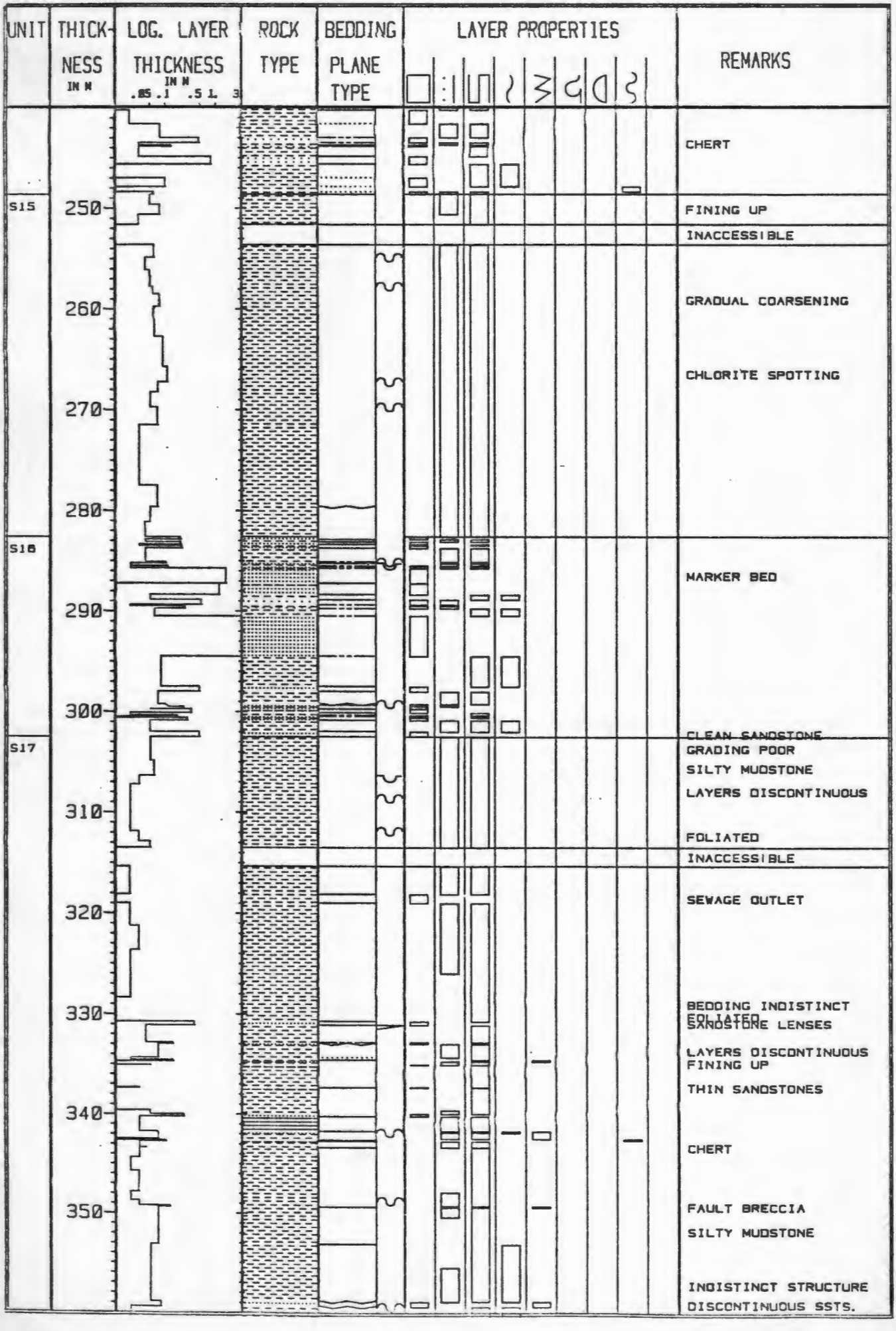
UNIT
THICKNESS IN M
LOG. LAYER THICKNESS IN M
.85 .1 .5 1.
ROCK TYPE
BEDDING PLANE TYPE
LAYER PROPERTIES
REMARKS
CHERT
S15
250
FINING UP
INACCESSIBLE
260
GRADUAL COARSENING
CHLORITE SPOTTING
270
280
S16
MARKER BED
290
300
CLEAN SANDSTONE
S17
GRADING POOR
SILTY MUDSTONE
LAYERS DISCONTINUOUS
310
FOLIATED
INACCESSIBLE
320
SEWAGE OUTLET
330
BEDDING INDISTINCT
FOLIATED
SANDSTONE LENSES
LAYERS DISCONTINUOUS
FINING UP
THIN SANDSTONES
340
CHERT
350
FAULT BRECCIA
SILTY MUDSTONE
INDISTINCT STRUCTURE
DISCONTINUOUS SSTS.

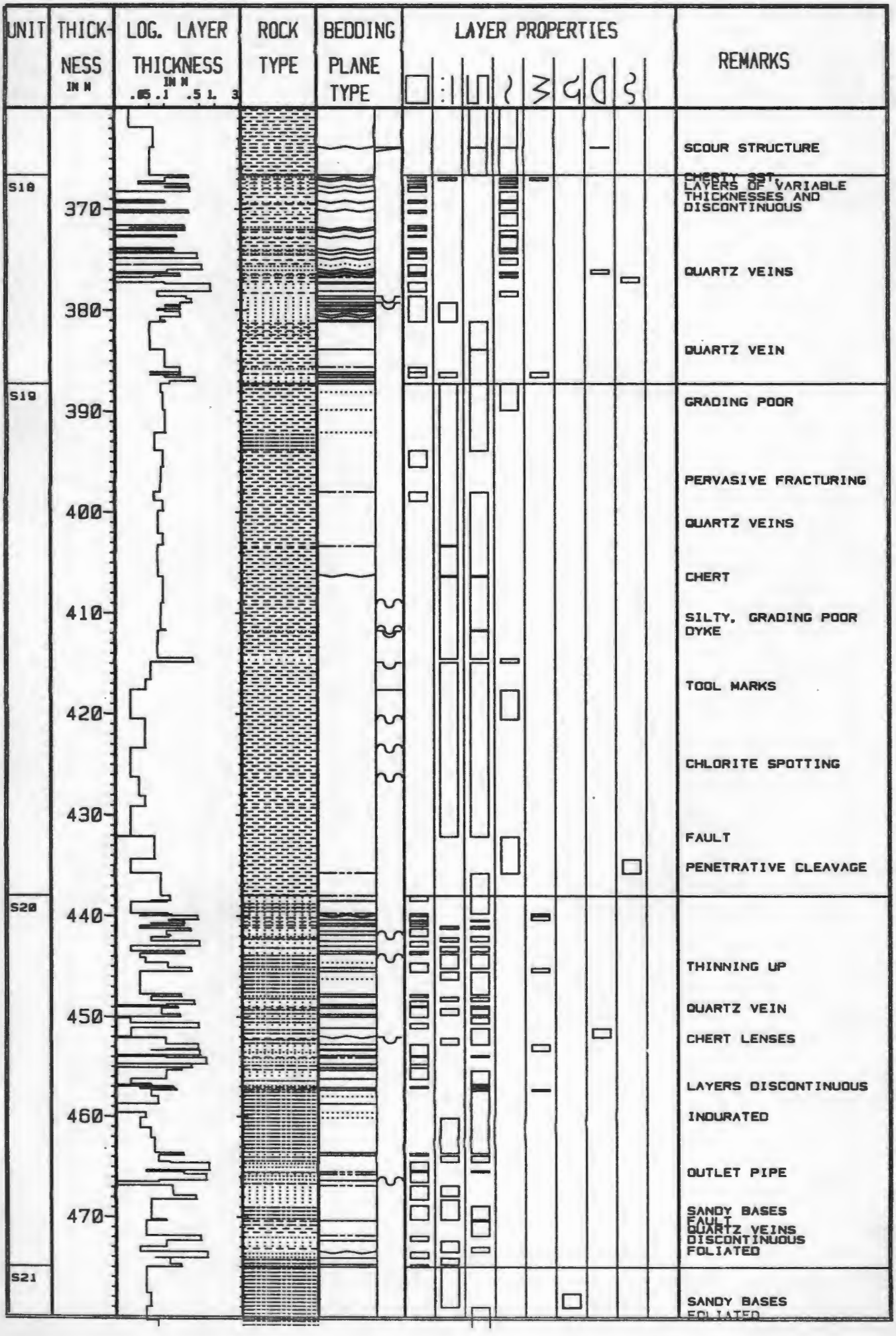
UNIT
THICKNESS IN M
LOG. LAYER THICKNESS IN M
.05 .1 .5 1. 3
ROCK TYPE
BEDDING PLANE TYPE
LAYER PROPERTIES
REMARKS
SCOUR STRUCTURE
S18
370
380
LAYERS OF VARIABLE THICKNESSES AND DISCONTINUOUS
QUARTZ VEINS
QUARTZ VEIN
S19
390
400
410
420
430
GRADING POOR
PERVASIVE FRACTURING
QUARTZ VEINS
CHERT
SILTY, GRADING POOR DYKE
TOOL MARKS
CHLORITE SPOTTING
FAULT
PENETRATIVE CLEAVAGE
S20
440
450
460
470
THINNING UP
QUARTZ VEIN
CHERT LENSES
LAYERS DISCONTINUOUS
INDURATED
OUTLET PIPE
SANDY BASES
FAULT
QUARTZ VEINS
DISCONTINUOUS
FOLIATED
S21
SANDY BASES
FOLIATED

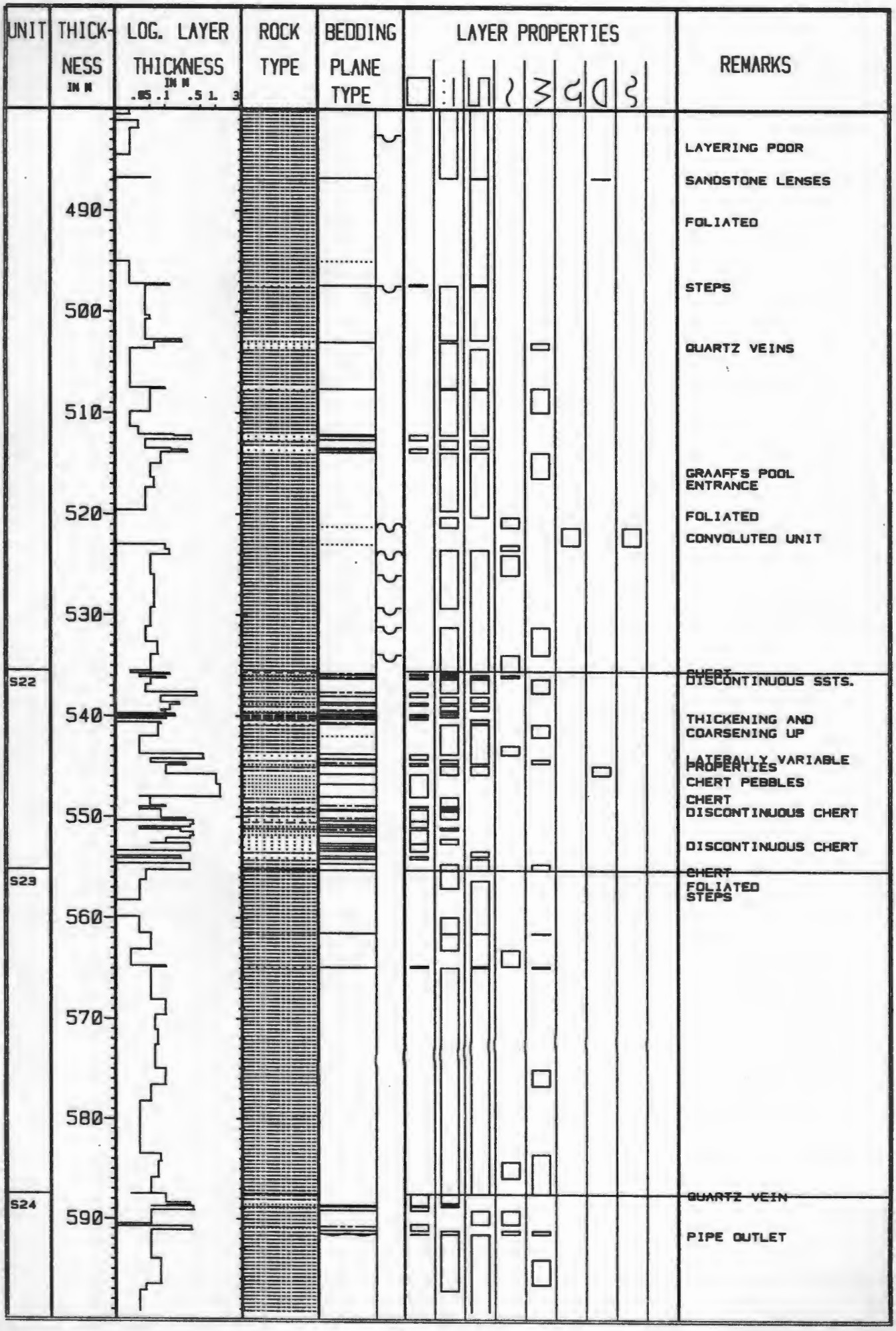
UNIT
THICK-NESS IN M
LOG. LAYER THICKNESS IN M .05 .1 .5 1. 3
ROCK TYPE
BEDDING PLANE TYPE
LAYER PROPERTIES
REMARKS
490
500
510
520
530
540
550
560
570
580
590
S22
S23
S24
LAYERING POOR
SANDSTONE LENSES
FOLIATED
STEPS
QUARTZ VEINS
GRAAFFS POOL ENTRANCE
FOLIATED
CONVOLUTED UNIT
CHERT
DISCONTINUOUS SSTS.
THICKENING AND COARSENING UP
LATERALLY VARIABLE PROPERTIES
CHERT PEBBLES
CHERT
DISCONTINUOUS CHERT
DISCONTINUOUS CHERT
CHERT
FOLIATED
STEPS
QUARTZ VEIN
PIPE OUTLET

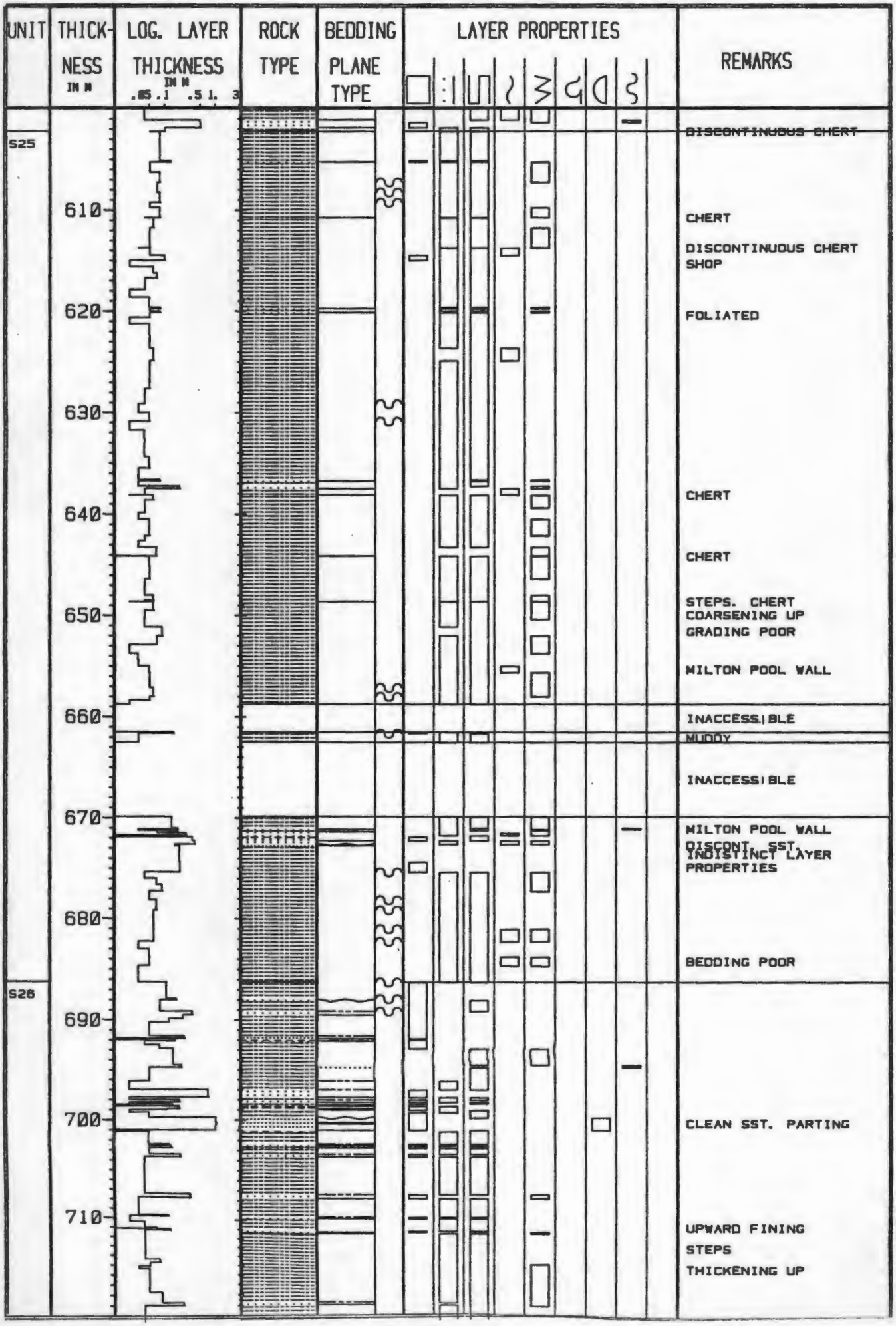
UNIT
THICK-NESS IN M
LOG. LAYER THICKNESS IN M .05 .1 .5 1. 3
ROCK TYPE
BEDDING PLANE TYPE
LAYER PROPERTIES
REMARKS
S25
S26
610
620
630
640
650
660
670
680
690
700
710
DISCONTINUOUS CHERT
CHERT
DISCONTINUOUS CHERT
SHOP
FOLIATED
CHERT
CHERT
STEPS. CHERT
COARSENING UP
GRADING POOR
MILTON POOL WALL
INACCESSIBLE
MUDDY
INACCESSIBLE
MILTON POOL WALL
DISCONT. SST.
INDISTINCT LAYER
PROPERTIES
BEDDING POOR
CLEAN SST. PARTING
UPWARD FINING
STEPS
THICKENING UP

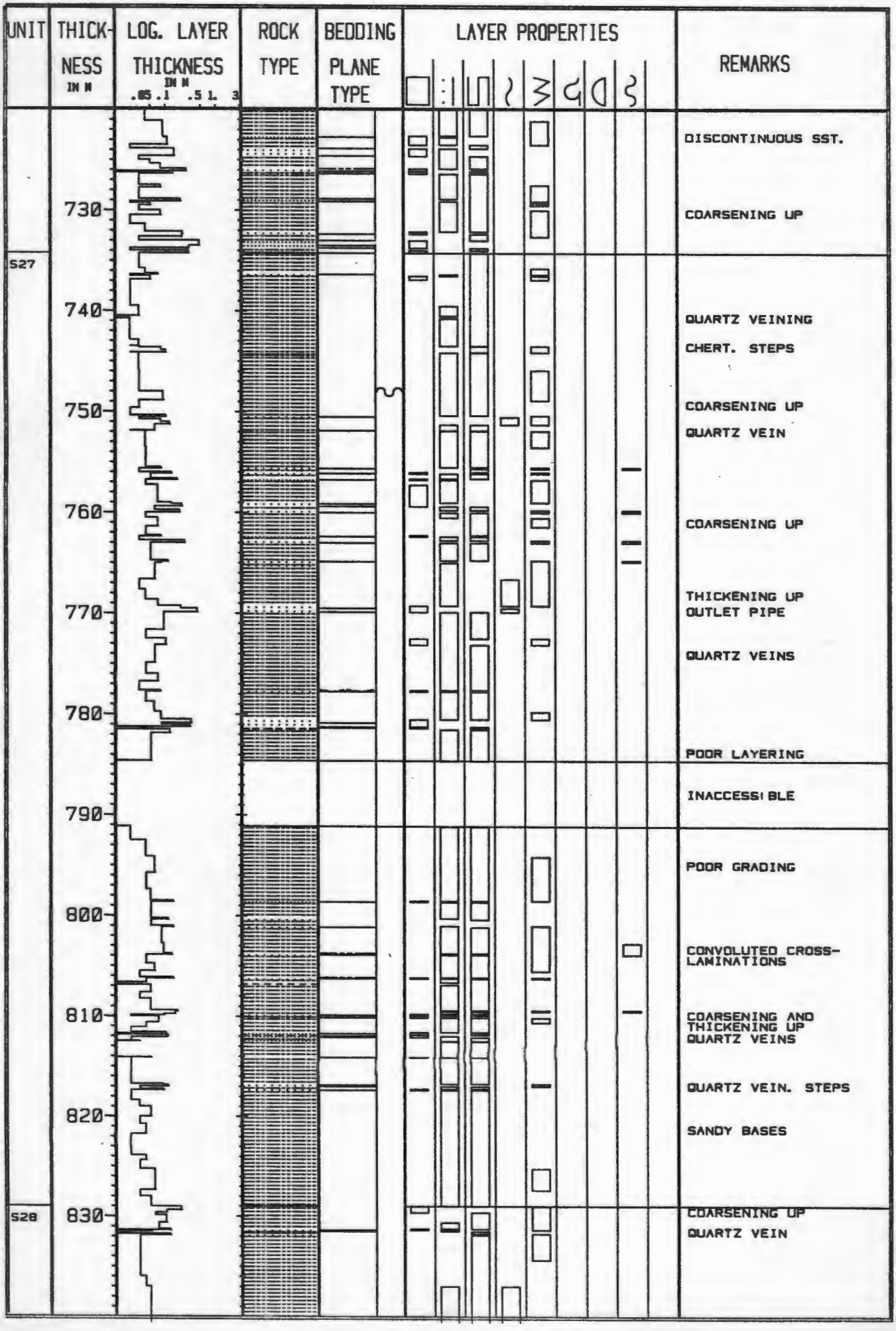
UNIT
THICK-NESS IN M
LOG. LAYER THICKNESS IN M .05 .1 .5 1. 3
ROCK TYPE
BEDDING PLANE TYPE
LAYER PROPERTIES
REMARKS
730
740
750
760
770
780
790
800
810
820
830
S27
S28
DISCONTINUOUS SST.
COARSENING UP
QUARTZ VEINING
CHERT. STEPS
COARSENING UP
QUARTZ VEIN
COARSENING UP
THICKENING UP
OUTLET PIPE
QUARTZ VEINS
POOR LAYERING
INACCESSIBLE
POOR GRADING
CONVOLUTED CROSS-LAMINATIONS
COARSENING AND THICKENING UP
QUARTZ VEINS
QUARTZ VEIN. STEPS
SANDY BASES
COARSENING UP
QUARTZ VEIN

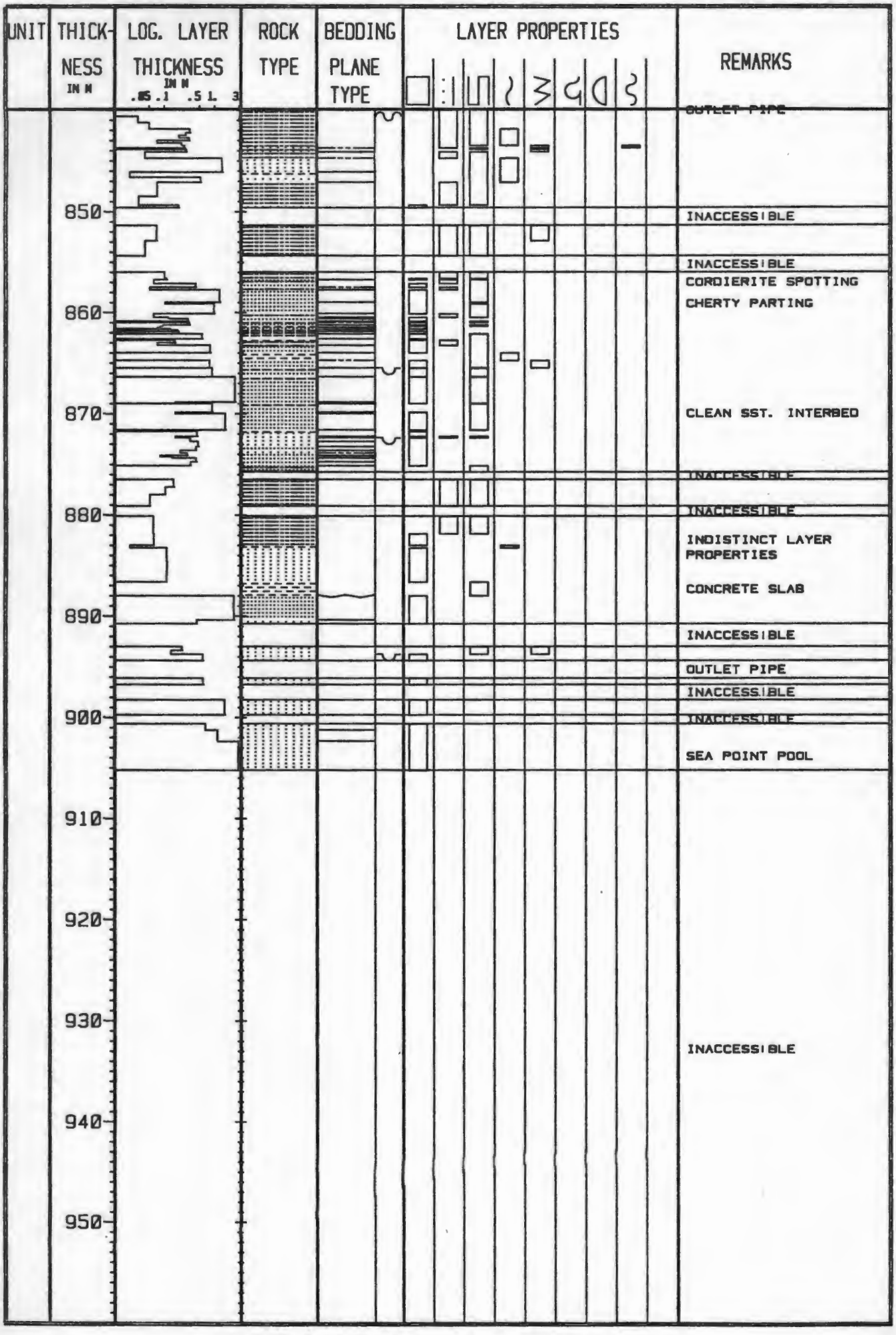
UNIT
THICK-NESS IN M
LOG. LAYER THICKNESS IN M .05 .1 .5 1. 3
ROCK TYPE
BEDDING PLANE TYPE
LAYER PROPERTIES
REMARKS
OUTLET PIPE
INACCESSIBLE
INACCESSIBLE
CORDIERITE SPOTTING
CHERTY PARTING
CLEAN SST. INTERBED
INACCESSIBLE
INACCESSIBLE
INDISTINCT LAYER PROPERTIES
CONCRETE SLAB
INACCESSIBLE
OUTLET PIPE
INACCESSIBLE
INACCESSIBLE
SEA POINT POOL
INACCESSIBLE
850
860
870
880
890
900
910
920
930
940
950

Graphic log of the NE limb, Rocklands Syncline.

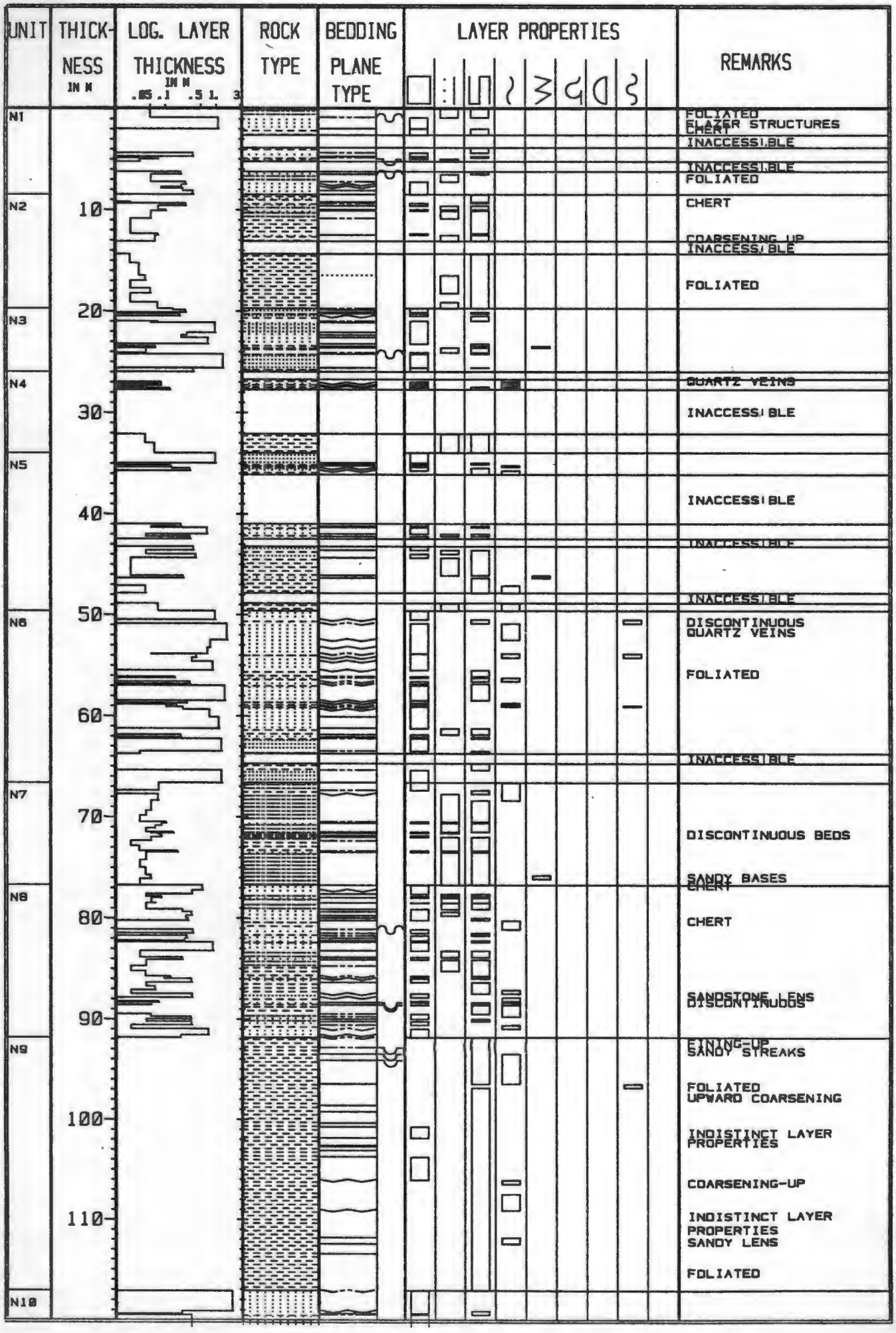

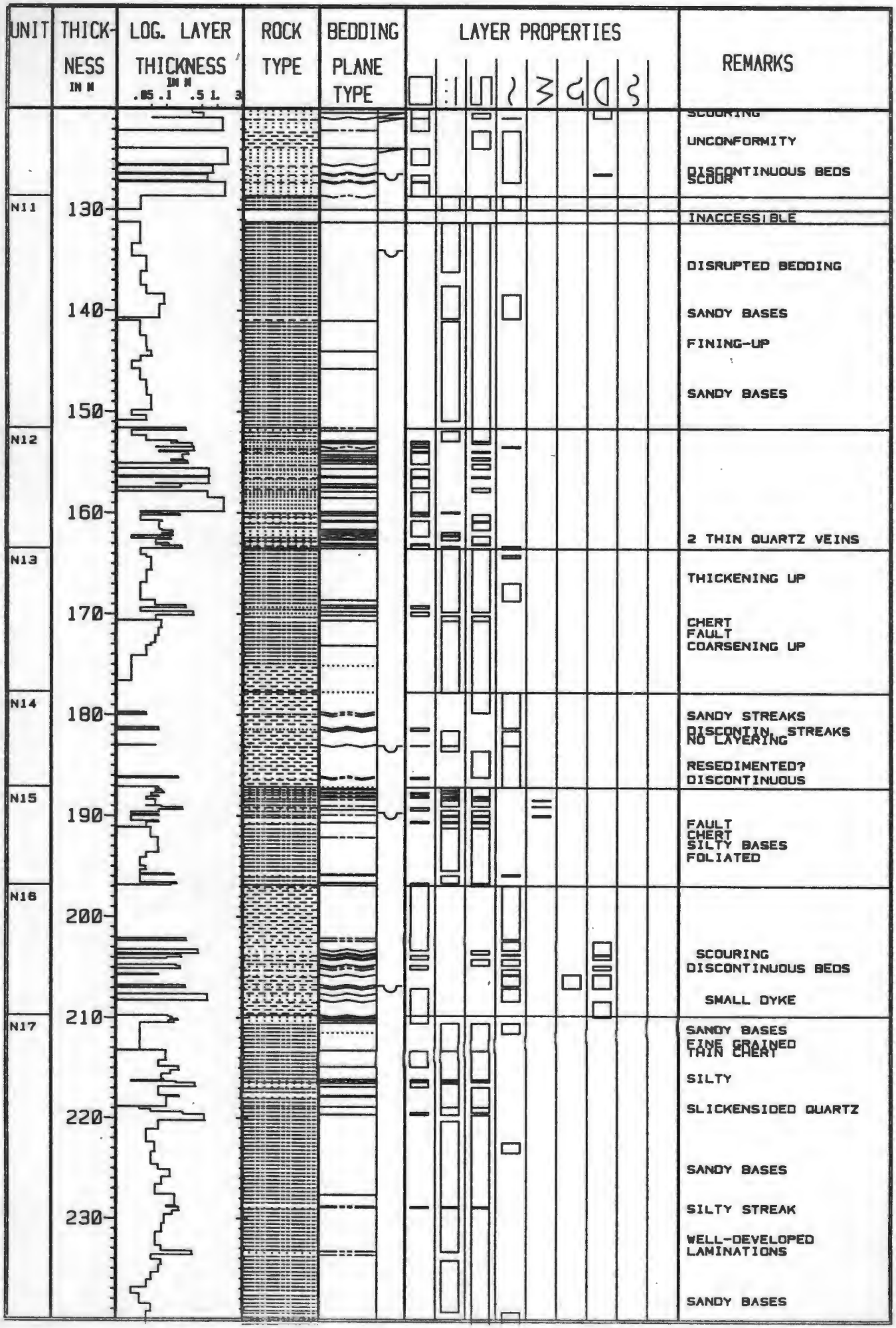
UNIT
THICK-NESS IN M
LOG. LAYER THICKNESS IN M .05 .1 .5 1. 3
ROCK TYPE
BEDDING PLANE TYPE
LAYER PROPERTIES
REMARKS
SCOURING
UNCONFORMITY
DISCONTINUOUS BEDS
SCOUR
N11
130
INACCESSIBLE
DISRUPTED BEDDING
140
SANDY BASES
FINING-UP
150
SANDY BASES
N12
160
2 THIN QUARTZ VEINS
N13
THICKENING UP
170
CHERT
FAULT
COARSENING UP
N14
180
SANDY STREAKS
DISCONTIN. STREAKS
NO LAYERING
RESEDIMENTED?
DISCONTINUOUS
N15
190
FAULT
CHERT
SILTY BASES
FOLIATED
N16
200
SCOURING
DISCONTINUOUS BEDS
SMALL DYKE
N17
210
SANDY BASES
FINE GRAINED
THIN CHERT
SILTY
SLICKENSIDED QUARTZ
220
SANDY BASES
230
SILTY STREAK
WELL-DEVELOPED LAMINATIONS
SANDY BASES

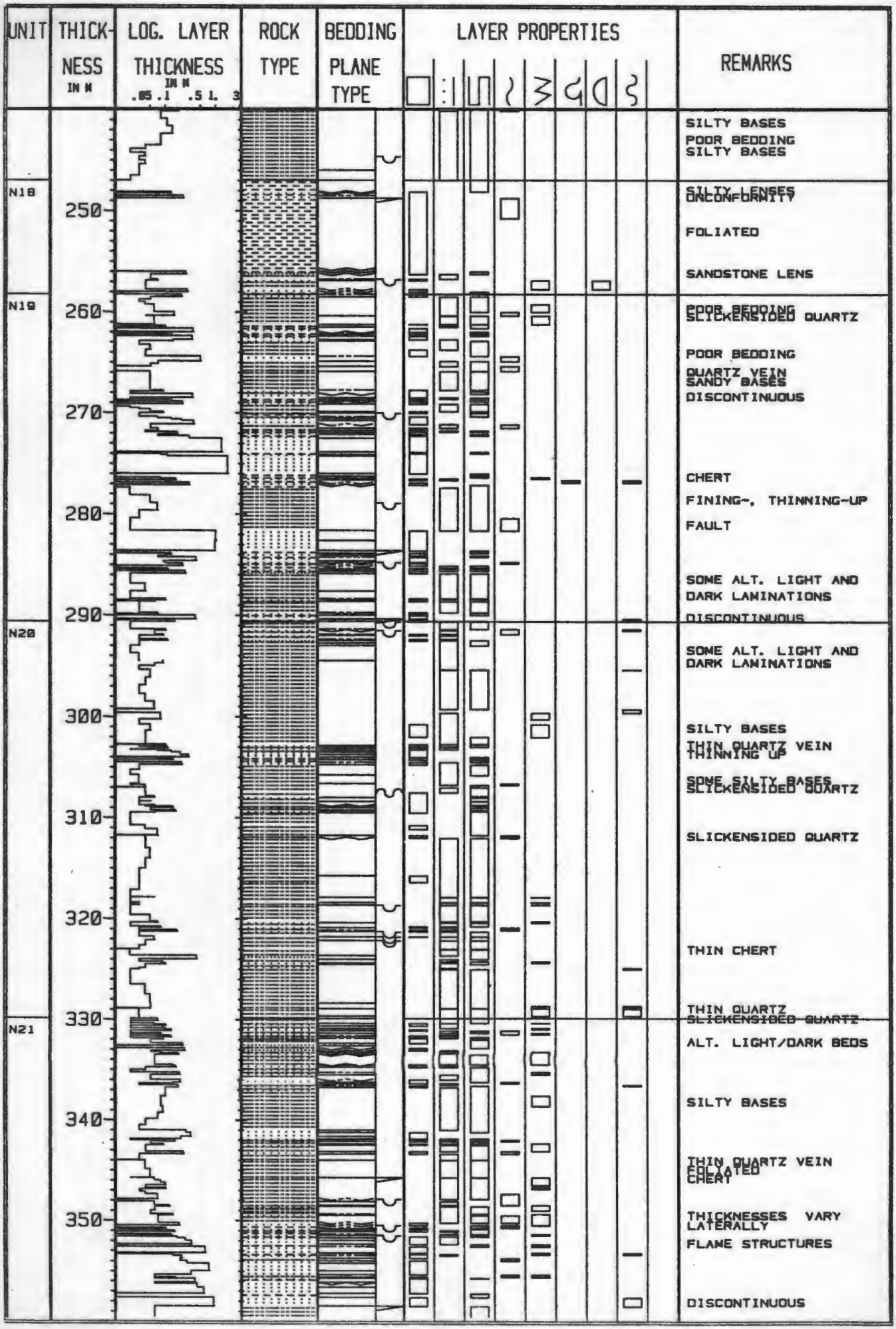
UNIT
THICK-NESS IN M
LOG. LAYER THICKNESS IN M .05 .1 .5 1. 3
ROCK TYPE
BEDDING PLANE TYPE
LAYER PROPERTIES
REMARKS
SILTY BASES
POOR BEDDING
SILTY BASES
N18
250
SILTY LENSES
UNCONFORMITY
FOLIATED
SANDSTONE LENS
N19
260
POOR BEDDING
SLICKENSIDED QUARTZ
POOR BEDDING
QUARTZ VEIN
SANDY BASES
DISCONTINUOUS
270
CHERT
FINING-, THINNING-UP
280
FAULT
SOME ALT. LIGHT AND DARK LAMINATIONS
DISCONTINUOUS
290
N20
SOME ALT. LIGHT AND DARK LAMINATIONS
300
SILTY BASES
THIN QUARTZ VEIN
THINNING UP
SOME SILTY BASES
SLICKENSIDED QUARTZ
310
SLICKENSIDED QUARTZ
320
THIN CHERT
330
THIN QUARTZ
SLICKENSIDED QUARTZ
N21
ALT. LIGHT/DARK BEDS
340
SILTY BASES
THIN QUARTZ VEIN
FOLIATED
CHERT
350
THICKNESSES VARY LATERALLY
FLAME STRUCTURES
DISCONTINUOUS

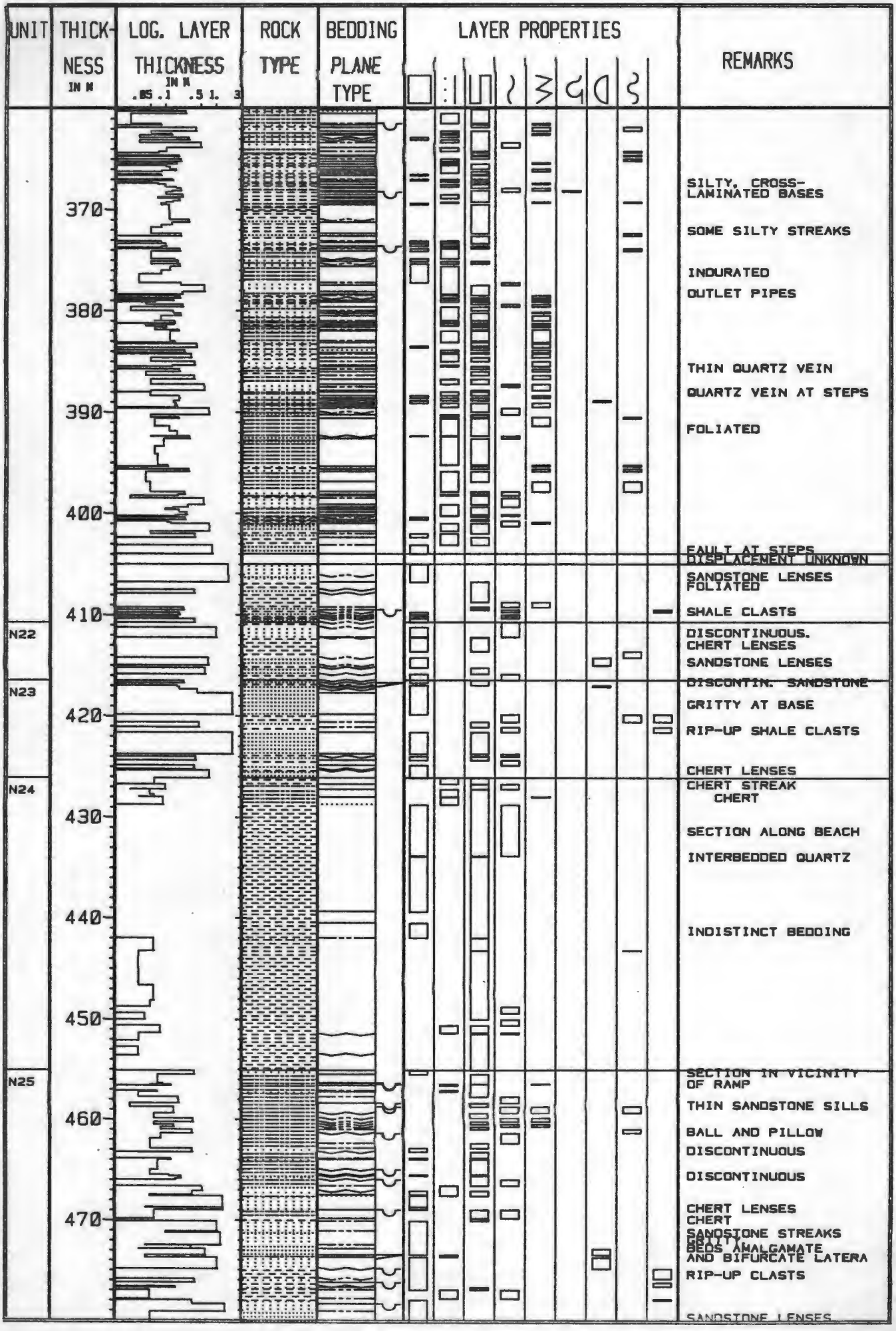
UNIT
THICK-NESS IN M
LOG. LAYER THICKNESS IN M .05 .1 .5 1. 3
ROCK TYPE
BEDDING PLANE TYPE
LAYER PROPERTIES
REMARKS
370
380
390
400
410
420
430
440
450
460
470
N22
N23
N24
N25
SILTY, CROSS-LAMINATED BASES
SOME SILTY STREAKS
INDURATED
OUTLET PIPES
THIN QUARTZ VEIN
QUARTZ VEIN AT STEPS
FOLIATED
FAULT AT STEPS
DISPLACEMENT UNKNOWN
SANDSTONE LENSES FOLIATED
SHALE CLASTS
DISCONTINUOUS. CHERT LENSES
SANDSTONE LENSES
DISCONTIN. SANDSTONE
GRITTY AT BASE
RIP-UP SHALE CLASTS
CHERT LENSES
CHERT STREAK
CHERT
SECTION ALONG BEACH
INTERBEDDED QUARTZ
INDISTINCT BEDDING
SECTION IN VICINITY OF RAMP
THIN SANDSTONE SILLS
BALL AND PILLOW
DISCONTINUOUS
DISCONTINUOUS
CHERT LENSES
CHERT
SANDSTONE STREAKS
BEDS AMALGAMATE AND BIFURCATE LATERA
RIP-UP CLASTS
SANDSTONE LENSES

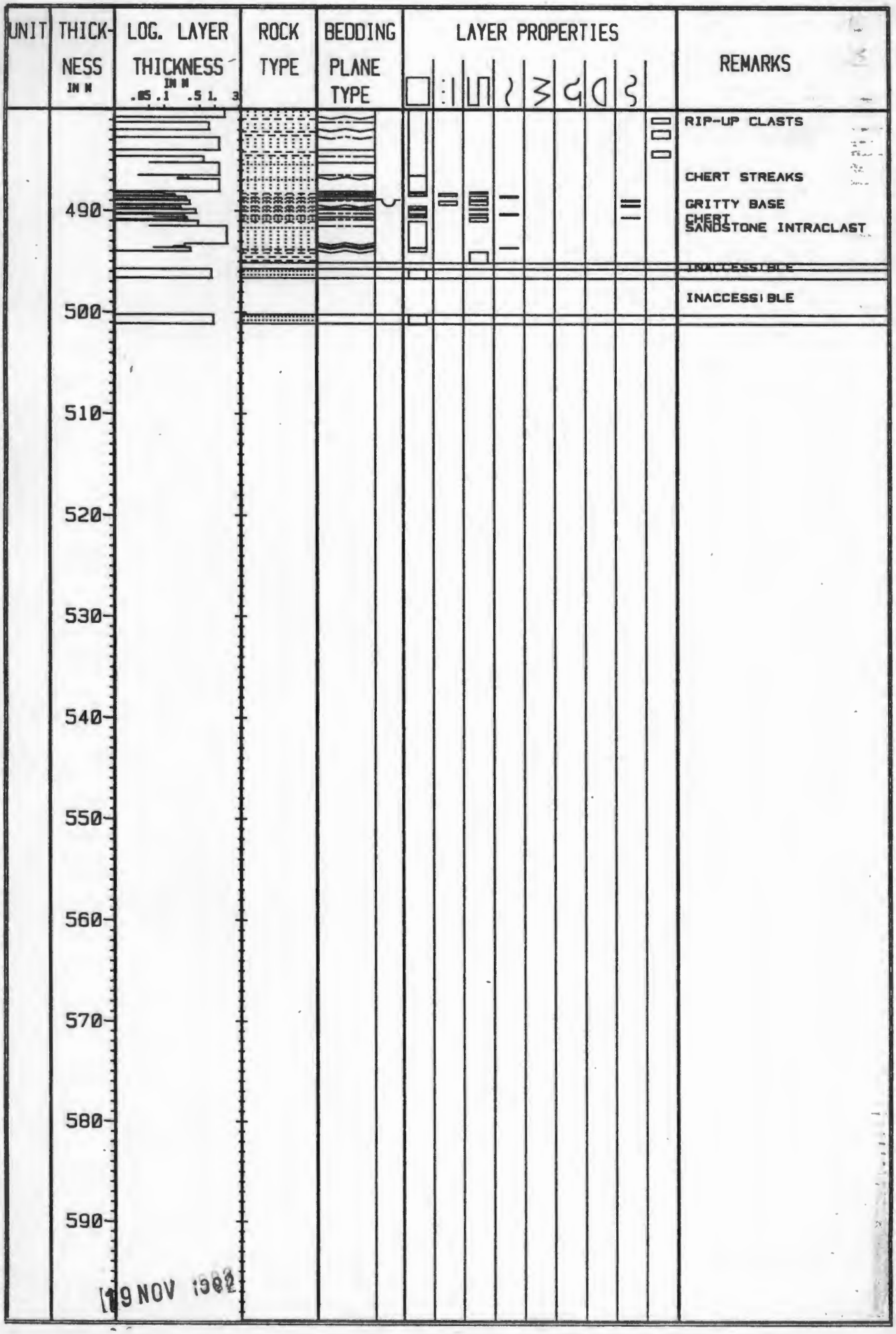
UNIT
THICK-NESS IN M
LOG. LAYER THICKNESS IN M
.05 .1 .5 1. 3
ROCK TYPE
BEDDING PLANE TYPE
LAYER PROPERTIES
REMARKS
RIP-UP CLASTS
CHERT STREAKS
GRITTY BASE
CHERT SANDSTONE INTRACLAST
INACCESSIBLE
INACCESSIBLE
490
500
510
520
530
540
550
560
570
580
590
19 NOV 1982

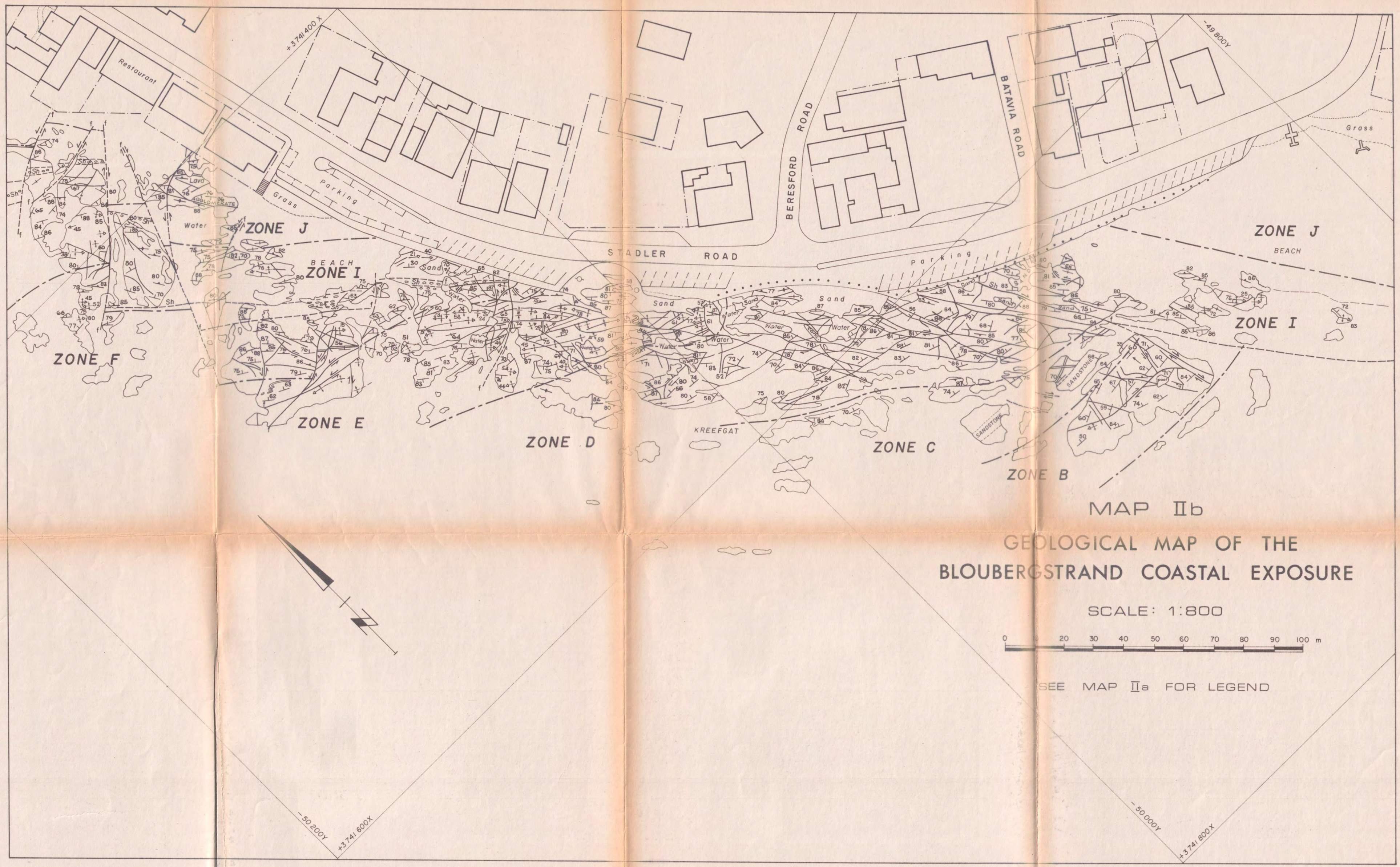

MAP IIb

GEOLOGICAL MAP OF THE BLOUBERGSTRAND COASTAL EXPOSURE

SCALE: 1:800

0 10 20 30 40 50 60 70 80 90 100 m

SEE MAP IIa FOR LEGEND

LEGEND

- Boudinage
- Shear zone
- Fault defined
- Fault assumed
- Joint
- Lithological boundary
- Strike and dip of layering.
- Strike of vertical layering.
- Strike and dip of foliation.
- Strike of vertical foliation.
- Trend and plunge of fold axis.
- Syncline axis.
- Anticline axis.
- Direction of younging.

MAP IIa

GEOLOGICAL MAP OF THE BLOUBERGSTRAND COASTAL EXPOSURE

SCALE: 1:800

0 10 20 30 40 50 60 70 80 90 100 meters

toilets
Blue Peter Hotel
POPHAM ROAD
Parking
-5200Y
SIR DAVID BAIRD DRIVE
PELEGRINE ROAD
JANSEN ROAD
BEACH
LOW WATER MARK
ZONE K
KLEINBAAI
GROOTBAAI
+3740800X
"Ons Huisie" Restaurant
STADLER ROAD
Memorial Cross
SAND AND BOULDERS
Water
WATER
DIE EILAND
ZONE J
ZONE I
ZONE H
ZONE G
BAMS ROCK
-5040OY
+3741200X
+3741000X
-5080OY
+3741400X

GEOLOGICAL MAP OF THE SEA POINT - MOUILLE POINT COASTAL EXPOSURE

MAP I

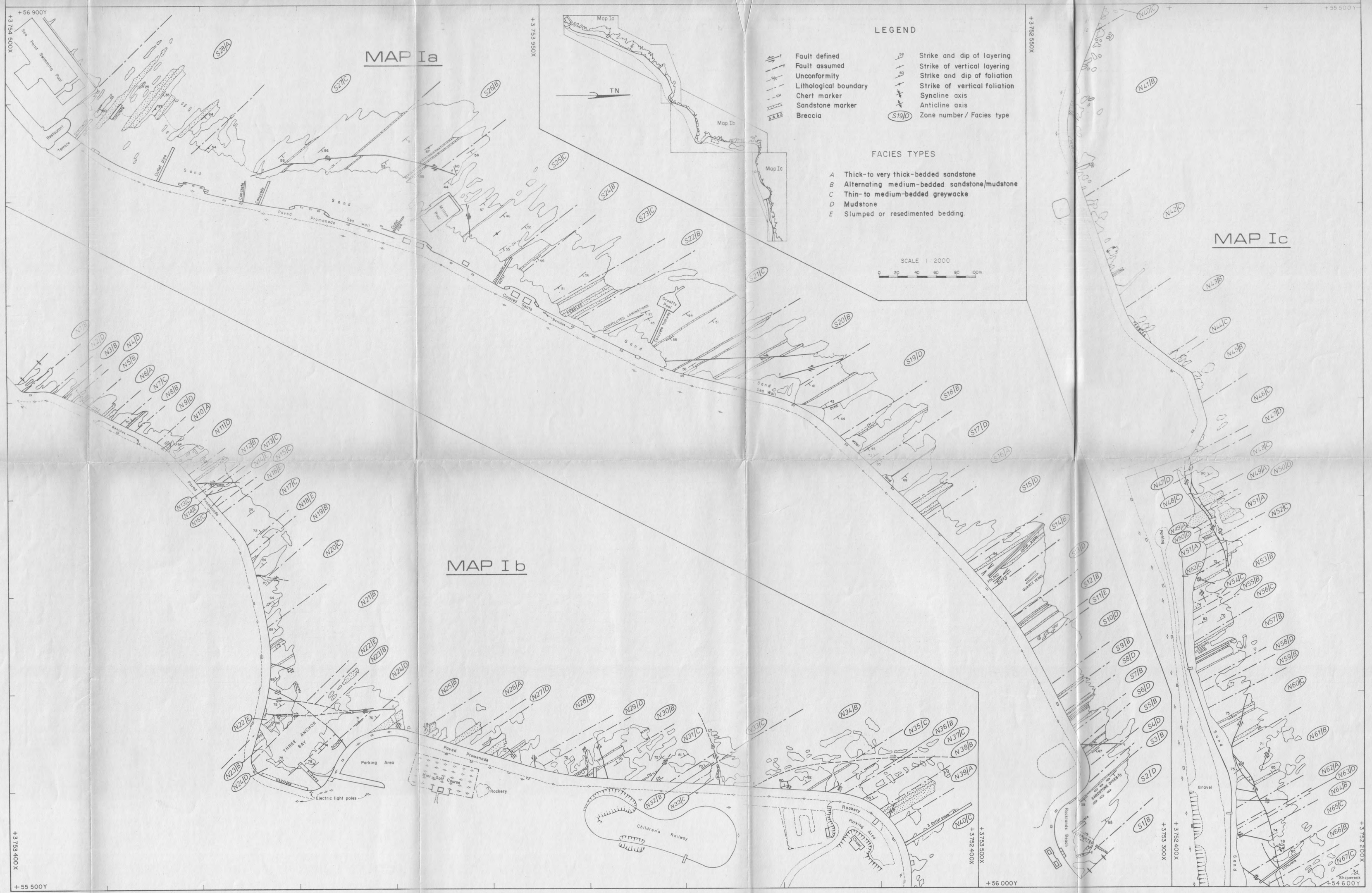

VAN REENEN STREET

Grass

Parking

BELLOY ROAD

Path

Grass

B E A C H

ZONE J

LOW WATER MARK

ZONE I

BOKKOMBAAI

Concrete

Water

Mermaids Pool

Sh

ZONE A

TABLE BAY

+ 3 741 800X

- 49 800Y

+ 3 742 000X

toilets

ZONE K

B E A C H

Sh

pool

Water

WATER

ZONE I

B E A C H

LOW WATER MARK

ZONE J

- 49 600Y

MAP IIc

GEOLOGICAL MAP OF THE BLOUBERGSTRAND COASTAL EXPOSURE

SCALE: 1:800

0 10 20 30 40 50 60 70 80 90 100 m.

SEE MAP IIa FOR LEGEND